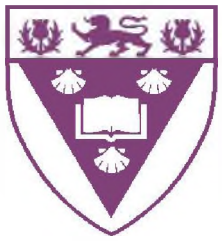

RHODES UNIVERSITY

Grahamstown • 6140 • South Africa

Exploration Potential for Copperbelt - Style Mineralisation in NW Province, Zambia; Soil Geochemistry as a targeting tool

By

John Mwamba

A dissertation submitted in partial fulfilment of the requirements for the degree of

MASTER OF SCIENCE
(Exploration Geology)

MSc Exploration Geology Programme
Geology Department
Rhodes University
P.O. Box 94
Grahamstown 6140
South Africa

February 2018

ACKNOWLEDGEMENTS

I am grateful; first and foremost, to my wife, family and children who have provided me with a stable homestead all these years I have worked as an Exploration Geologist often missing from home for many weeks at a time. I want to particularly thank them for their understanding and tolerance during my long periods of absence and for missing all important academic activities in their lives.

Prof. Yao, the previous Programme Director, is applauded for his contagious geology enthusiasm, technical input and academic involvements in the MSc Programme. He is appreciated for his generous sharing of knowledge on the geology of the Bushveld Complex during the Magmatic Module field trip of August 2014. Most sincere acknowledgements go to Prof. Jock Harmer for his constructive criticisms and technical guidance especially during presentations whilst on class field trip in March 2015. This dissertation would not be in this current form without his input. For this, I will be forever grateful.

Ashley Goddard is thanked for her administrative support during the entire period of my study at Rhodes. Her excellent administrative acumen made it possible for me to enjoy a stress-free stay at Rhodes allowing me to focus entirely on academics. Her efforts in ensuring my safe passage to and from Grahamstown are greatly appreciated.

The rest of the academic stuff at Rhodes; Dr.Prevec, Dr.Büttner, Dr.Skinner, and the entire Rhodes Geology Department staff are thanked for their input in making the university in general, and the geology department in particular, a library of knowledge and a conducive atmosphere for learning. All my classmates, my workmates, my teachers, my lecturers, authors of geology literature and others are thanked for helping shape my thoughts, thinking, ideas and outlook on many matters pertaining to life in its broadest sense. It is entirely impossible to claim ideas presented in this thesis as entirely mine as these people have helped put those thoughts into my mind. I am forever grateful.

Above all, I am thankful to God for his enduring love for me, for His guidance when all seems dark, for exercising patience with me whenever I go wonder bouts, and most importantly for sustaining my life on this universe that He created. Truly, He is my JEHOVAH JIREH.

DECLARATION

I, **John Mwamba**, declare this dissertation to be my own work. It is submitted in fulfilment of the Degree of Master of Science at the University of Rhodes. It has not been submitted before for any degree or examination in any other University or tertiary institution.

Signature of the candidate: .....  .....

Date: .....03/09/2017.....

DEDICATION

This thesis is dedicated to the memory of my late parents and the one man whose words long ago invigorated me to pursue higher learning.

ABSTRACT

The NW Province of Zambia is fast becoming a major significant mining district challenging to usurp the economic importance of the traditional Copperbelt Province that has been mined for nearly a century. With latest developments at Kansanshi, Lumwana and Kalumbila mines exploration efforts in the search for Copperbelt style mineralisation have doubled up in the province in recent months. Traditional methods of stream sediment and soil sampling, geophysics, aerial photo and Landsat imagery interpretations have been employed in exploration targeting campaigns.

This thesis asks the question: Can we use the Copperbelt geochemical footprint as a proxy to finding new copper deposits in NW Province? The challenge faced in such studies is that few geochemical datasets for old mines exist and the little that does is proprietary information. In some mines this dataset is entirely nonexistent – at least not in the public domain. Attempting to run orientation geochemical trials on such mines is not feasible at present due to maturity of mining and the levels of contamination of the natural environment that have occurred over several decades of mining.

However, in tackling this question few Copperbelt geochemical datasets from Baluba, Nkana, Mimbula, Nchanga, Bwana Mkubwa, Mufulira West and Lufubu North were used. The findings presented in this report are that for Copperbelt style mineralisation Cu/Co, Cu/Ni, Cu/Ag ratios in soil geochemistry data should be in the ranges of 0.25 to 0.48 provided geochemical studies occurred in residual soils. These ratios hold true for sediment hosted copper-cobalt mineralisation hosted at various stratigraphic levels within the Roan Group or in upper levels elsewhere on the Central African Copperbelt.

Geochemical dataset for the study areas presented in this report show that the soil geochemistry footprint in the province is not dissimilar to the soil geochemistry footprint of the traditional Copperbelt Province. This means there is great potential for finding Copperbelt style mineralisation in the province and other styles of mineralisation in which copper is associated with cobalt, lead, zinc, nickel, vanadium and molybdenum. The areas of study also possess requisite geological factors that are conducive to hosting Copperbelt style deposits. These factors include: favourable structural traps with similar trends to existing mines in the province, geophysical characteristics comparable to other deposits in the

province, right geological package known to host multi-type deposits in the Katangan stratigraphic sequence, and similar geochemical footprints observed on other deposits within the Lufilian fold belt. For this reason, geochemical dataset must not be looked at in isolation but should be treated in considerations with other factors and geological environment.

Keywords: *Copperbelt mineralisation, stream sediment, soil sampling, geophysics, Landsat imagery, Lufilian fold belt*

TABLE OF CONTENTS

LIST OF FIGURES

LIST OF TABLES

1. INTRODUCTION

The NW Province is the second largest province in Zambia with an aerial extent of over ten million hectares. It is home to three of Zambia's newest mines collectively boasting 4 major deposits namely: Kansanshi - 744.3Mt at 0.86%Cu measured/indicated resources; Enterprise - 40.1Mt at 1.07% Nickel; Sentinel - 1027.3Mt at 0.51%Cu measured and indicated resources (First Quantum Minerals Ltd, 2012) and Lumwana - 965.89Mt at 0.50%Cu reserves plus inferred resources (Barrick Gold Corporation, 2016). Consequently, the province is fast emerging as the new 'copperbelt' of Zambia challenging the traditional economic ascendency of the Copperbelt Province whose reserves have been progressively depleted. Though mining has occurred in the province since the early 1900s, it is only in recent times that mechanized mining has been implemented commencing with Kansanshi in 2005, Lumwana in 2010 and more recently Kalumbila where production ramp-up activities are currently underway.

The Lufilian Arc hosts all mineralisation in the Central African Copperbelt. It is an arcuate Pan-African structural belt that extends from the Zambian Copperbelt in the east to the Democratic Republic of Congo (DRC) in the north and to northeast Angola in the west. The Lufilian belt is subdivided into four major geological domains based on varying structural characteristics (De Swardt and Drysdall, 1964). These subdivisions from north to south comprise:

1. The External Fold and Thrust Belt (which hosts all the DRC deposits);
2. The Domes Region (where all Zambian Deposits are located);
3. The Synclinorial Belt, and
4. The Katanga High.

The Domes Region hosts all the major copper deposits in Zambia. This geological domain is characterised by arcuate chain of basement inliers at the core of domes which are enveloped by Muva supergroup quartzites and younger Katangan rocks. The Domes Region underwent deep and shallow level thrust tectonics which culminated into extensive hydrothermal alteration of both basement and sedimentary cover units (Porada and Berhorst, 2000).

Overall the stratigraphy of the Lufilian Arc comprises Paleo-Proterozoic gneisses and schists with Meso-Proterozoic Muva quartzites and granites forming the Basement Complex. The

Katangan Sequence which overlies the Basement Complex is internally subdivided into the *Lower Roan* - consisting of clastic units interspersed with siltstones and shales; the *Upper Roan* – consisting of mixed carbonates-siliciclastics and breccias; the *Mwashia* – comprised of carbonates, mixed carbonates-siliciclastics, siltstones and shales; the *Lower Kundelungu* – comprised of diamictite (Grand Conglomerat), carbonates, siltstones and shales; and the Upper Kundelungu – consisting of basal diamictite (Petit Conglomerat), dolomitic shales, pink limestones, sandy shales and sandstone.

All the four deposits in NW Province are unique in terms of mineralisation styles and in their stratigraphic position within the Katangan Sequence. The Kansanshi deposit is a vein-style Cu-Au mineralisation located within a complex sequence of N-S trending mineralised faults cutting Katangan metasediments of the Kundelungu series (Broughton et al., 2002), Lumwana is a Cu-U deposit hosted within slivers of basement gneisses and schists at the stratigraphic level of the - Roan Group – Basement Dome inter-phase (Bernau, 2007). The Kalumbila (Sentinel) Cu-Co-Ni deposit represents stratabound mineralisation located in the Mwashia carbonaceous shales/phyllites (Hitzman, 2011) whereas the Enterprise deposit is a hydrothermal nickel deposit occurring in Roan Group metasediments (Capistrant et al., 2015).

Despite the varying suggested ore models, all the deposits are similar to the Copperbelt mineralisation in that they occur in the Domes region in the arcuate Lufilian fold-thrust belt of Neoproterozoic age. The wide range of deposit styles being exploited in NW Province coupled with many areas possessing key geological footprints similar to the traditional Copperbelt deposits give hope for discovering more deposits in the province.

1.1. History of Exploration in NW Province

Written records of exploration activities in the province date as far back as the late 1800s coinciding with the arrival of Europeans in what was then known as Northern Rhodesia. George Grey, an emissary of Tanganyika Concession Limited - a company formed by Cecil Rhodes' friend R. Williams, first pegged the Kansanshi Cu-Au property in 1899 after being shown ancient workings by indigenous people. Tanganyika Concession Limited was formed solely to explore the areas around the Zambia-Congo DR border (Watts et al., 1991; Broughton et al., 2002). In the same year Tanganyika Concession Limited were shown old workings at Chambeshi Copper property on the Copperbelt by local chiefs.

With the re-discovery of Kansanshi (Cu-Au), Chambeshi (Cu), Kabwe (Pb-Zn) and Roan Antelope (Cu) exploration activities escalated everywhere in Zambia in the years leading up to the first World War. These exploration activities halted only during the periods of the First World War (1914-1918), the great depression (1932) and the Second World War (1945). Other Copperbelt deposits such as Nchanga and Nkana were discovered after the First World War. Exploration companies such as the Rhodesia Congo Border Concession Limited (RCBC) were actively exploring in the area between the Copperbelt and the Angolan border.

However, it was the period after the Second World War when a more comprehensive and systematic exploration was carried out in NW Province. The entire NW Province exploration ground was consolidated and shared among three main players namely; Rhodesian Selection Trust, American Metals (Amax) and Anglo-American Group. These majors utilised various subsidiaries to carry out regional exploration for copper, cobalt and uranium using geochemical techniques as the primary prospecting tool. It was during this period that most of the outcropping mineral showings were discovered and delineated. The vast extent of NW Province coupled with generally difficult access due to the large number of perennial streams, resulted in only the most obvious mineral occurrences and geochemical anomalies being followed up in any detail.

The period between the early 1950s and late 1970s remains the most productive period for the discovery of mineral occurrences and detection of anomalies in NW Province. Early exploration targeted copper anomalies in Katangan stratigraphy, copper with associated gold or zinc in Kundelungu group (upper parts of Katangan stratigraphy) and stratiform epigenetic mineralization similar to that found at Kipushi on the Congo DR side of the Copperbelt. Major mineral deposits and occurrences discovered during this period (Legg, 1973) include the Lumwana Cu-U-Au deposit (Malundwe & Chimiwungo), Kalumbila Cu-Ni-Co deposit, Kalengwa Cu deposit in Mufumbwe, Kalaba Cu deposit, as well as the Iron deposits around Kisasa - and several iron occurrences around Kasempa. In Mwinilunga the Luamata copper occurrences were noted in relatively unmodified stratiform sediments/metasediments as well as skarn metasomatic iron, copper and uranium showings in both unmodified stratiform sediments/metasediments and in modified metamorphosed/remobilized metasediments. Hydrothermal and metasomatic gold occurrences were discovered around Chovwe.

1.2. Location of Study Area

The study area comprised three adjoining large exploration licenses covering a total of 2443Km^2 located in NW Province of Zambia and situated in the Domes Region of the Lufilian Arc, a Neoproterozoic belt renowned for hosting world class copper-cobalt deposits of several types including typical Copperbelt style stratiform mineralisation, Kansanshi vein style, thick-skinned Lumwana basement type, Mwashia-hosted Kalumbila style, and the new emerging hydrothermal nickel deposits. The newly developed Kalumbila deposits are located about 30 km north of the study areas. Individually the areas are referred to as Solwezi, Mapunga and Matebo (**Figure 1**); collectively they were called the Solwezi Copper Programme (SCP).

The study area lies 260 km west of the Copperbelt town of Chingola and approximately 100 km southwest of Solwezi town. These licenses were part of a large portfolio of exploration ground in NW Province worked by VALE Zambia Limited before they exited Zambia in early 2015 as result of weakening commodity prices especially that of iron ore – the company's single-most important commodity.

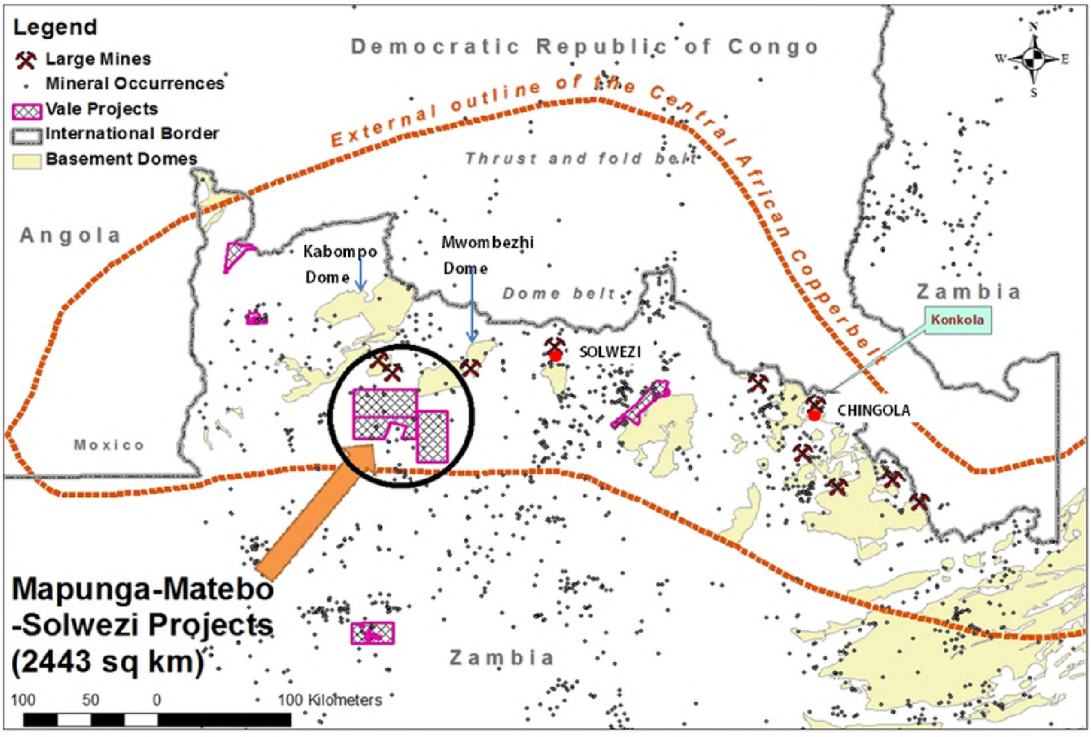

Figure 1: *Location map of the study area: 3 adjoining tenements measuring 2443 Km^2 (Vale Exploration Team, 2013).*

1.3. Exploration Potential for Copper-Cobalt Deposits in the Province

Prospective areas can be highlighted by extrapolation from the geological features and mineralisation characteristics of known occurrences. The most obvious key characteristics to use when narrowing down search areas include low magnetic signature bodies on the flanks of magnetic highs; soil geochemical anomalies beyond certain thresholds (discounting lithological interferences); high electromagnetic signature bodies; structural complexities; and most importantly good stratigraphic location within the Katangan stratigraphy. Good stratigraphic location refers to horizons with favourable geology that can effect entrapment or accumulation of metals from mineralising fluids.

Prospectivity in NW Province has already been demonstrated by the large number of mineral occurrences and geochemical anomalies discovered during the broad-brush exploration approach conducted in the early 1950s to the late 1970s. During this period over 20 mineral occurrences and geochemical anomalies were discovered. A compilation of these mineral occurrences and geochemical anomalies was done by Legg (1973) (**Figure 2**).

Of the more than twenty mineral occurrences only 3 deposits (Kansanshi, Lumwana, and Kalumbila) have recently been developed into producing mines. These deposits were the most obvious during the largely stream sediment geochemical sampling programmes of Rhodesia Selection Trust and Anglo-American Corporation. Kansanshi is the only exception as the deposit has seen intermittent mining from 1906 (Watts et al., 1991) to about 2005 when more continuous copper production was commenced by First Quantum Minerals Limited of Canada.

Several copper oxide occurrences have been mined and some are still being mined in the province. Whether these oxide caps have sulphide roots at depth is an area needing further investigation. Some of these copper oxide deposits include Kalaba, Kalengwa, Zambesia deposit in Luamata, Lalafuta in Kaoma, Karibarembi in Mufumbwe and Kimale near Mujimanjovu.

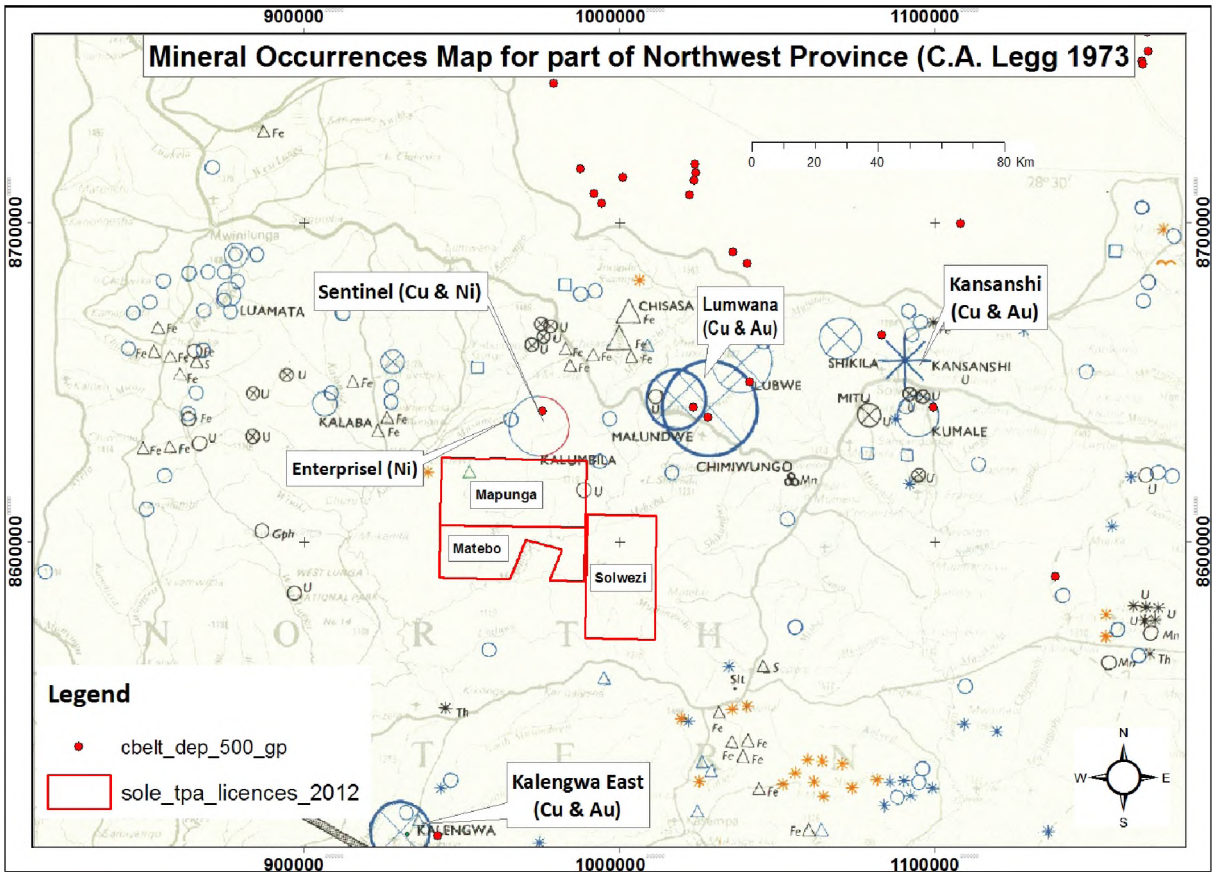

Figure 2: *Mineral Occurrence Map (Legg, 1973) showing location of study area Solwezi, Matebo and Mapunga.*

1.4. Research Outline

The research was conducted using soil samples collected in three contiguous tenements around the south-western flanks of the Mwombezhi dome. These samples were collected during the geochemical evaluation phase of exploration activities conducted by VALE Zambia Limited and supervised by the author. The samples comprised B-horizon soil collected in areas with clear residual soils, and termite mound soils collected in areas with suspected transported soils or dambos (shallow wetlands).

Geochemical investigations were conducted in these three areas as they were thought to possess a permissible combination of key geological factors required for orebody discovery. The areas are close to stratigraphic units that host mineralisation elsewhere on the Copperbelt (Basement gneiss-Lower Roan interface, Upper Roan-Lower Roan interface, Upper Roan-Mwashia interface). Another important factor for selecting these areas is their proximity (15-20km) to Kalumbila deposits and having similar structural complexity to Kalumbila and other

deposits within the Domes Region comprising high and low frequency magnetic domains with notable displacements near basement domes postulated to be conduits for transport of mineralizing fluids.

Analysis readings by a portable XRF spectrometer were used to select samples for dispatch to an analytical laboratory and by rule of thumb (based on historical geochemical surveys); all samples reporting Cu-Co concentrations above 40 ppm were sent for analysis at the ALS Chemex laboratory facility in Johannesburg. At the laboratory samples were homogenized after pulverization and digested in aqua regia before analysing for a suite of 51 elements by a combination of Inductively Coupled Plasma Mass Spectrometry (ICP-MS) and Atomic Emission Spectrometry (ICP-AES) with a +/- 10% precision. Assay analysis and interpretations were conducted using ioGAS, geochemistry software that allows rapid spatial visualization of large geochemical.

The research was aimed at identifying Cu-Co concentrations above normal background levels in the three tenements. Determination of background concentration and anomaly thresholds were undertaken using statistical methods. Any sample concentration above median plus two standard deviations (above the 95^{th} percentile) was deemed anomalous.

The author executed the soil sampling programme described in this thesis, planned the follow-up in-fill sampling programmes, managed the QA-QC sampling protocols prior to dispatch and after receipt of laboratory assays; and was solely responsible for the interpretations and discussions of geochemical assays to arrive at the conclusions presented herein. Apart from adding new information about this area through this study, the author has generated strong drill targets for potential economic copper, cobalt and zinc mineralisation.

1.5. Purpose of Research

The purpose of this research is to use soil geochemistry to try and identify anomalous elemental concentrations in order to determine the potential for metal accumulations in the subsurface which, in turn, might indicate potential for orebody discovery. Soil geochemistry is an integral part of mineral exploration techniques employed in Zambia particularly in NW Province where nearly all mineral occurrences and geochemical anomalies have been found by this mechanism using either stream sediment or the traditional residual soils (Kansanshi is the only deposit in the province whose discovery is not attributed to geochemistry: it was

mined by indigenous peoples way before geochemical techniques were introduced in the province). With the large body of knowledge existing from the Copperbelt mines and elsewhere in the region, analogues are drawn where known mineral assemblages from existing mines are used as vectors to finding potentially viable mineral occurrences in the study area.

Watts et al. (1991) recognised copper deposits of the NW Province to be an integral part of Zambia's future growth potential and recommended maximizing exploration efforts by developing sound geochemical sampling programmes and assay data evaluation techniques to speed up new deposit discovery. It is clear that methodically run geochemical sampling programmes will aid in locating new deposits as evidenced by the re-discovery of Kansanshi, Lumwana and Kalumbila deposits where meticulous soil sampling campaigns were important stages in early exploration endeavours by Cyprus Amax (Kansanshi), Equinox Minerals (Lumwana) and First Quantum Minerals (Kalumbila).

With this study it is hoped that light will be shed on the viability of the three exploration areas under study. The primary element of focus is copper with its associated elements cobalt and nickel.

1.6. Surface Topography

The study areas have generally flat lying landscape dominated by rivers, termite towers, flood plains and dambos. The areas are cut by four main rivers (Mwombezhi, Lualaba, Maheba and Mwafwe) and several crisscrossing perennial tributaries which posed access challenges (**Figures 3 and 4**). Surface relief is generally flat to gently undulating with low-lying areas mainly along river channels and dambos. Within the dambos are found patches of swamps and enumerate pimple/mushroom size termite mounds. Low lying and highland areas have elevations which range between 1150 m and 1250 m above sea level.

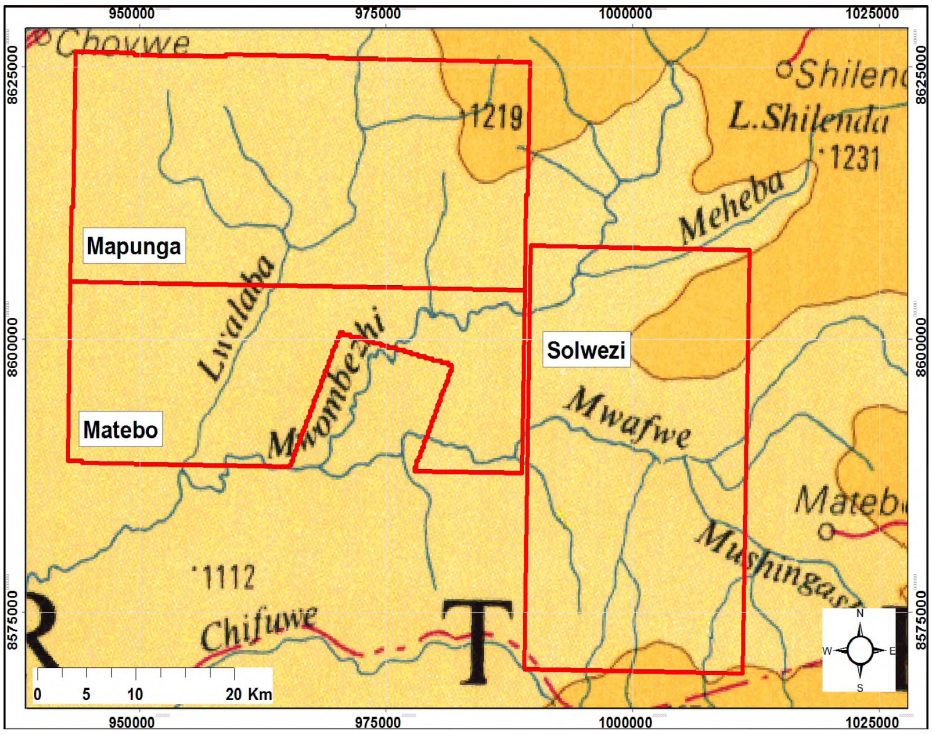

Figure 3: *Topographic Map showing topography of study area dominated by rivers (Surveyor General, 1986).*

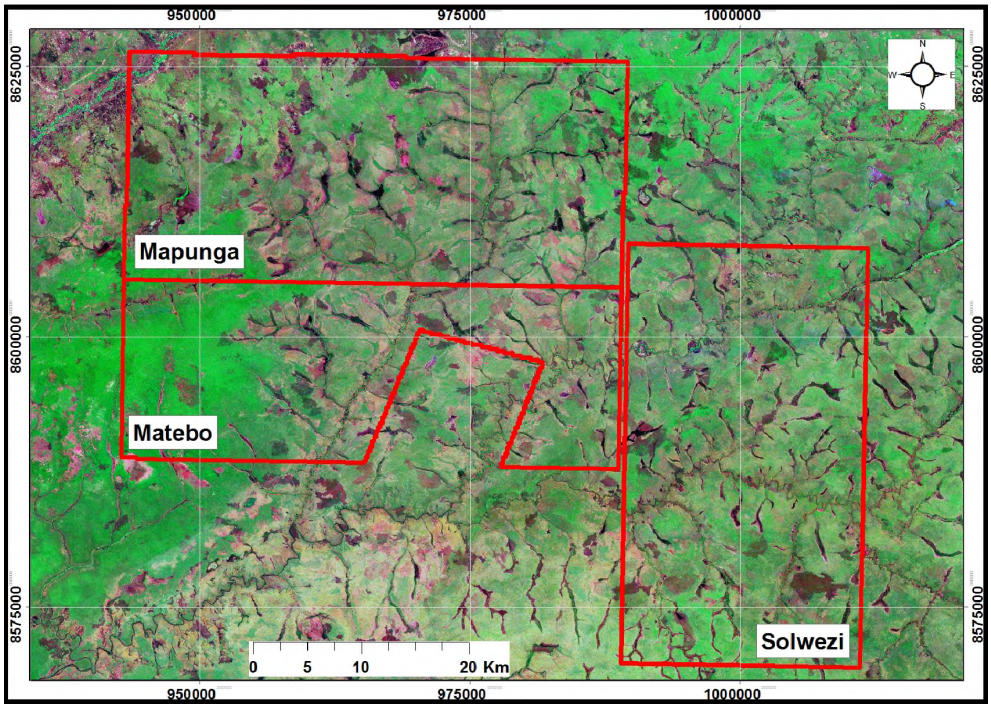

Figure 4: *Extract of a Landsat 7 image displaying visible and near infrared bands 3, 2, and 1 in red, green and blue (RGB) showing terrain of the study areas (serial number of the raw image = LE71730692001201EDC00).*

1.7. Vegetation and Regolith Formation

Miombo Woodland vegetation covers the study area (Edmonds, 1976). These woodlands are still preserved owing to the area falling within protected areas on the eastern flank of the West Lunga National Park. Miombo woodlands are generally deciduous and have closed canopy-light foliage (**Figure 5**). Sufficient light percolates through this closed canopy foliage to reach the ground where a continuous cover of grasses, herbs and other shrubs thrive. Leguminous species of Brachystegia longifolia, Isoberlinia and Julbernardia dominate Miombo Woodlands. Thick vegetation is commonly found along rivers where trees are tall and grass thick with nearly impassable bushy shrubs. A few open spaces found mainly on or around dambos and on areas covered by hard crusts of Ferricrete have short grass with sparse thin trees.

The soil survey unit of Mount Makulu Research Station in 1999 published a soil map of Zambia which depicts the study area to fall under what is known as ferralsols. These soil types occur in humid tropical and subtropical regions of the world on old and stable land surfaces. They are red, reddish brown or yellow weathered soils resulting from accumulations of aluminium or iron oxides. Flood plains and dambos have greyish black clayey, silt to loamy soils that are rich in organic matter and therefore are enriched in metal concentrations due to scavenging of metals from various surface sources.

Some open spaces have little amounts of soil due to presence of hard crust of laterite. The Kalahari white sands and silts cover a small portion in the southwest corner of the study area. Kalahari soil cover can be very deep and because of this fact, this portion of the study area was not sampled. Soil types in the study areas is consistent with what has been mapped throughout in the province; Kalahari sands and silts, flood plain silts and dambo clayey loams, residual clayey loams, lateritic and clayey soils (Key et al., 2004).

Figure 5: *Typical Miombo Woodland Vegetation found in study areas.*

1.8. Climate

The study areas experience subtropical climate with summer rains from November to April varying between 1200 – 1400mm per year; cold dry winter season from May to August and a hot dry season from September to October. Temperatures vary from mean maxima of 28-30^{o}C to mean minima of 12-15^{o}C. Temperatures are considerably influenced by altitude and the mean maxima are rarely attained at higher elevations.

2. REGIONAL GEOLOGICAL FRAMEWORK

The study area is located within the Lufilian Arc, an arcuate fold and thrust belt that extends from the Zambian Copperbelt to the Congolese Copperbelt in Katanga Province. The Lufilian arc is a northward-convex belt that consists predominantly of metasedimentary rocks of the Neoproterozoic Katanga Supergroup which hosts several giant-to medium-sized stratabound/stratiform copper-cobalt deposits. The arc is subdivided into four main regions (see **Figure 6**) with the most renowned being the domes region which host nearly half of the copper-cobalt mineralisation in the Central African Copperbelt (Selley et al., 2005; Armstrong, 2001).

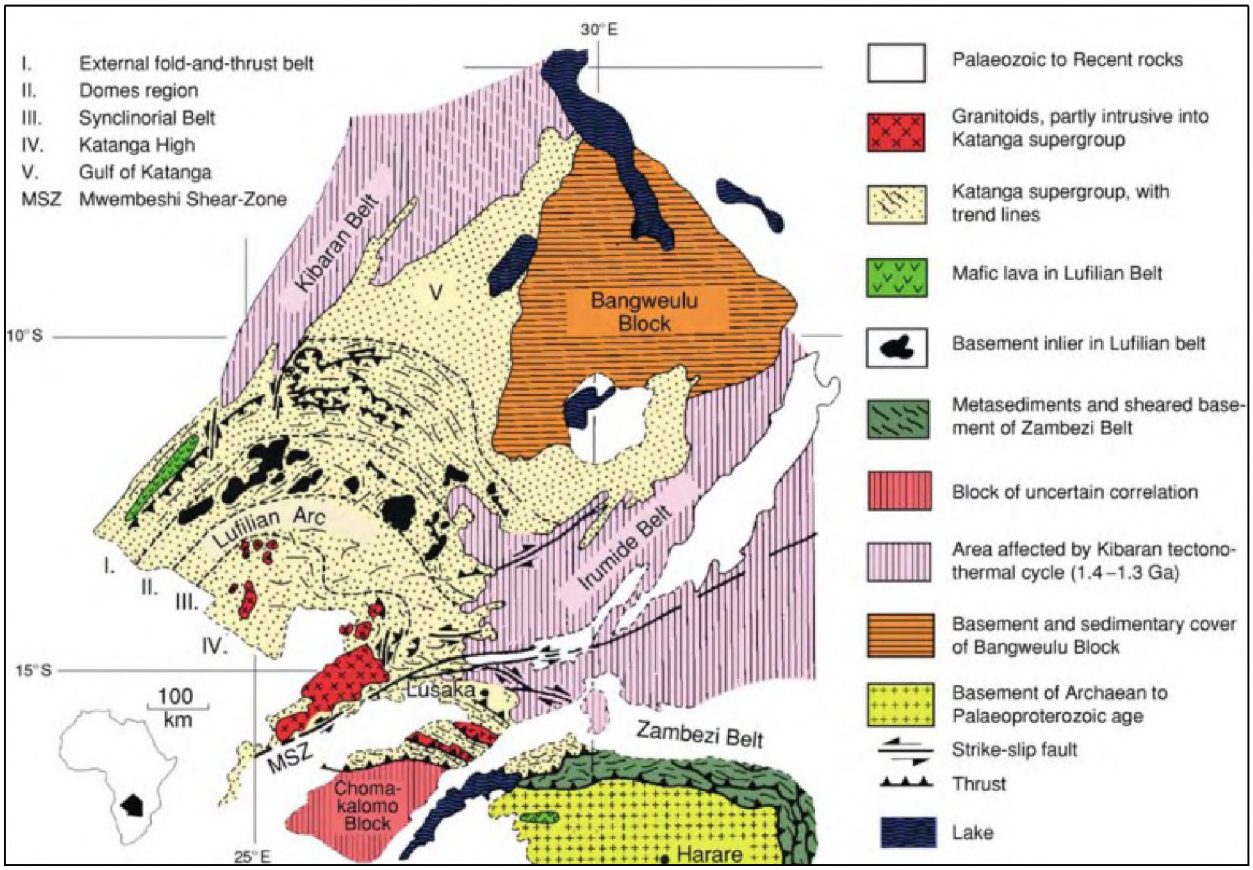

Figure 6: *Tectonic sketch map of the Lufilian Arc showing four main subdivisions most important of which is denoted II (Domes Region). Other important features on the map include, the Mwembeshi shear (MSZ) and the External fold thrust belt (region I) that host most of Cu-Co mineralisation in Congo DR (modified after Porada, 1989).*

The Lufilian fold thrust belt is bound to the N and NW by the 2.54 – 2.56 Ga Congo Craton (Key et al., 2001) and the ca. 1.38 – 1.37 Ga Meso-proterozoic Kibaran Belt (Kokonyangi et al., 2006). To the NE, the arc is bound by the ca. 2.0 – 1.8 Ga Paleo-proterozoic Bangweulu

Block (Unrug, 1982) whereas to the SE east it is constrained by the ca. 1.05 – 0.95 Ga Late Meso-proterozoic Irumide Belt (De Waele et al., 2006). The Lufilian Arc developed in response to the collision between the Congo and Kalahari Crustal plates (Porada, 1989).

2.1. Tectonic Setting of Lufilian Arc

The Zambian Copperbelt forms the southern part of the Central African Copperbelt in the Lufilian Arc. The Arc can be subdivided into five major subdivisions (Porada, 1989) – from northeast to southwest these are; Lufilian Foreland (Gulf of Katanga), the External Fold and Thrust belt, the Domes Region, the Synclinorial belt, and the Katanga High (**Figure 7**). All Zambian Cu-Co deposits are located within the Domes Region whereas the Cu-Co deposits of the Democratic Republic of Congo are restricted to the External Fold and Thrust belt. In broad terms each of the belts in the arc preserves evidence of Neoproterozoic extension during breakup and dispersal of the Meso-proterozoic supercontinent, Rodinia followed by later collisional deformation and metamorphism during assembly of central Gondwana (Selley et al., 2005).

The Basement rocks in Zambia comprise re-worked Archean and Meso-proterozoic metagranites, migmatites, metavolcanic and metasedimentary units which occur on the periphery of Lufilian arc as well as well exposed as basement inliers in the Domes Region (Johnson et al., 2005). The Lufubu schists which are dominantly sedimentary and volcanic rocks with granitoids - are the oldest recognised rocks in the Copperbelt forming a metamorphosed Paleo-proterozoic magmatic arc sequence (Mendelssohn, 1961; Master et al., 2005).

Tectonic evolution in the Central African Copperbelt was initiated by continental rifting with subsequent sedimentation which commenced around 880 Ma as recorded by U-Pb zircon ages from the Nchanga granite (Armstrong et al., 2005) generated by the breakup of the Rodinia supercontinent (Unrug, 1996; Kampunzu et al., 2009; Kampunzu and Cailteux, 1999). The intracontinental rift stage evolved into proto-oceanic rift stage from 765 Ma to 735 Ma (Key et al., 2001; Barron, 2003; Barron et al., 2003).

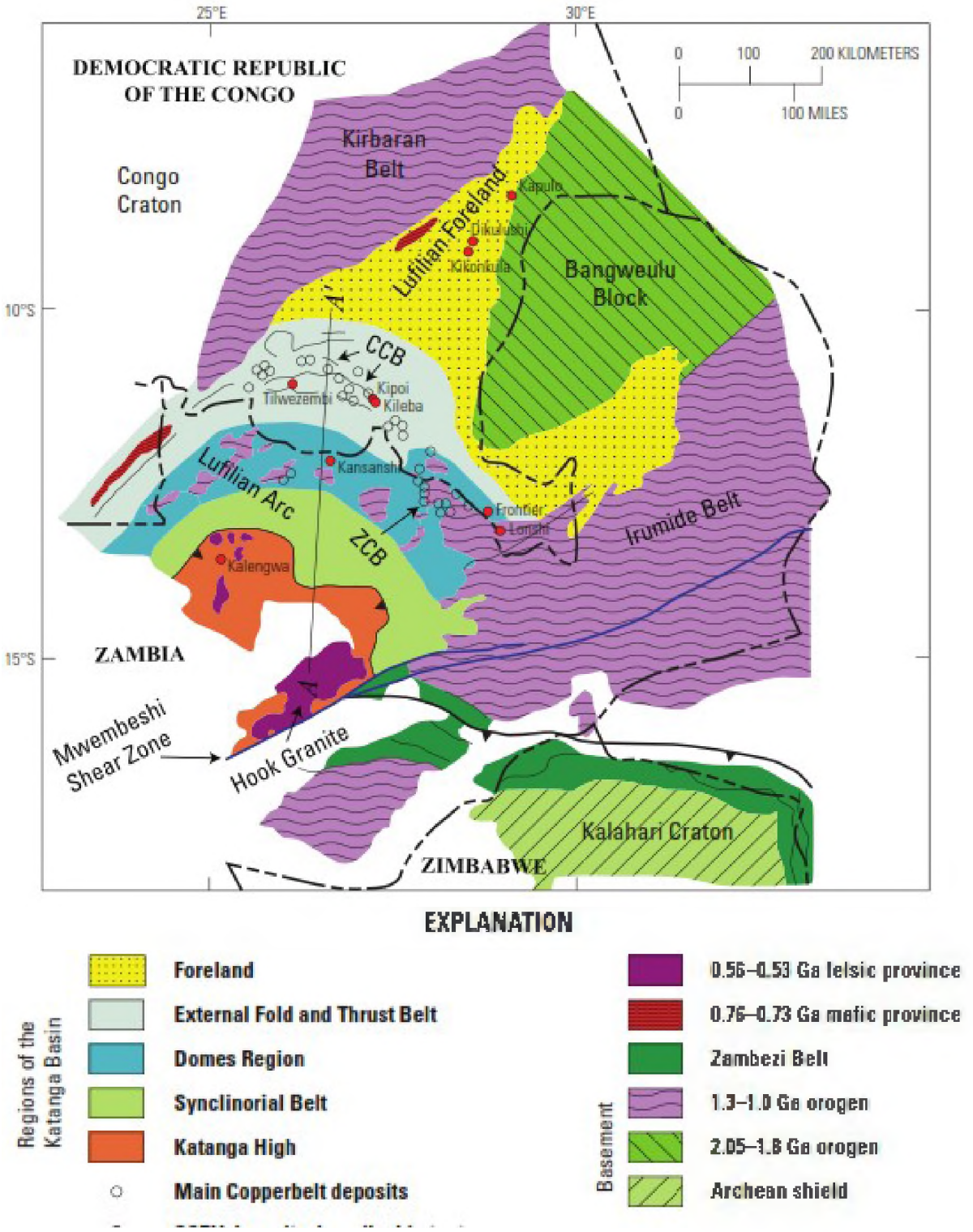

Figure 7: *Tectonic zoning of the Lufilian Arc and showing location of Zambian Copperbelt (ZCB) and Congo Copperbelt (CCB) (modified after Porada, 1989).*

Following deposition of the sedimentary sequences into the basin created by the extensional phase, convergence of the Congo and Kalahari cratons led to subduction of oceanic

lithosphere and resulted in eclogite formation at around 638 to 595 Ma (John et al., 2003; Kampunzu et al., 2009). Continent-continent collision between the Congo and Kalahari cratons occurred at 530 Ma (John et al., 2004; Kampunzu et al., 2009). This collision resulted in northwest and northeast directed thrusting in the western and eastern arms of the Lufilian Arc. Figure 8 shows Katangan rocks that are postulated to have been deformed contemporaneous with basement units.

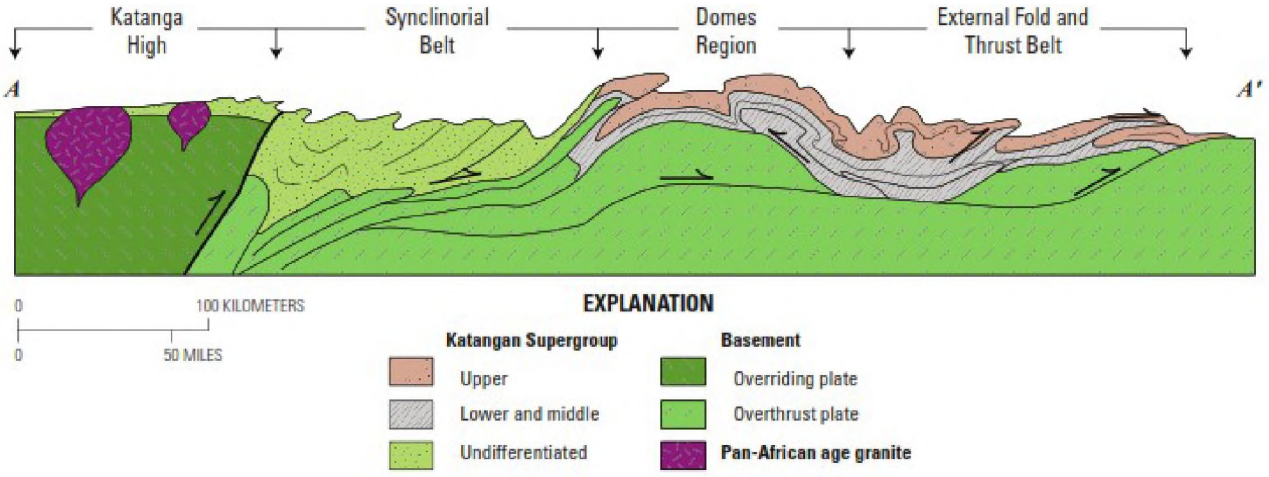

Figure 8: *Schematic cross section of the Lufilian fold belt. The section is drawn from line A-A' on figure 7 (modified from Selley et al., 2005).*

2.2. Lithostratigraphy of the Katanga Supergroup

The Katangan Sedimentary sequence in the Zambian Copperbelt uncomformably overlies basement units comprised of granites and Muva quartzites that form topographically prominent hills and ridges (Drysdall et al., 1972). The Katangan Supergroup is generally agreed to contain four major subdivisions, namely (from base to top), the Lower Roan Group – a siliciclastic dominated succession; Upper Roan – platformal carbonates with chaotic breccia and subordinate siliciclastics; Mwashia Group – carbonates and fine grained siliciclastic rocks; and Lower Kundelungu – glacial diamictites overlain by carbonate and carbonate bearing-clastic rocks (Selley et al., 2005).

The Lower portion of the Lower Roan Group is of coarse red beds overlain by a marine sequence of shale and siltstone with varying permeability and oxidation state. The major ore bodies occur at the top of the Lower Roan clastic sequence or within the basal portion of Lower Roan marine section; particularly in dark, though currently relatively organic poor,

siltstone shale designated the ore shale (Binda, 1994; Cailteux et al., 1994; Hitzman et al., 2005). The Ore Shale represents a regional, probably tectonically controlled, flooding surface (Hitzman et al., 2005).

The Lower Roan Group is overlain by a mixed clastic – carbonate – evaporite strata termed the Upper Roan Group which is distinguishable from the Lower Roan Group by the abundance of carbonate packages (Mendelssohn, 1961). The Upper Roan appears to have contained extensive evaporitic sediments, although according to Selley et al (2005) the evaporites were dissolved leaving only breccia complexes (largely strata bound but in places diapiric) and anhydrite to mark their former presence.

The breccia complexes lie at the top of the Upper Roan Group rocks. Beneath the breccia complex is a repetitive cycle of dolomite, anhydrite, dolomitic siltstone, highly ferruginous carbonates and minor intercalations of brecciated siltstone. Towards the base of the breccia complex lie beds of dolomitic shales interbedded with arkosic polymictic conglomerate and highly sheared amphibolites. At its top, the breccia complex is characterised by highly fractured, vugged and brecciated siltstone/shale followed by brecciated dolomite with abundant polymictic pebbles (clasts) of dolomite, shale, siltstone and amphibolites.

Overall, the Upper Roan Group contains extensive upward- fining cycles of sandstone, siltstones, dolomites, and anhydrite whereas the breccias contains rounded to angular polylithic intraformational fragments supported by crystalline matrix of carbonate, albite, quartz, anhydrite and chlorite (Selley et al., 2005). The known copper-cobalt mineralisation in the Upper Roan Group includes Tenke Fungurume, Kolwezi and Kalengwa (Hitzman et al 2012).

The Mwashia Group rocks overlie the Upper Roan Group which is predominantly a shale dominated sequence that grades upward from a carbonate-rich base to dominantly siliciclastic sequence culminating locally in starved black shale conditions. The Mwashia succession can be as thick as 600m in places dominated by carbonaceous, pyrite-rich shale and numerous mafic/felsic magmatic blocks (pyroclastics/intrusives) (Hitzman et al., 2005). The entire stratigraphic section of the Lufilian Arc is schematically shown in **Figure 9** below.

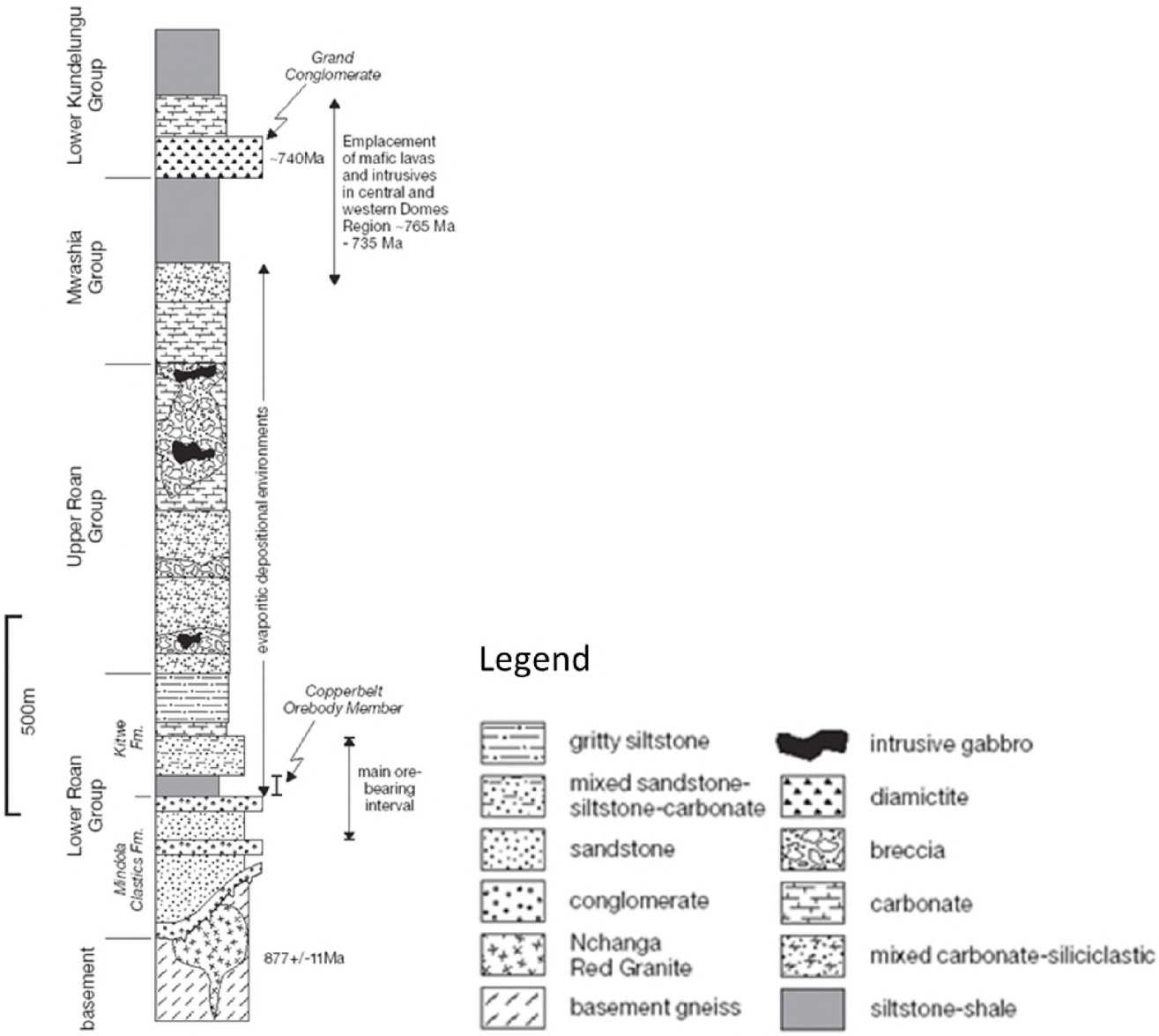

Figure 9: *Stratigraphic column of the Lufilian Belt (After Selley et al., 2005).*

Overlying the Mwashia are the shales, siltstones, glacial diamictites and carbonates of the Kundelungu Group. The basal unit of the Lower Kundelungu Group is the "Grand Conglomerate", a sequence of debris flows and diamictites containing interbeds of laminated siltstone and coarse lithic sandstone (Binda & Van Eden, 1972). An igneous event occurred throughout the African Copperbelt during Mwashia to Lower Kundelungu times that resulted in the emplacement of numerous gabbro sills in association with mafic/intermediate volcanic rocks in the Zambian Copperbelt (765-740 Ma; 1999; Key et al., 2001; Hitzman et al., 2005). A diamictite horizon also characterises the basal portion of the Upper Kundelungu Group and is referred to as the "Petit Conglomerat" which contains clasts of the underlying Katangan

rocks. Deposition of both the "Grand Conglomerat" and the "Petite Conglomerat" is correlated to the world-wide Sturtian glacial episodes during the Neoproterozoic Era. Fairchild and Kennedy (2007) constrains the age of the Sturtian glaciation to within 750 – 580 Ma. A Molasse sequence of dolomitic shales, pink limestones, sandy shales and sandstones make up the rock package of the upper Kundelungu.

2.3. Depositional history and Basin Evolution

The Lufilian basin is thought to have been developed from a hotspot-induced rift system characterized by localised bimodal magmatism which led to deposition of syn-rift clastic rocks involving basal siliciclastics deposited in fluvial environment and shallow marine clastics and carbonates with subsequent development of carbonate platform in slowly subsiding basin (Unrug, 1988; Cahen et al., 1984). The sediments deposited during this phase have a notable chemistry of high magnesium and high salinities in fluid inclusions suggesting presence of brines with high salinity (Greyling et al., 2005). During the initial stage of development the Roan basin was a restricted narrow NW-SE trending lagoonal basin separated from sea by a barrier platform (Unrug, 1988).

The second stage of basin development is thought to have occurred during an advanced phase of continental rifting marked by deposition of Mwashia Group and related magmatism. This supposition is derived from studies of the chemistry of mafic rocks within the Mwashia Group (Unrug, 1988; Wendorff, 2005a). Several meters-thick of volcanic units (basalt and basaltic andesite) belonging to the Mwashia Group have been mapped in Mwinilunga area, north-western Zambia (Key and Banda, 2000). In addition, dating of two gabbroic bodies in the Solwezi area (north-western Zambia) yielded ages of 745 +/- 7.8Ma and 752 +/- 8.6Ma (Barron et al., 2003) making them part of the extensional mafic magmatism associated with Mwashia Subgroup (Kabengele et al., 2003).

Following deposition of Mwashia the next stage involved the deposition of the Lower Kundelungu Supergroup involving a basal diamictite unit which is thought to be approximately 1200 m thick. During this stage banded iron formations and impure sandstones intercalated with diamictite at the same time interleaved with contemporaneous mafic activity sub-aqueously emplaced extensional magmas. The rocks deposited at this stage have E-Morb geochemical character which is interpreted to reflect a transition to

formation of true oceanic crust. Deposition of the Lower Kundelungu marks the maximum extension prior to compressional tectonics (Unrug, 1988; Cailteux et al., 1994).

The last stage of deposition involved the emplacement of Upper Kundelungu Group rocks interpreted to have accumulated during a phase of compression and transcurrent faulting. The Upper Kundelungu rocks consist of conglomerates and sandstones near the basin margin and siltstones and shales towards the basin centre, with over 1000m of arkoses at the top (Unrug, 1982).

There is an alternative view of Lufilian basin development that does not involve significant rifting. Because of lack of magmatism, deep-water rift-related sedimentary rocks and lack of syn-depositional fault systems there is a belief that the basin developed passively where the influence of eustacy outweighed that of slow subsidence rates (Mendelssohn, 1989; Binda, 1994). This model postulates progressive infilling and subsequent flooding of a highly irregular and deeply incised pre-Katangan landscape to account for pronounced facies and thickness variations in the Mindola Clastic Formations, and abrupt transition from a terrestrial to marginal marine systems (Selley et al., 2005).

2.4. Mineralisation Related to Basin Evolution

The Zambian Copperbelt contains many small to giant polymetallic deposits that are predominantly stratiform and stratabound but vein type mineralisation is not unusual (Kirkham, 1989; Key et al., 1989). The bulk of the copper-cobalt mineralisation (refer to **Figure 10**) are hosted in siltstones and shales (Konkola, Luanshya, Chambeshi) or sandstones (Mufulira, Chibuluma) in the Lower Roan Group although copper deposits have been identified in the entire Katangan stratigraphy e.g. post-kinematic vein style mineralisation at Kansanshi hosted in upper Roan to Lower Kundelungu; Kalumbila copper deposit hosted in Mwashia carbonaceous shale; Kamoa (DRC) located in the western foreland in the conglomeratic diamictites of the Lower Kundelungu and even in the basement shear zones as observed at Samba and Lumwana. Mineralisation occurs as disseminations, shear zone hosted, pre-folding vein hosted, post-folding vein hosted and as oxidation-supergene mineralisation (Selley et al., 2005).

Copperbelt deposits have many primary and secondary copper ore minerals (Notebaart and Vink, 1972) but the most dominant ones are simple hypogene minerals which include

chalcocite, bornite, chalcopyrite, pyrite, and carrollite with main gangue mineralogy being K-feldspar, phlogopite, sericite, muscovite, albite, carbonate, quartz, rutile, anhydrite, pyrite, and pyrrhotite (Selley et al., 2005).

Stratiform mineralisation appears to be stratigraphically controlled within the Lower Roan Group siliciclastic and mixed units hosted in the euxitic bituminous-rich rocks of the lagoonal facies. Mineralisation is restricted to stratigraphic interval between basement and carbonate units with carbonate reefs controlling the lateral extent of mineralisation (Fleischer et al., 1976). In stratiform mineralisation there are three main metal associations; Cu-Co-Fe, Cu-Fe, and Cu-Co-Fe-Ni-U-Au-PGE with primary uranium mineralisation occurring below the zone of Cu-Co with which it shares an antipathetic relationship. Metal and mineral zoning defined by chalcocite-bornite-chalcopyrite-pyrite is present at regional scale with the southern Copperbelt rich in Cu-Co-U-Ni; the central zone rich in Cu-Co with decreased U and Ni; and the northern zone having only traces of mineralisation (Unrug, 1988).

Metal zonation observed in the Copperbelt is said to be an effect of higher solubilities of iron-rich sulphides compared to those of copper-rich sulphides during precipitation from copper-bearing fluids (Rose, 1989). Copper-rich sulphides will precipitate out of fluids earlier than iron-rich sulphides which tend to stay longer in the ore-bearing fluid and precipitate farther away from the source during fluid migration. This understanding is used in exploration to interpret and make certain assumptions about the direction of the ore bearing fluid. This metal zonation is observable both in lateral and vertical extents on most Copperbelt deposits at scale of several tens of meters to several kilometres (Mendelssohn, 1961). Metal zonation, and conversely, ore fluid flow appears to have been from east to west (from the Kafue anticline to the west).

Stratabound mineralisation is said to be proto-ores for epigenetic mineralisation associated with the deposition of the Lower Kundelungu Supergroup contemporaneous with mafic igneous activity during the third stage of Katangan basin evolution (Unrug, 1988; Sales, 1962). Sulphide mineralisation occurs as veinlets, stringers, disseminated grains, patches as well as disseminations parallel to and crosscutting the bedding (Selley et al., 2005). Disseminated mineralisation is hosted mainly in sandstones whereas ores of Pb-Zn association are hosted in Lower Kundelungu platform carbonate rocks. However, Cu-Au mineralisation is not restricted to carbonate rocks as they can occur as patches, disseminated

grains or as veinlets. Two main types of mineral associations are common for stratabound mineralisation, namely Pb-Zn-Cu-Ge-Ag-Cd-V (Kipushi, Kabwe) and Cu-Au-Fe- Mo (Kansanshi). Stratabound mineralisation is interpreted to be related to magmatism associated possibly with Kundelungu rifting phase due to mixing of crustal and igneous-related hydrothermal S and Pb isotopes (Unrug, 1988). High geothermal gradients induced by crustal rifting caused convective circulation of metal-rich basinal fluids which reacted with diagenetic pyrite resulting in replacement of Fe by Cu, Co, Ni, Zn, Pb and other metals.

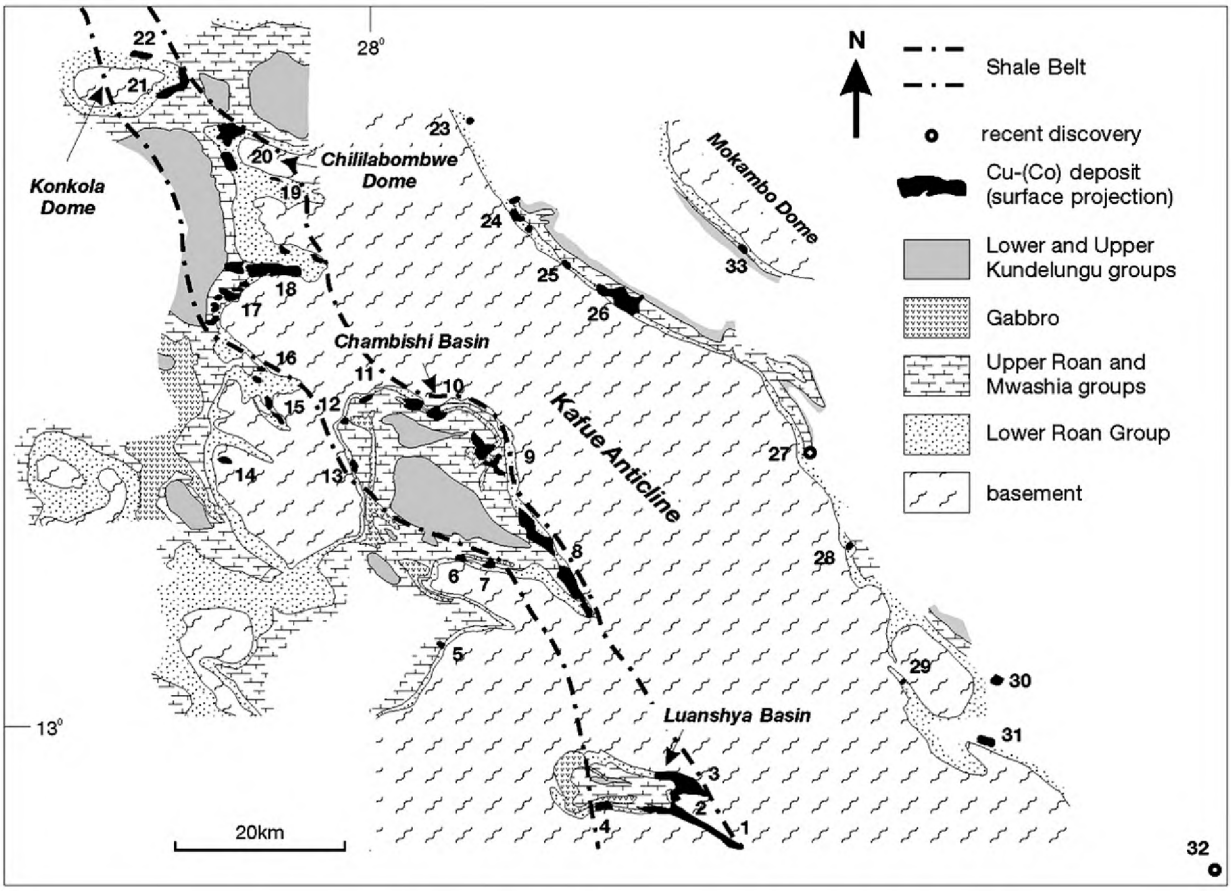

Figure 10: *Schematic illustration of Copperbelt and distribution of Cu-Co deposits in Zambia (1 – 33; from Selley et al., 2005). Deposit 26=Mufulira, 1 = Luanshya, 20 = Konkola, 5=Chibuluma; 10 = Chambeshi.*

2.5. Orogenesis; Structure, metamorphism and magmatism

The current arcuate configuration of the Lufilian belt resulted from a single polyphase orogenic event termed the Lufilian Orogeny. This Pan African Orogeny marked the last period of widespread orogeny and the formation of extensive mountain chains in Africa. The

Pan Africa orogenic event was also an era of widespread glaciation in Africa with glaciogenic deposits appearing in many Pan African belts almost at the same time (Cahen et al., 1984). Interpretations of structural data from the Lufilian belt led Cahen et al. (1984) and Coward and Daly (1984) to conclude that two major deformation phases (D1, D2) of the Pan African Orogeny affected the Lufilian Arc.

The initial deformation phase caused north to north-eastward directed thrusting and folding which resulted in south verging back-thrusting and back-folding involving both basement and sedimentary cover. This deformation phase resulted in tectonic superposition of sedimentary units deposited in different environments and displacement of Katangan units aided by evaporitic minerals in lagoonal facies. Economically significant tectonic breccias and shear zones developed which incorporated mineralised fragments during thrusting and associated fluidization of evaporites. These breccias consist of mega-fragments of Roan Supergroup units including stratiform Cu-Co mineralisation. D1 produced syn-kinematic regional metamorphism with metamorphic isograds broadly parallel to structures and degree of metamorphism increasing from outer zone southwards where white schists and high pressure eclogites have been mapped south of the Domes Region.

The second deformation phase which occurred between 750 – 700 Ma (Porada, 1989) was responsible for the present arcuate shape of Lufilian belt. This deformation phase caused clockwise rotation of the eastern block of the Lufilian belt accompanied by a left-lateral strike slip faulting resulting in escape-block tectonics due to impingement of Kalahari craton into Congo craton (Kampunzu, 1998). Earlier formed D1 structures were refolded in northerly direction during D2 deformation. D2 structures affected younger strata in northwest Zambia and Congo and resulted from northerly directed tectonic movement. Greenschist facies metamorphism is recorded in the external fold and thrust belt whereas in the Domes Region metamorphism upgrade to amphibolite facies.

Lufilian thrusting and folding episodes had an effect of remobilizing stratiform Lower Roan ores concentrating them along phyllosilicate-rich ductile shear zones and within major thrust horizons (e.g., Cu-Co rich ores of Shaba hosted in mega breccias). Proto-ores associated with Kundelungu extensional tectonism were remobilised into epigenetic Pb-Zn-Cu-Ag ores at Kipushi and Kabwe as well as Cu-Au-U-Co-Ni veins at Shinkolobwe, Kalengwa and Kansanshi. Pb-Zn deposits at Kabwe and Kipushi consist of pipe-like orebodies which are

clearly linked to faults. These deposits resulted from successive pulses of hydrothermal fluids which produced several paragenetic metal associations such Pb-Zn-Fe; Cu-Co-Mo and Cu-Ag (Unrug, 1988). In the Domes Region and at Shinkolobwe, in the DRC, uranium-rich polymetallic deposits occur as network of veins in brecciated or sheared host rock with several remobilization cycles of uranium related to successive thermal events.

The Domes Region of the Lufilian Arc comprises many granitic bodies dated between 570-530 Ma (Porada, 1989) and interpreted to be collision-related intrusives which resulted from magmatic events and were accompanied by contact metamorphic and metasomatic processes. These processes formed skarns and hydrothermal vein deposits. Skarn mineralisation is spatially related to small hypabyssal syenitic intrusions with main paragenetic association being magnetite-copper sulphide-phosphate and commonly occurring in brecciated zones in the periphery of intrusions. Hydrothermal mineralisation which resulted from collisional magmatism have metal associations comprising Au-Fe-Cu-Ag-Bi commonly occurring in veins and shear zones especially those related to the ENE-WNW trending Mwembeshi Shear Zone.

2.6. Genetic Models; Origin of Mineralisation

In the last century, many models have been proposed in an attempt to explain the genesis of sediment-hosted copper-cobalt deposits in the Central African Copperbelt – by far the world's most important metallogenic province of this type (Sillitoe et al., 2017). A historical review of the development of metallogenic theories were summarised by Sweeney et al., (1991;). The main questions surrounding the various genetic models centred on the sources of copper and cobalt; the timing of mineralisation; and the physicochemical conditions of metal emplacement (Sweeney et al., 1991).

According to Brown (1997, 2005), emplacement of copper deposits requires the circulation of a low-temperature chloride-rich brine in rift filling footwall red beds, probably driven by meteoric recharge in adjacent highlands. Descending oxygen-rich meteoric water may become saline (either by leaching of footwall evaporites or by mixing with brines draining down from contemporaneous evaporite pans) and evolve toward a moderately oxidised brine as oxygen is consumed during the diagenetic reddening of the initially non-red coarse grained clastic rift sediments. Under these conditions, pore solution attains maximum leaching capability and transport copper from red beds. Sediment-hosted copper deposits may form

where the brine crosses a redox boundary into reduced sulphide-rich grey beds (Brown, 1997).

In the early days of mining, an *early epigenetic, intrusion-related hydrothermal model* for the genesis of sediment-hosted copper deposits was put forward by several authors (Gray, 1929; Bateman, 1930; Davidson, 1931; Jackson, 1932; Sales, 1962; Unrug, 1988). In this model, hydrothermal mineralising fluids were introduced after deposition, lithification and deep burial of the sediments. Hydrothermal fluids originated from deep-seated, subaerial igneous rocks which caused crustal rifting with subsequent leaching resulting in high level penetration or circulation of metal-bearing fluids. This model postulates a source of metals from convective recirculation of hot basinal fluids driven by high geothermal gradients associated with crustal rifting in the Lufilian. It explains the origin of both stratiform and epigenetic mineralisation in two stages of hydrothermal activity. In the first stage pulses of metal-bearing hydrothermal fluids associated with Lufilian rifting in early Kundelungu interacted with primary or diagenetic pyrite, which in this model, was deemed a metal trap causing replacement of iron by Cu, Co, Ni, Zn, Pb and other metals. The next stage involved a second pulse of metal input related to compactional dewatering of the Lower Kundelungu pelites. Hot fluids leached ore metals from mafic volcaniclastics redepositing these in underlying more permeable Lower Roan sediments. This would explain the presence of Ni and PGMs which have mafic volcanic affinities.

When studies reviewed the nature of the granite (Basement) and Katangan meta-sediment contact to be erosional rather than intrusive, the epigenetic hydrothermal model was discredited (Mendelssohn, 1961). In its place, the *Syngenetic (syn-sedimentary) genetic model* gained support (Garlic, 1961; Garlic and Fleischer, 1972; Davis, 1954). In this model, copper was deposited at the same time as the host rocks; the source of metals being from erosion of continents and sediments transportation in rivers in solution as well as adsorbed on clays. The model links mineralisation to sedimentation of the host rocks (Brems et al., 2009). Sulphide precipitation occurred in reductant, stagnant waters with high bacterial activity (Fleischer, 1984). However, this model was rejected for its inadequacy to explain systematic correlation between lateral and vertical sulphide zonation and transgressive-regressive cycles along with mineralisation discontinuities within single lithostratigraphic units (Annels, 1974; Sweeney and Binda, 1994).

The widely accepted genetic models are the *early, intermediate to late diagenetic models* which developed from studies of diagenetic processes in sedimentary rocks (Brems et al., 2009; Sillitoe et al., 2017; Sweeney and Binda, 1989). These models contend that sulphides were precipitated during large-scale chemical reaction of host rock and its pore fluid with metalliferous brine (Bartholome et al., 1971; Annels, 1984; Selley et al., 2005; Unrug, 1988). Copper and its accompanying cobalt or silver were introduced during diagenesis of the host sediments (Brown, 1997; Hitzman et al., 2005). Diagenetic models highly emphasise the role of evaporites and evaporitic brines in the genesis of copper-cobalt mineralisation (Brems et al., 2009). In the late diagenetic model proposed by Unrug (1988) metals were derived from leaching of volcanoclastic fragments contained within Lower Kundelungu sediments.

More recently, *a syn-orogenic model* was proposed by McGowan et al. (2003). This model attempts to explain the genesis of sediment-hosted copper deposits on the basis of structural and petrographical observations only. The model emphasises the importance of late phase of mineralisation/remobilisation related to Lufilian orogeny (Brems et al., 2009) which tend to enrich the orebodies most notably in hinge zones of tight to isoclinal folds. On the basis of field and isotopic data from Nchanga mine, McGowan et al (2003) proposed this syn-orogenic epigenetic model in which metal and sulphate-bearing hydrothermal fluids were introduced into quartzo-feldspathic units during basin inversion, with sulphide derived from thermochemical reduction of sulphate near the sites of deposition.

2.7. Geochemical footprint

Geochemistry has been utilised as a principle exploration tool for discovering shallow mineralisation in the Copperbelt and elsewhere in the region albeit with some challenges due to the regions low topographic relief and extended period of weathering that led to some areas having considerable thicknesses of soil cover in excess of 30 meters (Diederix, 1977). Early prospectors on the Copperbelt heavily utilised geochemical sampling campaigns to discover blind orebodies by pitting, trenching and auger drilling areas with anomalous copper in soil. These early prospectors also realized the occurrence of 'copper clearings'- open areas devoid of trees and grass but awash with small plants with pale blue flowers. Upon experimental investigations seeds of these plants were observed to germinate only in solutions containing greater than 50ppm copper and thrive in soils of over 500ppm copper (Diederix, 1977). The copper flowers (*Becium centraliafricanum/B. homblei*) are copper

tolerant and copper accumulating and do commonly have yellow leaves (Maisse et al., 1978; Brummer and Woodward, 1999).

Orientation geochemical surveys were performed on some of the Copperbelt mines where surface workings did not adversely pollute the natural environment (Salisbury, 1961). The assay method employed at the time was mainly the dithizone-carbon tetrachloride technique which is fully described by Govett (2010). This is a colorimetric method for the determination of small amounts of copper, zinc, cobalt, lead and other elements that occurs in rocks and soils. The dithizone reagent (*diphenylthiocarbazone, phenylazothionoformic acid phenylhydrazide*) was used mostly due to its high sensitivity. Sample digestion was achieved using hydrofluoric-perchloric acid and sodium carbonate with resulting solutions extracted (separation of copper, zinc and lead from most of the other constituents of the sample in the main solution) with a carbon tetrachloride solution of dithizone in a slightly basic medium in the presence of citrate. Thus, copper zinc and lead formed *dithizonates* which dissolved in carbon-tetrachloride whereas the major constituents of the sample remained in aqueous phase. The carbon tetrachloride layer was separated and shaken with dilute hydrochloric acid to dissolve zinc and lead into the aqueous phase leaving only the copper complex in the carbon tetrachloride, which was then evaporated to dryness. The residue was ignited to cupric oxide and dissolved in hydrochloric acid with the copper in solution determined by extractive titration either with dithizone-carbon tetrachloride at acidic pH or by mixed-colour calorimetry with the same reagent in acid solution.

Thus, historical geochemical data generated by the dithizone-carbon tetrachloride assay technique makes it possible to construct comparisons and predicting soil geochemical signatures to be expected in new areas explored for sediment-hosted copper and cobalt mineralisations. One such survey was conducted over the Baluba deposit on the Copperbelt between 1954 to 1959 where both stream sediment and soil samples were collected across and over the sub-cropping mineralised ore shale (lower roan) previously traced by trenching, pitting and auger drilling. Results from this survey revealed copper in soils overlying the orebody to be in the range 200-800 ppm averaging at 460 ppm whilst cobalt in soils of between 20 – 80 ppm. Sharp anomaly peaks were observed even though they were displaced 30-60 m down slope of sub-cropping orebody. Copper-cobalt ratios were in the order of 1:10.

Similar surveys were conducted on the Nkana mining lease particularly on the Mindola N Extension area where the environment had not been disturbed by surface workings. Only values for copper exists for the geochemical survey carried out above the sub-cropping 6 m wide orebody grading at 3.7% Cu and extending for 2 km in strike length. Soil cover of up to 8 m were recorded and leached zone above orebody of between 12 m to 106 m with oxide zone extending a farther 50 m beyond the leached zone to about 150 m. The mixed sulphide-oxide zone extended down to 180 m in this orebody. Copper in soil directly above the sub-cropping orebody ranged between 200 – 400 ppm over areas of the orebody that was relatively un-leached (1-4% Cu) and 100 – 200 ppm Cu overlying areas of sub-cropping orebody that was leached (0.2 – 0.9% Cu) with 50 – 150 ppm Cu range directly above extensively leached orebody (0.05 – 0.2% Cu). Copper values in surface soils closely mimicked leaching patterns in the ore below. Background copper in soils was in the order of 70 ppm with anomaly threshold taken to be roughly 100 ppm Cu.

At Mimbula copper deposit near Nchanga, geochemical sampling was completed in 1958-9 and revealed anomaly of the range 300 – 2000 ppm Cu directly above sub-cropping ore zone. Stream sediment sampling from headwater dambos draining the mineralised area attained copper values ranging between 1000 – 10,000 ppm and cobalt values ranging between 13 – 800 ppm (0-90 cm below surface) and 7- 45 ppm Co collected at 5 m below surface giving a copper-cobalt ratio of roughly 1:12.

At Nchanga overlying the sub-outcropping Dambo Lode area near the copper clearing peak copper values attained were in the order of 5000 ppm with soils overlying banded sandstone reporting average values of 350 ppm copper about 200 m south of the main orebody. Background values ranged between 50 – 80 ppm copper.

Elsewhere on the Copperbelt geochemical surveys in the late 1950s established background and anomalous values of copper and cobalt in freely drained soils. For example at Luansobe, northwest of Mufulira, anomalous range of 150 – 400 ppm Cu over 300m-thick deeply leached soils overlying ore mineralisation with 25 - 100 ppm Cu established as background. Similar ranges were obtained in Lufubu North on soils overlying sub-outcropping ore (200 – 550 ppm Cu anomalous) with background values in the range 30 – 75 ppm Cu. Anomalous cobalt range overlying orebodies was established to be between 20 – 80 ppm with background values in the range 7 – 14 ppm. As long as the peneplane topography was flat

anomaly peaks directly overlain sub-outcropping mineralisation. In sloping landscape cobalt anomalous values decreased rapidly to background upslope from mineralisation for short distances of up to 60 m whereas down slope anomalous values tended to extend farther, to up to 550 m.

A complete list of soil geochemical backgrounds and threshold values over Copperbelt deposits for geochemical surveys performed in the 1950s were compiled and reported in Salisbury, (1961). These tables are reproduced in this document as **Table 1** and **2** below. In recent times, modern studies on Copperbelt deposits have established geochemical fingerprints in terms of mineral associations, major elements and minor ones (McGoldrick et al., 2003). These associations are well entrenched in the minds of Copperbelt explorers and are extensively utilised in the search for similar styles of sediment-hosted mineralisation. Copperbelt deposits and occurrences have the following distinct mineral associations: Cu, Co, Zn, Pb, Ag, Ni, Ba, (Mo, V, U, Re, Ge). Potassium and barium enrichment often accompany copper deposition (Hayes, 1990; Sutton and Maynard, 2005).

Copper is a very good pathfinder element in soils and stream sediment sampling for sediment-hosted copper deposits in diverse weathering and climatic conditions. Cobalt, silver, antimony, arsenic, barium, mercury and on rare occasions, vanadium, molybdenum and uranium are also used as pathfinders for sediment hosted copper.

Table 1: *Range of background, threshold and probable anomalous copper values for freely drained soils in the vicinity of various ore zones of the Copperbelt (modified after Salisbury, 1961).*

Locality	A Zone Peak (B-horizon)		Background		Threshold (ppm)	Statistical Anomaly (ppm)
	Range (ppm)	Average (ppm)	Range (ppm)	Average (ppm)		
Nkana/Mindola	60 – 390	210	15 – 80	50	70	100
Baluba	200 – 800	450	30 – 100	70	100	150
Chambeshi	150 – 600	340	20 – 100	50	75	150
Mimbula	250 – 500	300	30 – 120	80	150	200
Nchanga Dambo Lode	5000	5000	80 – 100	100	150	200
Nchanga N Limb	120 – 150	125	35 – 50	50	80	120
Bancroft S Orebody	150 – 180	160	10 – 100	50	75	100
Fitwaola	90 – 150	120	15 – 60	35	55	75
Konkola E	80 – 120	100	20 – 60	40	50	75
Konkola W	-	-	10 – 50	25	-	-
Chibuluma	100 – 150	120	25 – 70	40	70	100
Fitanda	70 – 150	120	30 – 60	50	70	100
Bwana Mkubwa	70 – 150	120	10 – 70	30	65	100
Nkana S Limb Orebody					70	100
Mufulira W	150 – 250	200	25 – 100		75	120
Luansobe	150 – 450	250	25 – 100	50	100	150
Nchanga Lamprophyre dyke	250 – 375	300	30 –50	60	75	100
Fipimpa	300 – 2500	500+	20 – 120	80	150	200
Lufubu South	150	150				
Lufubu North	200 – 550	300	30 - 75	50	100	150

Table 2: *Cobalt dispersion data in near-surface freely drained soils over different rock types in background areas on the Copperbelt ((modified after Salisbury, 1961)*

Bedrock type	Horizon	Depth (m)	Range (Co_ppm)	Average Background (ppm)
Lufubu Schist (Baluba)	A1	0 – 1	3 - 5	4
	A2	1- 6	2 - 7	5
Lufubu Schist (Solwezi)	A1	0 – 1	3 - 8	5
	A2	1- 6	7 – 13	10
Granite (Mimbula)	A1	0 – 1	5 – 13	6
	A2	1- 6	7 – 14	10
Granite (Solwezi)	A1	0 – 1	6 – 10	7
	A2	1- 6	7 - 10	8
Mwashia Shale (Solwezi)	A1	0 – 1	10 – 15	5
	A2	1- 6	10 - 20	6
Gabbro (Chambeshi)	A1	0 – 1	25 – 40	13
	A2	1- 6	25 - 43	15

3. LOCAL GEOLOGY

3.1. Regional Setting

The study area lies in the Domes Region of the Lufilian fold belt, an arcuate zone of basement inliers whose cores consists of migmatised gneisses and amphibolites of the Wamfumbu Gneiss Complex (Klinck, 1977) which are in turn enveloped by meso-proterozoic Muva Supergroup quartzites and overlain by Katangan rocks. Tectonics within the Domes Region were characterised by deep and shallow level thrusts which culminated in extensive hydrothermal modifications of both basement and sedimentary cover. Study areas are located south of the Mwombezhi, and southeast of the Kabompo Domes (**Figure 11**). These areas are in a well-known mineral district which hosts the Lumwana copper, Sentinel copper and Enterprise nickel deposits. Sentinel and Enterprise have published measured and indicated resources of 1027.3Mt at 0.51% Cu and 40.1Mt at 1.07% Ni respectively.

Nyungu prospect, located a few meters to the northeast of the study area, was investigated in the late 1980s following up on soil geochemical anomaly of above 500 ppm Cu. Two holes spaced 450 m apart were drilled which intersected zones of mineralisation grading at 1.66% Cu over 3.4 m and 1.1% Cu over 8 m (Freeman, 1988). This prospect was re-investigated this prospect in the early 2000s by Anglo-American Corporation who, upon sinking scout drill holes, confirmed multiple lenses of low-grade mineralisation over a minimum N-S strike extent of 800m. Copper mineralisation was shown to be associated with cobalt, uranium and gold. For example, one reverse circulation drillhole intersected 47 m at 0.56% Cu with 0.19% Co, 0.48 g/t gold and 252 ppm U (Woodhead, 2001).

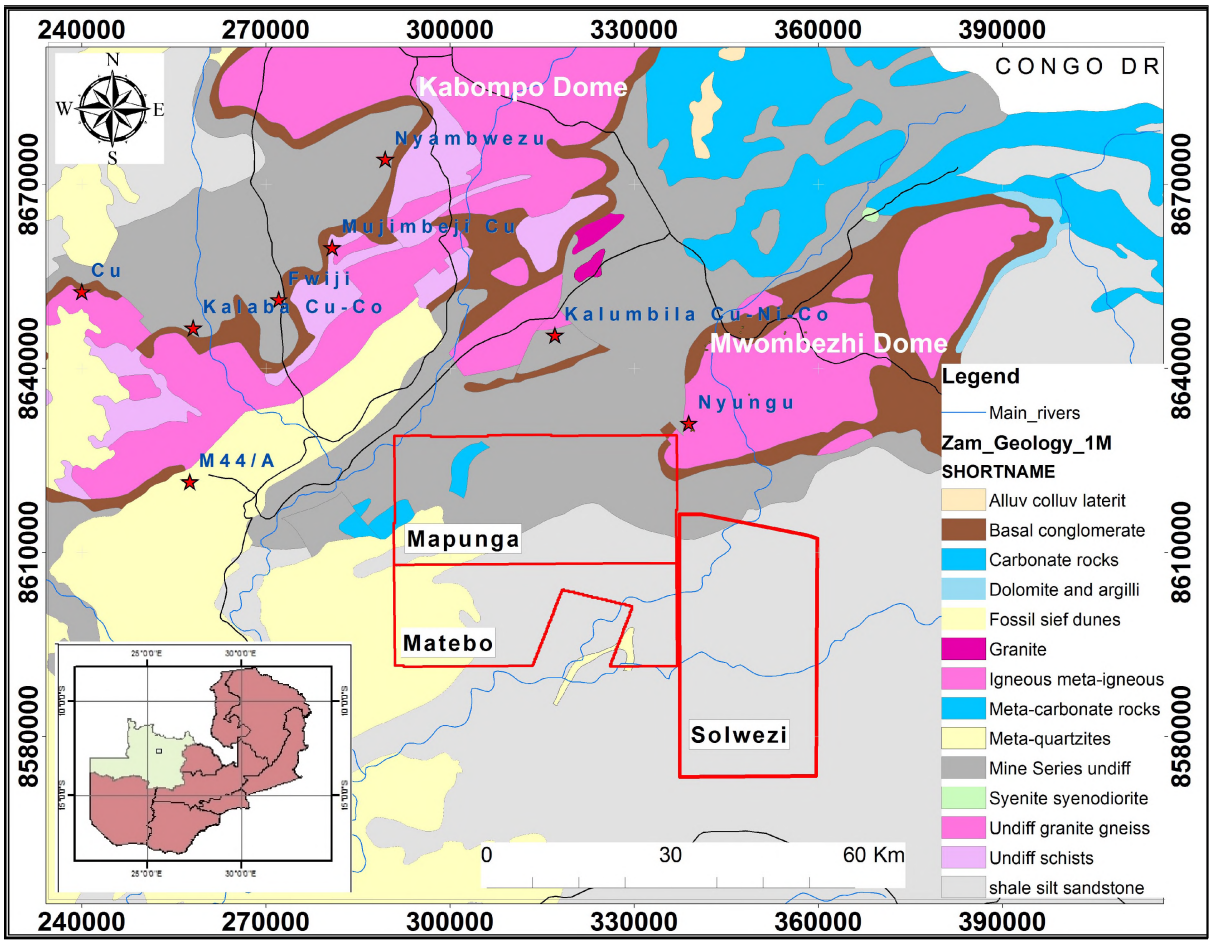

Figure 11: *Regional Geology Map of Zambia showing location of study area (Mapunga, Matebo and Solwezi) along with Sentinel (Kalumbila) and Nyungu prospects.*

3.2. Local Geological Setting

The study areas are covered by northeast trending basement biotite-scapolite-hornblende gneisses, migmatites and amphibolites that are overlain by aluminous schists, magnesium-rich talcose schists, white quartzites and minor quartz pebble conglomerates of the Wushingwi Formation at the base of the Katangan Supergroup. According to Klinck (1977), the Wushingwi Formation is correlated to the *Lower Roan Group* of the Katanga Supergroup. These rocks tend to form prominent ridges in the area (Steven and Armstrong, 2003). Overlying the Wushingwi Formation is a sequence of scapolite-biotite schists, granofels, biotite-carbonate-kyanite-garnet schists, meta-sandstones and various marbles belonging to the Wamikumbi Formation which is correlated to the *Upper Roan Group*. Succeeding the Wamikumbi Formation is another sequence of schists (biotite-scapolite-actinolite-garnet-carbonate) and arenites belonging to the younger Luigishi Formation, a correlateable

equivalent of the *Mwashia Group*. Overlying the Katangan rocks are the unconsolidated Kalahari sands of the Zambezi Formation (Klinck, 1977).

The geology map of Mapunga and Matebo (**Figure 11**) was compiled at a scale of 1: 250, 000 by Appleton (1978) and first published in 1984. On this map, (**Figure 12**), fine and coarse grained biotite gneiss and migmatites of the Basement Complex cover the top right corner of Mapunga area. These units are overlain by a small sliver of Lower Roan unit which is characterized by talc-kyanite-hematite quartzite and phlogopite schist. The Lower Roan unit is succeeded by biotite garnet schists that coexist with graphitic rocks and marbles of the Upper Roan. Overlying the Upper Roan are the psammitic biotite schists of Mwashia age. Lower Kundelungu rocks and unconsolidated Kalahari supergroup sands of the Zambezi formation cover the lower part of the study area. Kundelungu rocks are characterized by calcareous, dolomitic, plus non-calcareous meta-argillites and quartzites. In the southwest corner of the map the Katangan rocks are covered by loose sands whose thickness increases westwards.

Rock outcrops are few in the two areas and are mainly exposed in stream beds and in places where pitting and trenching have taken place. Laterite exposures are widespread covering discontinuous patches of ground made up of pisolitic brown soils devoid of any vegetation. A few insitu boulders of granites and mafic rocks were mapped during soil sampling campaigns and these coincided with what Appleton (1978) referred to as diorite intrusives on his 1984 1: 250,000 geology map of Ntambu Area, NW Zambia (red unit sitting on NW-SE trending structure on **Figure 12**).

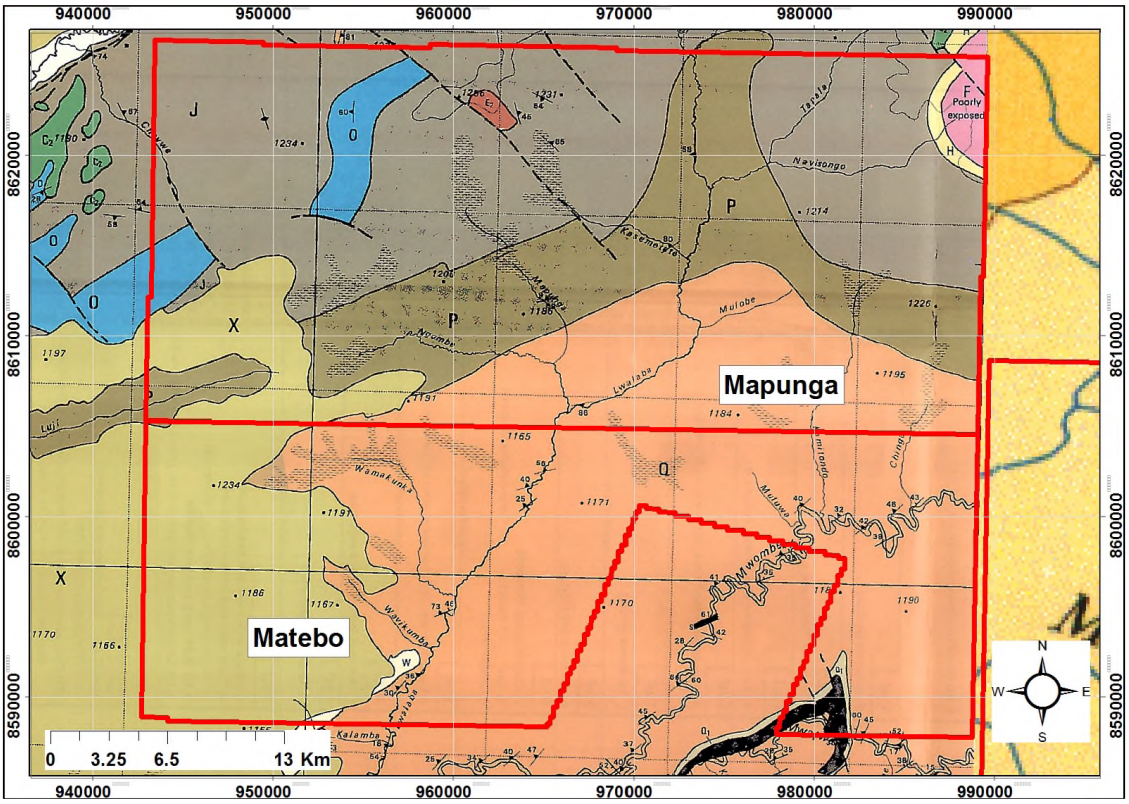

Figure 12: *Geology Map of Mapunga and Matebo, 1: 250, 000 scale. Pink unit at top right corner (F) =Basement; Unit P (brown) = Mwashia, unit Q (orange) =Lower Kundelungu; Unit X (yellow) = Kalahari sands.*

The adjacent licence area to the right of Mapunga-Matebo areas **(Figure 13)** was mapped between 1977 and 1980 at a scale of 1:100,000 (Loughlin, 1978). In producing this geology map, heavy reliance was placed on aerial photo interpretations, regional airborne magnetics, reviews on published Copperbelt literature and field traverses mainly along streams and rivers where scarce rock exposures could be found. All the rock outcrops in the area are ascribed to the Katangan Supergroup sequence and correlated to the well-known Copperbelt geology.

The oldest rocks in the area are the carbonates of the Chafugoma Marble Formation equivalent to the *Mwashia Group* of the Copperbelt. These carbonates are fine-grained, dark grey, very hard and dense. They are well exposed along the Mushingashi and Mwafwe rivers where fine-grained massive to well-laminated calcareous siltstones, and silicified shales occur in abundance. These calcareous siltstones and silicified shales are ascribed to the overlying Kundelungu Group dominated by thinly banded siliceous ironstones, calcareous siltstones, para-conglomerates and strongly silicified shales. Floats of ironstone occur in abundance in the area, they possibly represent sub-outcropping, discontinuous iron-rich

bodies. River exposures of siltstones and silicified shales occupy areas of low magnetic frequencies and have shallow dips to the north appearing to represent series of recumbent anticlines (Loughlin, 1978).

The Solwezi Licence area is entirely covered by Kundelungu metasediments with only a small central zone covered by river exposures of dark grey dense and moderately magnetic Mwashia marble (**Figure 13**).

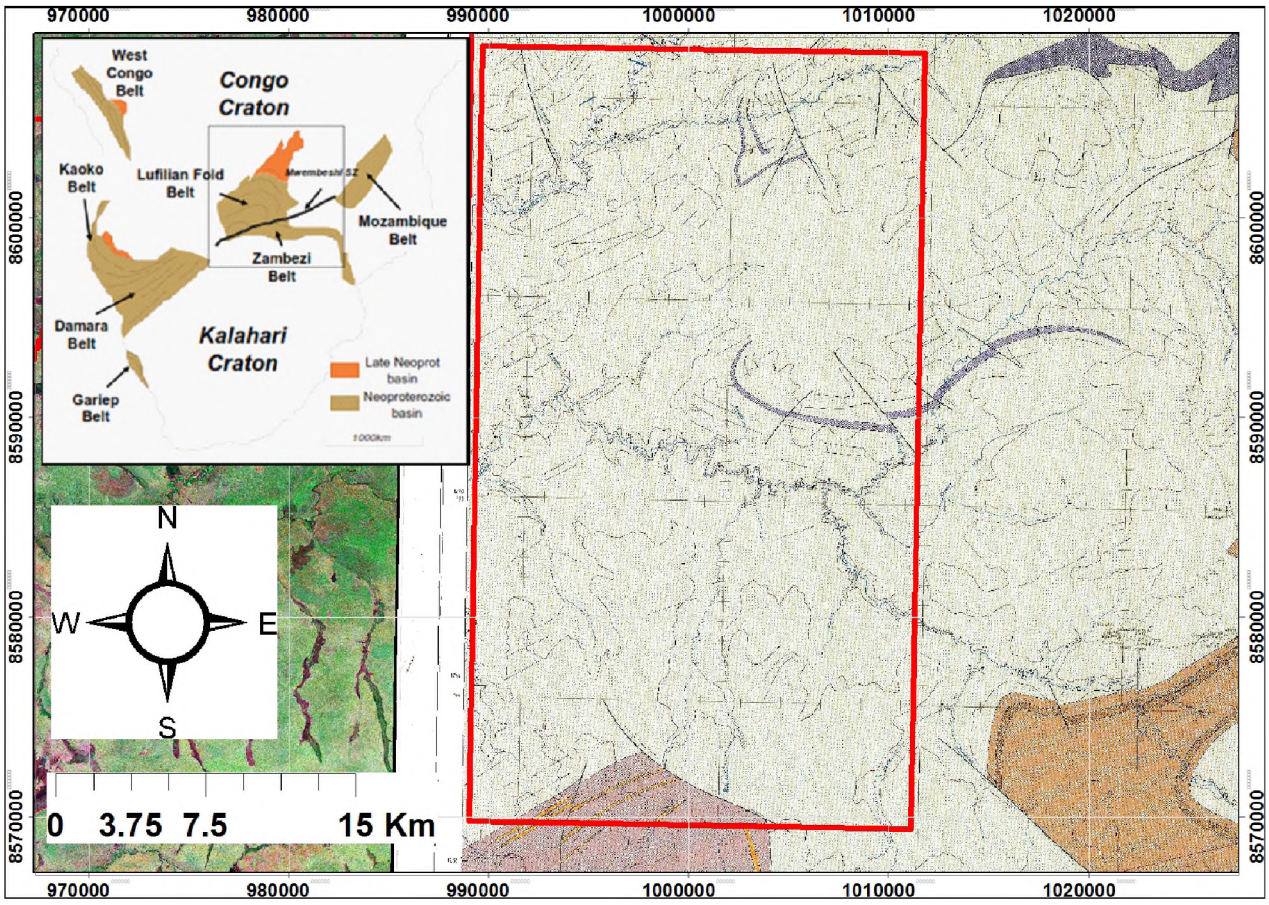

Figure 13: *Geology Map of Solwezi tenement (1:100, 000; after Loughlin, 1978). Kundelungu rocks cover whole area save for Mwashia grey marble (centre) and undifferentiated mine series rocks at the bottom.*

4. OVERVIEW OF EXPLORATION GEOCHEMISTRY

Exploration geochemistry has been used to locate mineral deposits for many decades since scientists discovered that soils overlying sub-outcropping mineral deposits are enriched in those elements constituting the deposit and that this enrichment is sufficiently different from the soil chemistry of the area surrounding the deposit (Moon et al., 2006). The difference between the geochemical features of soil overlying the deposit and the surrounding area is termed a geochemical anomaly whilst the chemistry of surrounding soils is termed the background or containing "normal" concentrations.

In mineral exploration, exploration geochemistry is therefore, focused on identifying anomalous metal concentrations in surface materials and establishing whether these anomalous levels relate to weathering and element dispersion from a buried orebody. Exploration geochemistry is used to locate sites of buried mineral deposits having no obvious visible surface expression. Once these sites are pinpointed, other exploration techniques (e.g. geophysics, pitting, trenching and ultimately drilling) can be applied to test the assumption that anomaly is related to secondary orebody processes.

4.1. Scientific Rationale

Geochemical exploration hinges on the premise that metal ions or elements of particular metals are mobile under certain physical or chemical conditions. These metal ions- or elements will move from their source to a given sample point thereby enhancing the concentration of that element beyond its crustal abundance at that point which then allows for its detection if that sample point is tested.

Groundwater plays a key role in dispersing metal ions and forming concentration halos which decrease in intensity with increasing distance from the source. These phases form either by reaction with oxygen (oxidation), reaction with water (hydrolysis) or acid action (reaction with acidic substances – formed when CO_2 dissolves in water). Metal ions adsorb onto clays which have high ion-exchange capacities; adsorb onto goethite; form complexes with organic material; or collect onto pedogenic carbonates (Bau, 1999). Pedogenic carbonates are secondary materials consisting of authigenic carbonate-developed locally within soils rich in calcium carbonate and usually formed in shallow transported soil horizon typically in arid and semi-arid climates. In residual soils, we sample mineralised but decomposed material

whose geochemical signature is *in situ*. In transported material the geochemical signature must have been added to the media by post mineralisation events.

4.2. Methods employed

Most geochemical surveys target stream sediments, termite mounds or soil as a sampling media. If soil is chosen as sampling media, it must be determined whether it developed in situ or was transported from another location. This can be done by digging a shallow pit and mapping the soil profile. Most soil profiles have a thin layer composed of quartz fragments usually called the stoneline. If the stoneline holds a large proportion of rounded quartz fragments compared to angular ones, there is a good chance the soil is a transported soil.

Stream sediment sampling involves sampling sediments in the bed of a watercourse and analysing either finer or coarser sieved fractions depending on target mineralisation (i.e. finer seized fractions for copper and coarser sieved fractions for gold). With stream sediment sampling care must be practiced to take samples from the same medium; from the bed of the stream and not mix with those samples from the banks of the stream as these might be of different age and composition (Ryan et al., 2004).

Most often, stream sediment sampling is employed to identify potentially prospective districts rather than to identify individual deposits or groups of deposits. Such surveys are multi-element and multi-commodity in approach rather than targeting specific commodities or styles of deposit (Anand et al., 2014). Compared to a soil sample, stream sediment represents a greater area of coverage and has different backgrounds and threshold abundances for each element. It is for this reason that stream sediment sampling is nearly always followed up with soil sampling to pinpoint locations of buried deposits.

Soil sampling is routinely performed on residual soils and rarely on transported soils unless analytical methods such as Mobile Metal Ion (MMI) and specialised interpretive skills described in Anand et al. (2009) are readily available.

Termite mound samples represent an alternative sampling media in areas where surface soils are suspected to have been diluted by windblown barren sand (transported material), in dambos or in areas where termite mounds have broken through a lateritic duricrust and brought residual material to the surface. Only those termite cathedrals larger than 1m in height are sampled and these must be widely distributed throughout the sampling grid at

sufficient density to be of use. Termite mounds are thought to be residual soil brought up from considerable depth, up to 30-40 m in Central Africa and greater than 200 m in Botswana (Tooms and Webb, 1961). The material is generally very fine-grained with little to no coarse material being carried onto the mounds by the termite, reflecting the carrying limits of the termites.

4.3. Usefulness of geochemistry

Geochemical exploration is a powerful tool for narrowing down the search area in mineral exploration. Critical to the sampling process is knowledge of target deposit style(s) being sought, for this will not only determine the assay technique to be employed and what elements to be included in the assaying package but also what sieved sample fraction would provide the most geochemical response. Knowing pathfinder elements and understanding other metals associated with specific deposit styles prove very useful in interpreting geochemical results.

For geochemical data to be meaningful, appropriate layers in the regolith profile must be targeted making sure that all samples are taken from a common horizon throughout the sampling campaign. Sieved sample fractions that give the best geochemical response are selected based on results of orientation sampling conducted usually at the beginning of the sampling campaign or chosen based on recommendations from either literature or historical geochemical surveys. Appropriate analytical techniques recommended for specific deposit styles whose assays are sufficiently precise and accurate must be employed in order to detect anomalies. Apart from knowing what elements to assay for it is equally important to know approximately what concentrations are expected in the sampled environment.

Many published works exist that explain the theory of geochemistry with a bias on sampling theory and detailing sampling procedures and protocols relevant to mineral exploration. The most complete explanations on the subject can be found in Levinson (1974) and Rose (1989).

4.4. Identifying geochemical anomaly

Once the data is received from the analytical laboratory, the accuracy and precision of the assays must first be assessed. This is done through the use of control samples submitted (preferably "blind" i.e. not identified) with the survey samples: control samples include blanks (material not known to contain the metal of interest) to check for contamination during

sample preparation and laboratory background (contamination of machines, reagents, etc.); duplicates to assess precision and certified standards to check for accuracy of results.

Once the quality of the assays has been established, one needs to domain samples according to the lithology they overlie (if it is known) since different rock types will produce different background and anomaly thresholds. For example, areas underlain by gabbros will have high copper backgrounds compared to areas underlain by sandstones. If this is not taken into account, particularly in interest areas underlain by both sedimentary and mafic rocks (i.e. sandstones and basalts/gabbros), low geochemical signature deposits in sandstones might be overlooked as background due to high copper contribution from mafic area to the background concentration. Grouping the data into geochemical domains may also be defined by alteration, regolith type or topography of the sampled area. Of utmost importance is to have large, representative datasets for each domain.

Anomaly thresholds are conventionally determined using non-parametric statistical methods. Common methods most often employed for anomaly threshold definition include: 1) literature comparison, 2) standard deviations, 3) histograms, 4) log probability, 5) spatial analysis and 6) orientation survey comparisons. Literature comparisons are done with average abundances (or range) of selected minor and trace elements in various natural media (Levinson, 1974) or with characteristics of the known deposit style being sought. Standard deviations, histograms and log probabilities are generated from manipulation of the geochemical datasets. Spatial analysis is achieved by plotting geochemical data as point assays or graduated symbols on either geological (i.e. lithology, structural, regolith) or geophysical (i.e. magnetics, gravity, electromagnetics) map backgrounds and determining prospective areas based on physical location and prior knowledge of target deposit characteristics. Orientation survey comparison involve establishing a geochemical profile of known deposit by running 2 or more sampling lines across the deposit and comparing the assays with the assays from unknown target area.

In this study, the first 5 methods of anomaly threshold definition are used, with particular emphasis on literature comparison, spatial analysis and standard deviation. The minimum anomaly threshold used as the first order anomaly is defined by nearly 4 times the standard deviation, which coincides with the 95^{th} percentile of the sample population of the domain.

5. METHODOLOGY

This study aims to assess the potential for detecting and defining Cu-Co deposits in the study areas using soil geochemistry as a primary assessment tool. In this chapter an outline of soil sampling protocols is given along with procedures put in place at both sampling and analytical stages to ensure data quality. Selection of the soil sampling method was based on past experiences at Kansanshi, Lumwana and Kalumbila deposits where the technique worked successfully in highlighting geochemical contrast between the deposits and surrounding non-mineralised areas.

5.1. Grid Spacing and Orientation

Soil sampling over the study areas was designed with the sediment-hosted-stratiform, Kansanshi vein-type and the Lumwana basement type mineralisation models in mind. Soil sampling grids were designed at regional scales of 2000m x 200m and 1000m x 200m with grid orientation based on regional geology and/or aeromagnetic trends. This grid spacing was selected based on cost considerations and the requirement for at least 2 samples to fall in the anomaly. Areas that showed elevated copper concentration detected by handheld XRF (HHXRF) were revisited and resampled to verify those elevated values. When verification sampling confirmed results of the first sampling, infill grids were designed in those areas at tighter spacing 500m x 200m).

Known geological and aeromagnetic information indicated an east-west trend to the geology: as a consequence the sampling grid lines were aligned North-South (**Figure 14**). In a few instances where anomalous soil geochem appeared to crossing prominent lineaments infill grids were re-orientated to transect those lineaments at right angles.

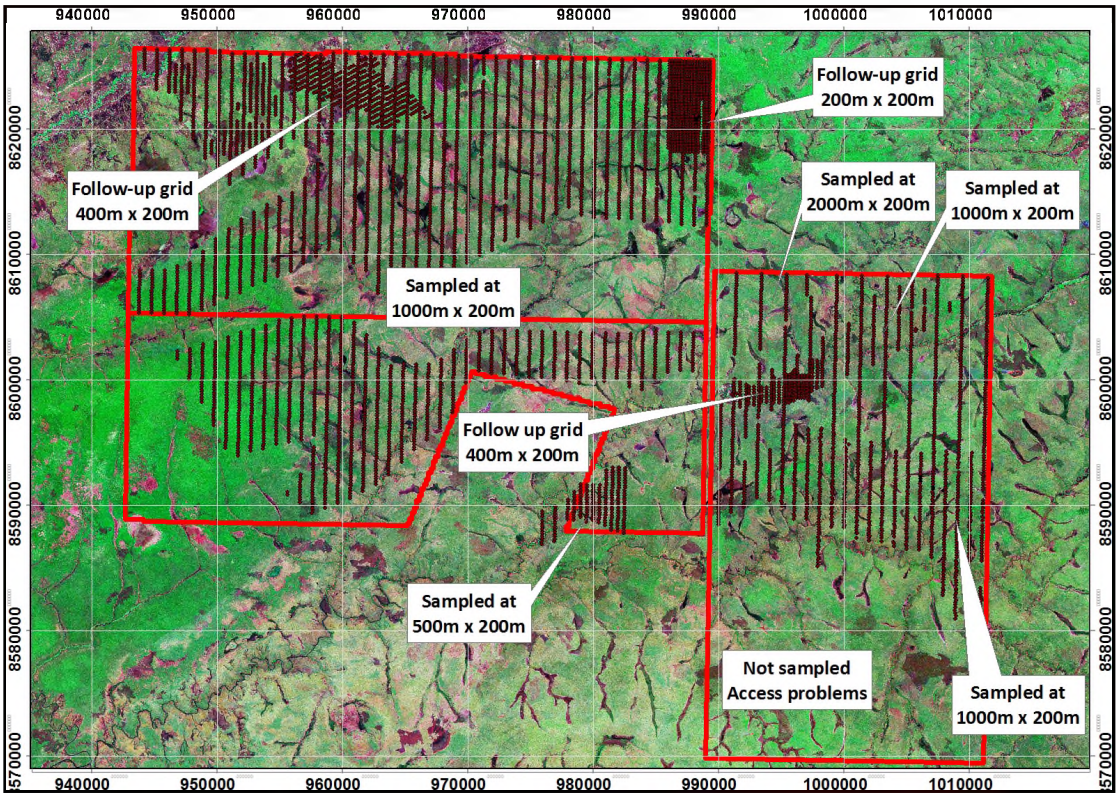

Figure 14: *Satellite image of the study areas showing the extent of the sampling grids together with orientations.*

5.2. Sample Collection and Handling

Prior to commencing sampling, a 140 cm deep orientation pit was dug with the view to expose the full soil profile and determine the best horizon for sampling. Three horizons were recognised in this pit; a top 10 cm thick grey layer made up of organic debris (humus, dead plants and partly decomposed plants), a 55 cm thick yellowish layer comprised of fine clay soil with abundant plant matter (roots), and the bottom 75 cm of brown ferricrete. Between the clay zone and the ferricrete there was a 17 cm thick band of pisolitic soil which gradually tended to ferricrete downwards. This band contained few subrounded quartz grits, iron concretions (pisoliths) and minor pebbles (stoneline).

The orientation pit was assessed using a HHXRF spectrometer to analyse three samples; one taken near the top of the clay zone, one near the base of the clay zone and the third sample from the laterite horizon (**Figure 15** and **Table 3**). These samples were sieved to minus 180 microns before assaying. This study showed that the sample from the base of the clay zone (B-horizon) gave a higher geochemical response of 85 ppm Cu compared to 38 ppm Cu in the

upper sample and 76 ppm Cu in the ferricrete sample. On the basis of these results, and the general knowledge that most Copperbelt geochemical anomalies were detected using the minus 180 micron size fraction of soil samples, it was decided to use this fraction in the exploration exercise.

Figure 15: *Orientation pit used to check optimal soil horizon for sampling.*

Table 3: *Layers in orientation pit with respective XRF Cu concentrations*

Depth (cm)	Description	Cu_ppm
0 - 10	Organic debris; humus	Not tested
10 - 65	Clay soil	85
65 - 82	Pisolitic Soil	38
82 – 140	Ferricrete; duricrust	76

Soil and termite mound sampling was conducted in two sampling campaigns; one in August 2012 and the second between May and August of 2013. The two campaigns collected 7613 conventional soil samples and 840 termite mound samples for a total of 8453 samples. Predetermined grid sampling points were located in the field using hand-held GPS. All locality data was determined using WGS84 datum and UTM Zone 35S projection. Sample locations were stored in the GPS, and recorded on sample log sheets along with other

important sample attributes such as: soil colour, soil condition (dry, moist, wet), landscape setting (hill slope, valley, dambo, vegetation) to aid later interpretations.

At each sample point, a 50 cm radius area was cleared of organic debris prior to digging a 35-70 cm deep sample pit into the B-horizon of the soil profile. Digging was done with a mattock and a plastic scoop used to collect the sample. Samples were collected at base of the pit after removing any fallen debris. Samples were approximately 4 kg in size and stored in labelled plastic bags with sample identification tags inserted and attached to the bags. In some cases, particularly where sample pits fell on slightly elevated terrains characterised by very hard ferruginous saprock with abundant quartz fragments (possibly eroded ridges), samples were pre-screened with a 2 mm stainless steel sieve in the field and -2 mm fractions bagged for further screening at the field camp. This was done in order to increase the size of fine portion of the sample. This pre-screening was performed on approximately less than one percent of the total samples collected in the campaign.

In the field every 20th sample was duplicated by collecting a fresh sample a few centimetres proximal to the 'original' sample. A fresh pit was dug very close to the parent hole and a new sample collected from the same horizon in the soil profile as in the parent hole. One would argue that this was not a typical duplicate sample but we know that even in the same sample pit collecting samples at different depths in the same soil horizon can produce variances in metal concentrations.

The bulk sample collected in the field, weighing approximately 4 kg, was sieved using a 180 micron aperture sieve to produce roughly 500 g of -180 micron sample fraction. The -180 micron sample was split into two, one half was for analysis and the other retained as a reference along with the +180 micron fraction. In some instances the -180 micron sample was not sufficient for splitting: in those cases only the +180 micron fraction was retained and the entire -180 micron sample used for analysis. Splitting was done by simply dividing the sample into two halves without using the riffle splitter since sieved sample fractions were usually not large enough to be split without bias on the Riffler (**Figure 16**).

Prior to laboratory assaying all samples (termite and soil) were first tested by HHXRF spectrometer, a cost cutting procedure that ensured that only those samples from promising areas were sent to the laboratory. The practice furthermore enabled quick decision making in

the field regarding where to add infill sample lines to better define and identify anomalous zones.

Figure 16: *Sample size collected in the field. (A); average bulk sample with smallest sieved sample size; (B); smallest sieved fraction could not be spilt by Riffler without bias.*

Termite samples were collected only on termite towers of greater than 1 m height. Four samples were taken on opposite sides of the mound: north, south, east and west; at a height approximately halfway up the mound. These four sub-samples were subsequently combined into one sample and bagged ready for analysis.

5.3. Field Analysis Procedures – Handheld XRF

Field analysis of termites and soil samples were performed using an Olympus Innov-X HHXRF spectrometer, a device that determines the elemental composition of a material by identifying elements in the material and quantifying the amounts present of those elements. This spectrometer is programmed to perform a 15-second calibration run at initial device start-up to check its hardware conditions. No sample testing can be run without successfully completing a calibration check, which is done either within the docking station accompanying the spectrometer or by shooting a x-ray beam through a standard calibration coupon that is supplied with the device. Calibration checks were performed every 4 hours even though the instrument manufacturer recommends performing calibrations once every 10 hours. Check standards were measured immediately following calibration checks.

In addition to testing the spectrometer with standards provided by the manufacturer, certified reference materials (CRMs) from laboratories were used at a rate of 1 in 20 samples; results of which were checked against standard assays before proceeding with further sample tests.

Since testing was accomplished by placing HHXRF spectrometer against the sample bag, it was important to routinely clean the measuring window of the instrument to remove dust.

Measurements were done in 3-Beam Soil mode set to read the following 30 elements by default: K, Ca, S, P, Cl, Ti, V, Cr, Mn, Fe, Co, Ni, Cu, Zn, W, Hg, As, Pb, Bi, Se, Th, Rb, U, Sr, Zr, Mo, Ag, Cd, Sn, and Sb. Each sample was tested for a recommended minimum counting time of 1 minute (20 seconds per beam) reporting assay results in parts per million (ppm). Increasing counting times marginally the improved accuracy of analyses but long counting times also reduced the number of samples that could be processed in a given day. Over 200 samples were assayed in a single day and results were downloaded from the HHXRF onto excel spreadsheets for processing and analyses. Those assays with incomplete counting times were deemed erroneous and flagged for re-testing.

5.4. QAQC Sampling Protocols

Certified Reference Materials (CRMs) containing concentration levels of the metals of interest – comparable to those anticipated in the soil samples – were inserted blind with unknown samples along with duplicates at rate of 5% (1 every 20) for both HHXRF and laboratory analyses. Blinding of CRMs was achieved by removing them from their original sachets and re-packaging in similar pouches as the rest of unknown samples. However, even with this level of blinding experienced laboratory chemists may be able to detect which are control samples in the batch based solely on sample colour, sample quantity and sample texture (standards are commonly very finely ground pulps).

At the laboratory a partial digestion method was employed which uses aqua regia, a 3: 1 mixture of hydrochloric and nitric acids to dissolve sulphides, carbonates, phosphates, chlorites and oxides contained in the samples. Aqua regia is a very popular acid digestion for exploration geologists due to its low cost of determination for most sedimentary deposit pathfinders. However, major rock-forming and resistant minerals such as silicates are not completely digested and will yield only a partial determination of those associated elements. For this reason data from an aqua regia leach is considered as representing only the leachable portion of the analyte (acid leachable portion of the elements) and reading by a combination of ICP-MS and ICP-AES is used to report the widest possible concentration range. This

combination of aqua regia digest with ICP-MS and ICP-AES finish allows for low detection limits in soil and sediment surveys that require ultra-trace analytical sensitivity.

5.5. Comparison of HHXRF and Laboratory Assays

Portable X-ray Fluorescence spectrometry is a non-destructive technique useful in effecting quick, on the spot analysis of metal concentrations. It is a technique which does not destroy the analytical specimen. It not only identifies but quantifies total element concentrations in the specimen. A high energy primary x-ray beam from HHXRF analyser strikes a sample causing atoms in the sample to become unstable. Electrons in the nucleus of the unstable atom interchange orbitals in order to regain stability and, in the process emit secondary x-ray beams (photons) with wavelengths characteristic to specific elements present in the sample. The HHXRF captures this secondary x-ray beam and identifies the elements.

Analyses at the laboratory were done by first bringing the specimen into solution using acids prior to reading by ICP-MS/AES. This technique not only completely destroys the specimen; it is also limited to determinations of the acid leachable portion of the elements. After digestion the sample is introduced into hot argon plasma as aerosol droplets where it dries, molecules dissociates and electrons removed from components thereby forming singly-charged ions which are then directed into a mass filtering device known as the mass spectrometer. The mass spectrometer sorts ions by their mass-to-charge ratio such that at any given time only one mass-to-charge ratio is allowed to pass through the mass spectrometer from the entrance to the exit where a detector counts individual ions exiting the mass filter. Thus, ICP-MS technique achieves lowest possible detection limits with highest levels of productivity.

HHXRF assays represent only those points on a sample that are measured. If no sample homogenisation is done, geochemical results for those measured points do not represent the elemental concentrations for the entire sample. This analytical bias was minimised by sieving samples to minus 180 micron (homogenised) fraction.

5.6. Sample treatment at Laboratory

Samples were analysed at ALS Chemex laboratory facility in Johannesburg in South Africa. Samples were submitted as minus 180 micron powders which only needed drying at 110°C prior to partial digestion and analysis. The ME-MS41 multielement geochemical package

offered by ALS Chemex was employed which reports concentrations on a suite of 51 elements extracted into an aqua regia digestion. Concentrations are determined by a combination of inductively coupled plasma spectrometry (ICP-MS) and atomic emission spectrometry (ICP-AES). According to ALS in their commercial brochures, this analytical technique has a lower limit of detection of 0.2ppm to 0.01% (detailed in Table 4).

Table 4: *Detection ranges (as lower – upper limit of detection) for elements reported in the ME-MS41 Package*

Concentrations as ppm (unlabelled) or percent							
Ag	0.01 - 100	**Cs**	0.05 - 500	**Mo**	0.05 - 10,000	**Sr**	0.2 - 10,000
Al	0.01% - 25%	**Cu**	0.1 - 10,000	**Na**	0.01% - 10%	**Ta**	0.01 - 500
As	0.1 - 10,000	**Fe**	0.01% - 50%	**Nb**	0.05 - 500	**Te**	0.01 - 500
Au	0.2 - 25	**Ga**	0.05 - 10,000	**Ni**	0.2 - 10,000	**Th**	0.2 - 10,000
B	10 - 10,000	**Ge**	0.05 - 500	**P**	10 - 10,000	**Ti**	0.005% - 10%
Ba	10 - 10,000	**Hf**	0.02 - 500	**Pb**	0.2 - 10,000	**Tl**	0.02 - 10,000
Be	0.05 - 1,000	**Hg**	0.01 - 10,000	**Rb**	0.1 - 10,000	**U**	0.05 - 10,000
Bi	0.01 - 10,000	**In**	0.005 - 500	**Re**	0.001 - 50	**V**	1 - 10,000
Ca	0.01% - 25%	**K**	0.01% - 10%	**S**	0.01% - 10%	**W**	0.05 - 10,000
Cd	0.01 - 1,000	**La**	0.2 - 10,000	**Sb**	0.05 - 10,000	**Y**	0.05 - 500
Ce	0.02 - 500	**Li**	0.1 - 10,000	**Sc**	0.1 - 10,000	**Zn**	2 - 10,000
Co	0.1 - 10,000	**Mg**	0.01% - 25%	**Se**	0.2 - 1,000	**Zr**	0.5 - 500
Cr	1 - 10,000	**Mn**	5 - 50,000	**Sn**	0.2 - 500		

5.7. Geochemical Data Analysis (Software)

A combination of ArcMap 10.2.2, MS Excel and ioGAS 5.2 was used in this exercise to evaluate and report the geochemical results. ioGAS is specifically geochemical analysis software. It is an essential geochemist toolbox that has a multitude of customised tools for advanced data analysis of large multivariate data sets. It relies on a dynamically linked graphical environment and has capabilities of exporting directly to Google Earth, ArcMap and MapInfo GIS platforms.

6. RESULTS

Geophysical and geochemical survey campaigns were independently executed in the three contiguous study areas making up the Solwezi Copper Programme (SCP). These surveys primarily targeted deposits of the Copperbelt or Kansanshi types but not excluding the possibility of the IOCG style mineralisation.

6.1. Geophysical Survey

The SCP area was covered by an airborne magnetic and radiometric survey flown at 35m average ground clearance at 150 m line spacing with tie lines every 1500 m covering a total of 11,625 line kilometres. Processed line data and interpretations were done in Geosoft Voxi and Model Vision Softwares.

Magnetic data are useful in identifying structural features such as folds and faults and very helpful in delineating prospective areas for further targeting. Every rock has a magnetic susceptibility which depends on its mineralogy. Brines passing through these rocks cause changes in rock's internal petrophysical properties (i.e. alteration) and can produce magnetic susceptibility contrasts which may be used to identify fold structures, delineate magnetic rocks from non-magnetic rocks and locate magnetic minerals (i.e. pyrrhotite) that may be associated with viable mineralisation (e.g. pentlandite). Furthermore, magnetic data can provide information on the depth to basement (i.e. thickness of sedimentary cover) or top of the causative feature.

Previous regional surveys have shown that Lower Roan units characteristically show low magnetic signature, whilst Upper Roan units have low to medium magnetic susceptibility response and Mwashia rocks generally have higher magnetic signatures (Saraswatibhatla, 2013, Carey et al., 2012).

The additional cost of recording radiometric as well as magnetic data during an airborne survey is small and so both types of data are routinely gathered. Radioelement data provide information on the variations in the concentrations of uranium (*U*), Thorium (*Th*) and potassium (*K*) in the survey area and can be useful in delineating different geological domains. Uranium content often increases from ultrabasic/basic rock units to acidic rock units, although uranium response can exponentially increase up to 2000 times immediately

after the rainfall (Saraswatibhatla, 2012, 2013). Thorium (*Th)* may increase or decrease in hydrothermal alteration.

Radiometric data is commonly depicted using "ternary images" (**Figure 21**) in which the intensities of each channel are assigned a colour: K – red, Th – green and U – blue. The responses are combined to produce a single RGB colour map. Granitoids are known to give elevated *U* and *Th* values. In order to enhance variations, ratios such as between U*/Th, Th/K, K/Th* are useful. For example, the ratio K/Th can be used to distinguish intrinsically high K intrusives from extrinsically K-rich alteration zones.

Figures 17, 18 and 19 show Total Magnetic Intensity (TMI), Reduced to Pole (RTP) and Analytical Signal (AS) magnetic images respectively. The total magnetic intensity image was generated from values ranging from 29500 to 34000nT with a mean value of 31500nT. The high values are purple and orange representing underlying rocks with appreciable magnetic susceptibilities. The blues and greens represent rocks with lower magnetic susceptibilities. A gradual change in colour indicates a gradual change in the magnetic field strength; a consequence of either steady change in magnetic susceptibility of rocks near surface, burial of rock unit of relative constant magnetic susceptibility, or gradual introduction of new unit at depth. An abrupt change in colour indicates an abrupt change in magnetic susceptibilities.

The background values are quite different between southern part and northern part of the survey. Notable on all magnetic images (TMI, RTP, AS) there are 2 distinct magnetic domains distinguished by northwest-southeast trending high magnetic bodies in the northern part of the survey area (top left and top right corners), and the northeast-southwest trending linear to curvilinear high magnetic bodies in the central zone. All magnetic anomalies were assessed on the ground to eliminate false anomalies that could be generated by cultural activities (e.g. wire fencing, power lines, coaxial cables etc.). The helicopter-supported ground-proofing exercise identified intrusives (syenites, gabbros) to be responsible for high magnetic susceptibility responses in the top half of the study area (magnetic bodies with NW-SE trends). All northeast-southwest trending high magnetic bodies in the central zone were observed to be metasedimentary rock units (marbles, calcareous siltstones, dolomitic marbles and siliceous shales).

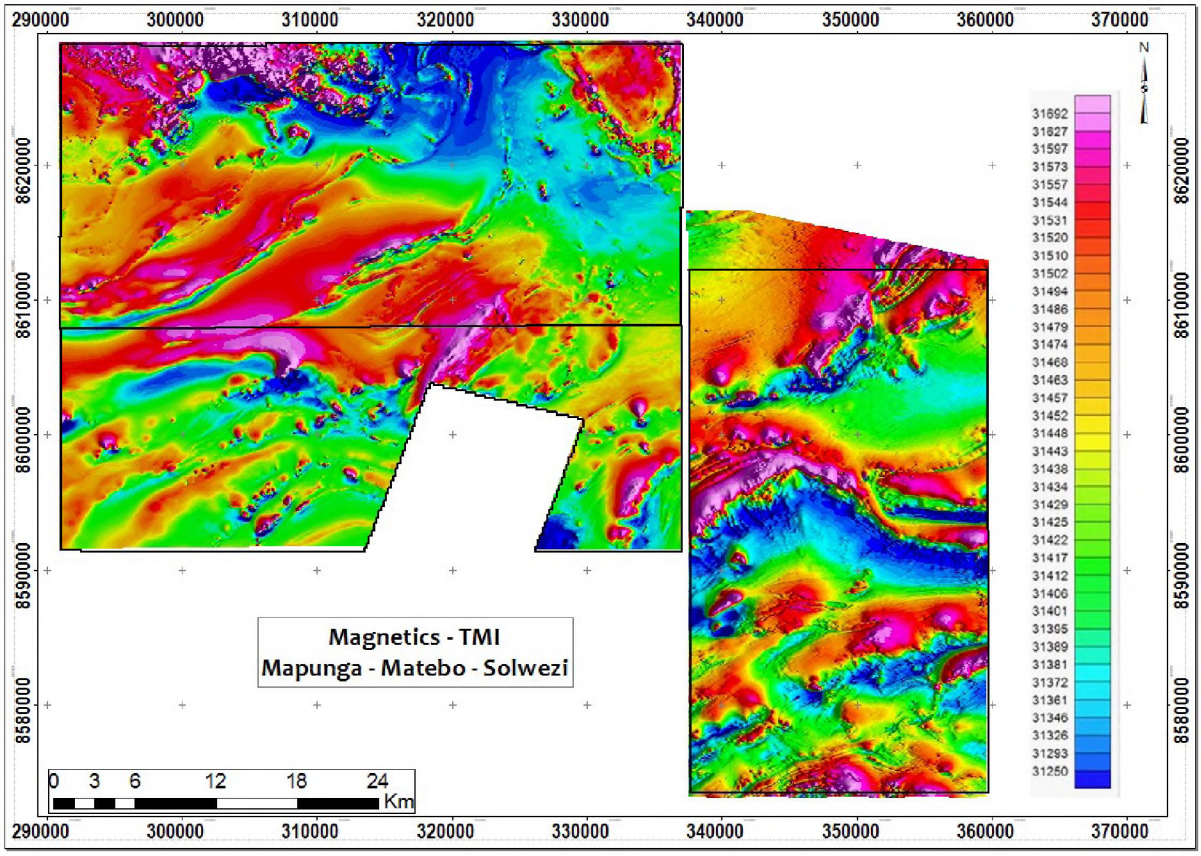

Figure 17: *Magnetic intensity map (TMI) covering the study areas. Intrusive rocks occupy the top half of area and have a general NW-SE trend. NE trending linear features were observed to be metasedimentary rocks.*

TMI images depict total magnetic susceptibility strengths of underlying geology of a surveyed area. Magnetic bodies in the two interpreted magnetic domains differ in appearance (magnitude, texture and trend). The NW-SE trending bodies have a stippled pattern characteristic of intrusive rocks and this appearance is clearly observed on the analytical signal map in which intrusive units appear as a cluster of isolated blobs (**Figure 19**). In the central zone, linear features have a smooth and continuous appearance and they seem to be stacked, a common observation in areas underlain by stratified or layered metasedimentary bedrock of differing magnetic susceptibility intensities. Outcrops of banded carbonate rocks were observed in this area during fieldwork.

Reduced to pole magnetic images (**Figure 18**) are produced from computation of TMI maps to produce a magnetic map that would result had the area been surveyed at the magnetic pole. In this way, all magnetic susceptibility intensities on RTP images are assumed to be from induced magnetic effects of underlying bodies whose magnetic intensities are placed directly

above the causative features. This is useful when interpreting structural features (faults, folds) and subsequent locating them in the field. By obtaining locations from an RTP image where magnetics suggested the presence of intrusive bodies, granites and gabbros were accurately located in the field.

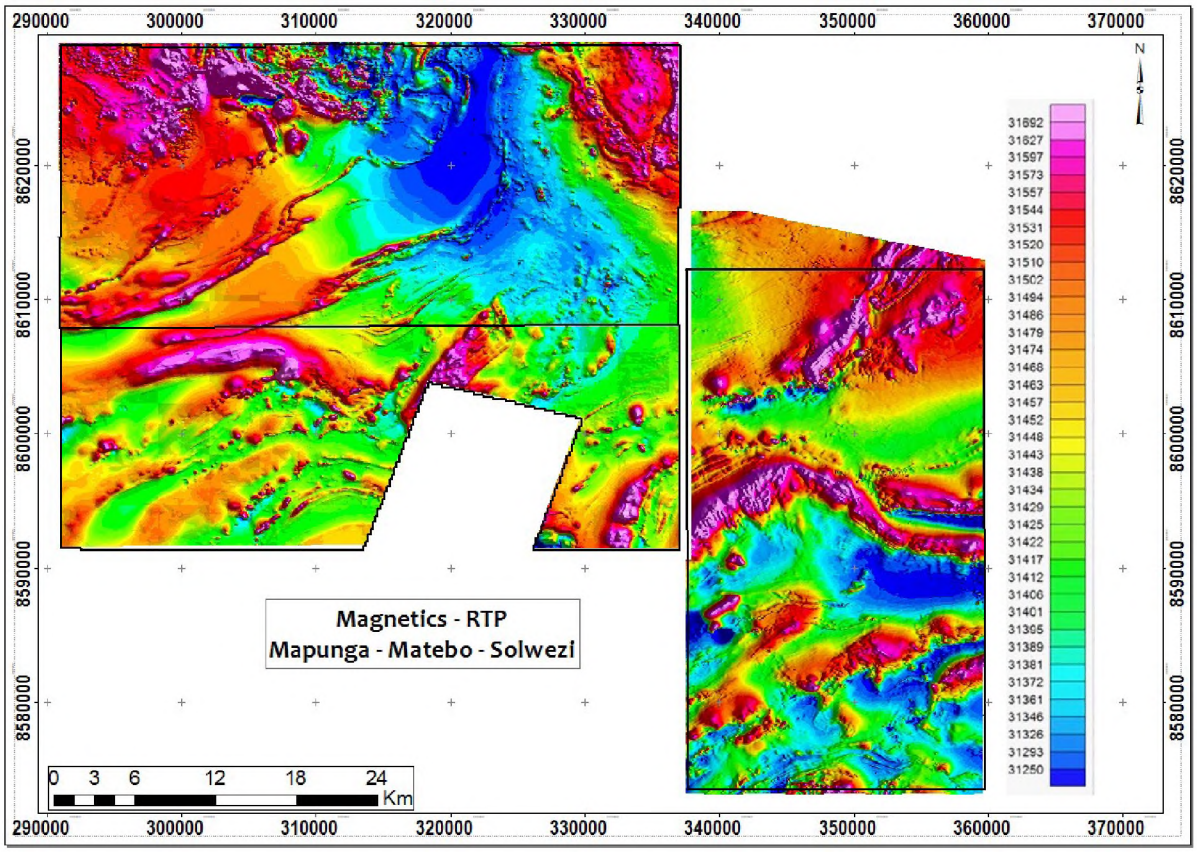

Figure 18: *Reduced to pole (rtp) magnetic image covering the study areas drawn from magnetic intensities ranging between 31250nT and 31615nT. The intrusive unit in the top right corner maps the southwestern edge of Mwombezhi Dome.*

The top right corner coincides with a section of mapped basement unit belonging to the Mwombezhi Dome (**Figures 11 & 12**). A major NW trending structural lineament appears to separate the northern area which has intrusive rocks from the southern area hosting metasedimentary units. Intrusive bodies in the top left corner appear to have intruded the country rocks through this lineament.

Analytical Signal anomaly maps (**Figure 19**) simply mark the magnetic contrast of magnetic minerals in rock units. Since magnetic minerals are randomly oriented in intrusive rocks and do not entirely make up the rocks (compared to metasedimentary units in which they often form continuous layers) intrusive bodies appear as discontinuous and isolated blobs forming

stippled patterns, which can easily be distinguished on maps. In the study area, the northern portion has these stippled patterns in the left and right corners interpreted to host intrusive rocks. This interpretation is in agreement with regional geology mapping (**Figure 11**) and was confirmed in the field by outcrop mapping. Further, conversion of TMI data into gravity data by mathematical computations to produce a pseudo-gravity image (**Figure 20**) show very dense bodies in the two areas in the northern part interpreted to host intrusives.

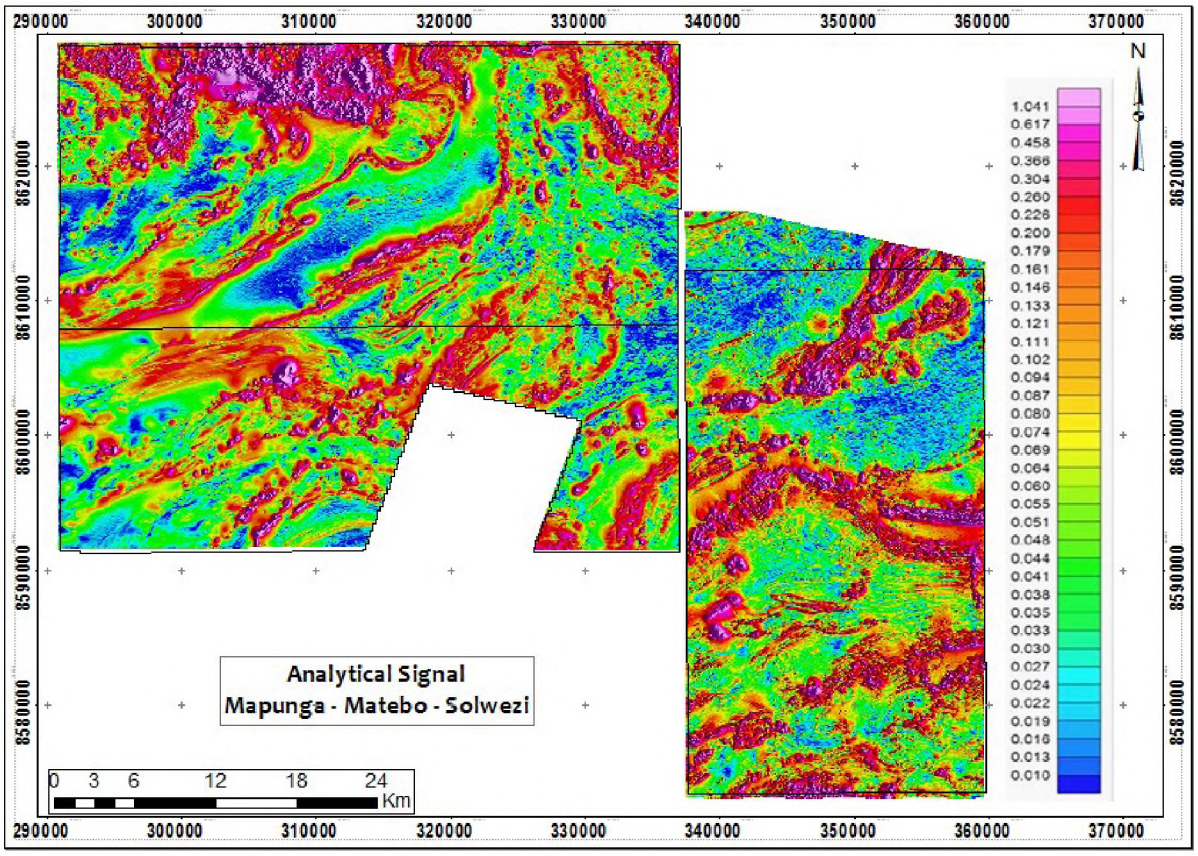

Figure 19: *Analytical Signal of TMI showing a dome structure (top right corner) and syenites (top left) identified by stippled pattern and gravity data (refer to figure 20).*

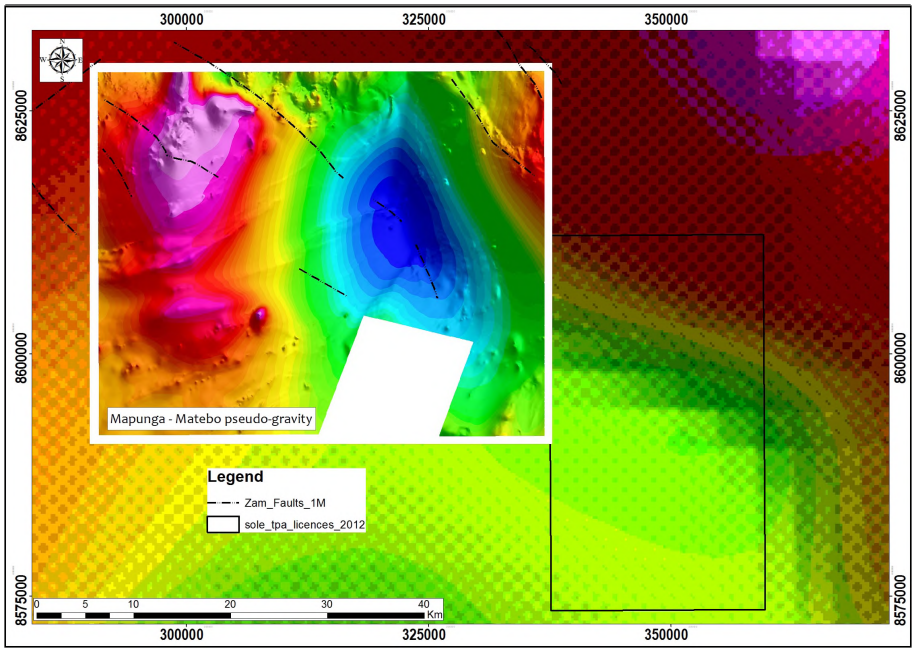

Figure 20: *Pseudo-gravity image of Mapunga and Matebo areas superimposed on regional ground gravity data. This image was generated from conversion of TMI data into gravity data by mathematical computations. Dense subsurface coincides with basement rocks at top right corner and syenite intrusive zone at top left of image. Dashed lines are large scale lineaments interpreted from regional magnetics.*

Radioelement data are used only for mapping purposes due to their limited depth of penetration (~30 cm). Used in connection with magnetic data they are useful in fine-tuning interpretations of subsurface geology. Figure 21 shows a combined U, Th and K ternary image generated from uranium values ranging between 3 – 250 counts per second (cps), thorium values ranging between 2 – 234 cps and potassium values ranging between 3 - 343 cps. Immediately apparent on this image are the high concentrations of all radioelements (U, K, Th; reddish purple zones) in areas interpreted from the magnetic images to be underlain by granitoids. These areas are on elevated grounds (**Figure 22**) compared to the rest of the area. Thorium and uranium (yellowish green and blue zones) almost exclusively cover low-lying wetlands to the south of the area (thorium and uranium have high solubilities and are thus considered highly mobile in surficial environments). This suggests alteration activity as well as movement of soil down slope. With this observation, interpretation of soil geochemical anomalies should consider a possible shift of anomalies from their origin. The area underlain by Kalahari sands is well marked to the southwest corner of the study area (represented by colour white). This area is shown to be lacking in radioelement activity and was completely ignored during geochemical sampling programmes.

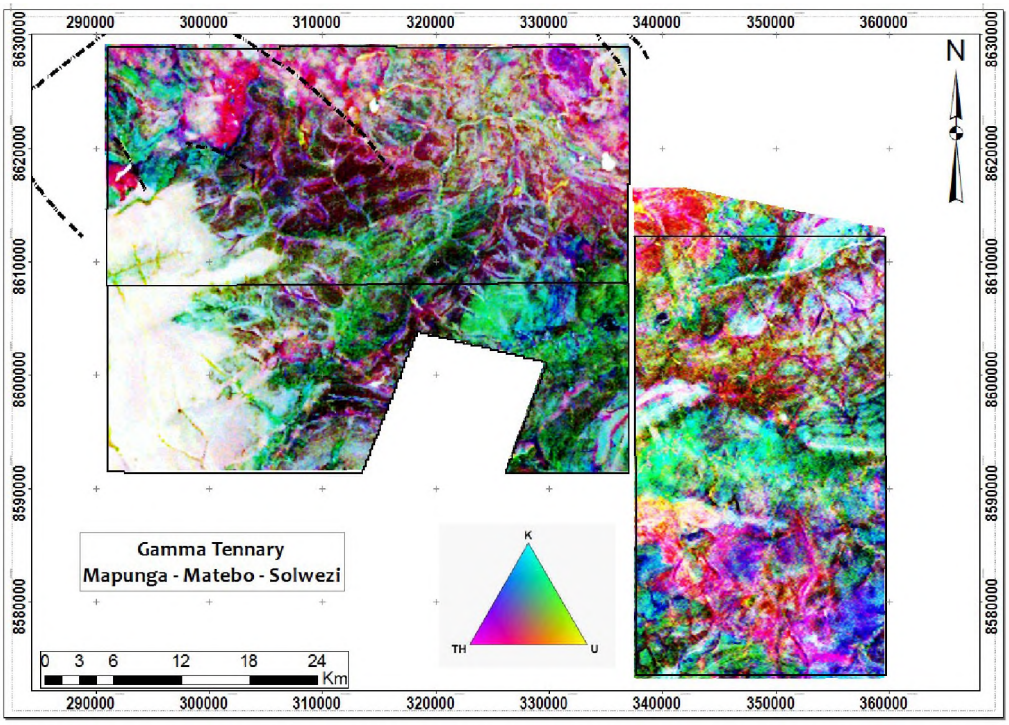

Figure 21: *Radiometric image (Ternary) covering study areas; generated from combination of radioelements Uranium - U, Thorium - Th and Potassium - K (Red =K-rich, Green =Th-rich, Blue = U-rich).*

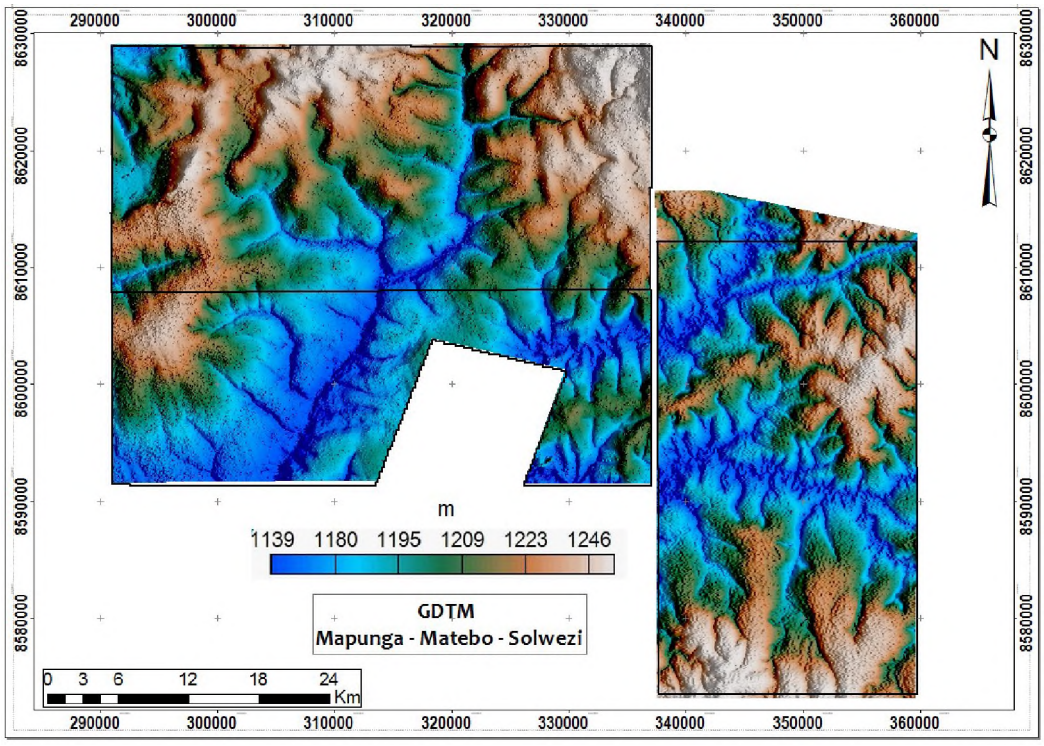

Figure 22: *Topographic map showing colour-shaded elevation of the study area. Ground has a general slope to the southwest and rivers and streams occupy lowest points (deep blue colour).*

6.2. Geochemical Survey

Planning the geochemical survey was helped by insights obtained from the geophysical survey data. Sampling grid orientation and follow-up infill grids were guided by interpreted structures from magnetics and pseudo gravity data. The decision not to take samples in a portion of the Matebo grid was made based on gamma ternary data that predicted thick recent transported soil cover, which was later confirmed during the soil geochemistry campaign. Magnetic data suggested 2 magnetic domains in the study area: a northern-most section comprising high magnetic susceptibility rocks characterised by basement domes and syenite intrusions both of which have a general NW trend; and the rest of area of low magnetic susceptibility but with a stacked, NE orientated high magnetic rocks interpreted (and supported by gravity) to host a sedimentary / metasedimentary package.

Sampling campaigns in these 3 study areas were instituted independently and, therefore, the results of the surveys are presented similarly. HHXRF was used as a screening tool in the field to select samples for wet chemical analysis.

Figure 23 compares HHXRF results with assay results by aqua regia digestion and ICP-MS/AES finish. The graphs show both HHXRF and wet chemistry assays identifying the same anomaly clusters, albeit with different concentration values. HHXRF reported much higher copper concentrations than ICP-MS assays and this difference was notably wider in samples that had lower iron content (figure 24). The reason for this could be that HHXRF was apparently undertaking an over-correction to the copper concentrations at low contents of iron (Fe<2%) resulting in artificially inflated contents of copper by HHXRF.

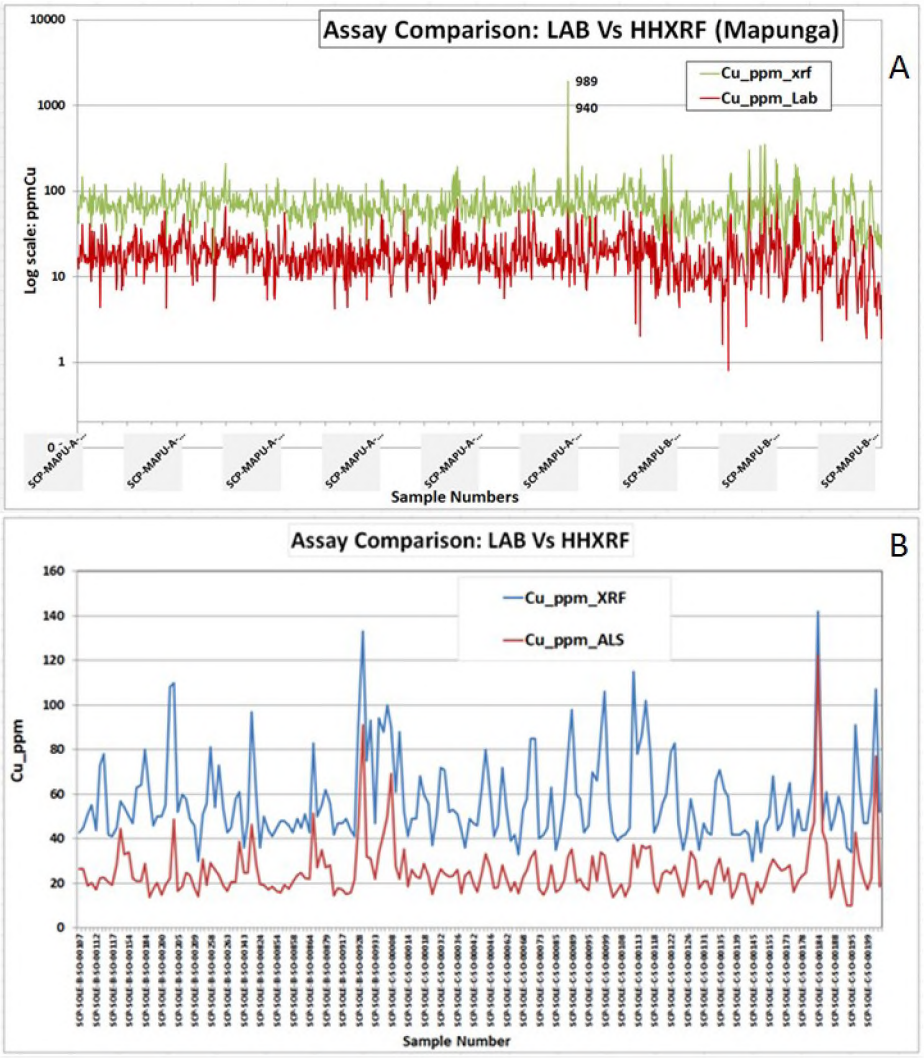

Figure 23: *Graphs showing plots of laboratory copper assays versus assays reported by HHXRF in Mapunga (A) and Solwezi (B) areas. The same anomalies were identified by both these assay methods.*

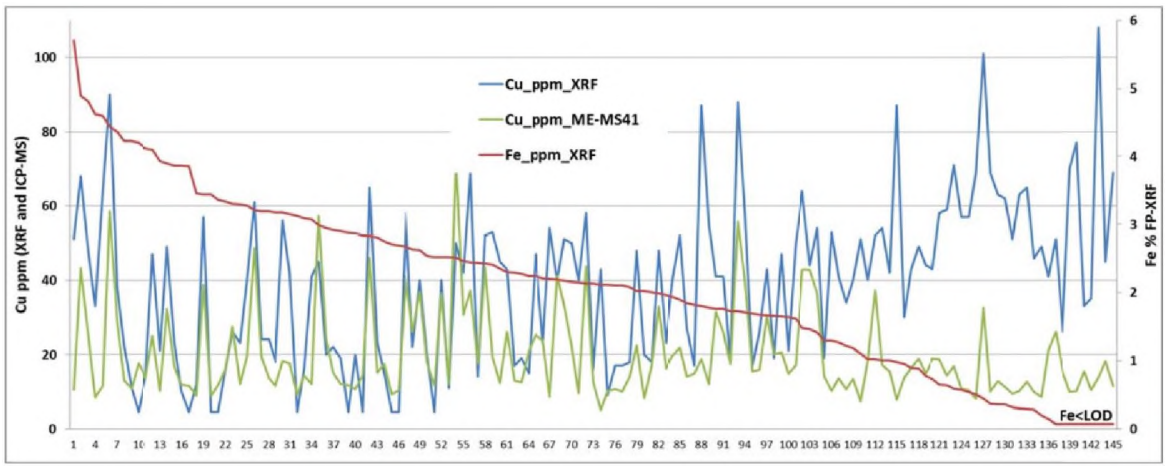

Figure 24: *Graph showing effects of iron on HHXRF and Laboratory assays. At Fe<2% there is a wider disparity between laboratory and HHXRF assays.*

6.2.1 QAQC

Of the 1861 samples analysed at ALS, quality control insertions with the samples comprised 115 aliquots of CRMs and 89 field duplicates equating to 6.2% CRM insertion and 5.3% duplicate insertion. These levels meet the minimum requirements (Snowden, 2011) of 5% insertion of each QAQC type (5% Standards, 5% duplicates). Three (3) CRM types were utilised in the sampling exercise. These were:

- OREAS45d: 345ppmCu (+/- 16ppm by aqua regia and ICP-OES/MS)
- GBM996-6 : 25ppmCu (+/- 4ppm by 3AD, 4 AD and ICP, AAS and XRF)
- GBM908-1: 74ppmCu (+/- 6ppm by 3AD, 4AD and ICP, AAS and XRF)

QAQC data for the copper in OREAS45d, GBM996-6 and GBM908-1 are shown in figures 25, 26 and 27 on the basis of their certified values. For the purposes of exploration, the results from the CRM would be considered acceptable for copper.

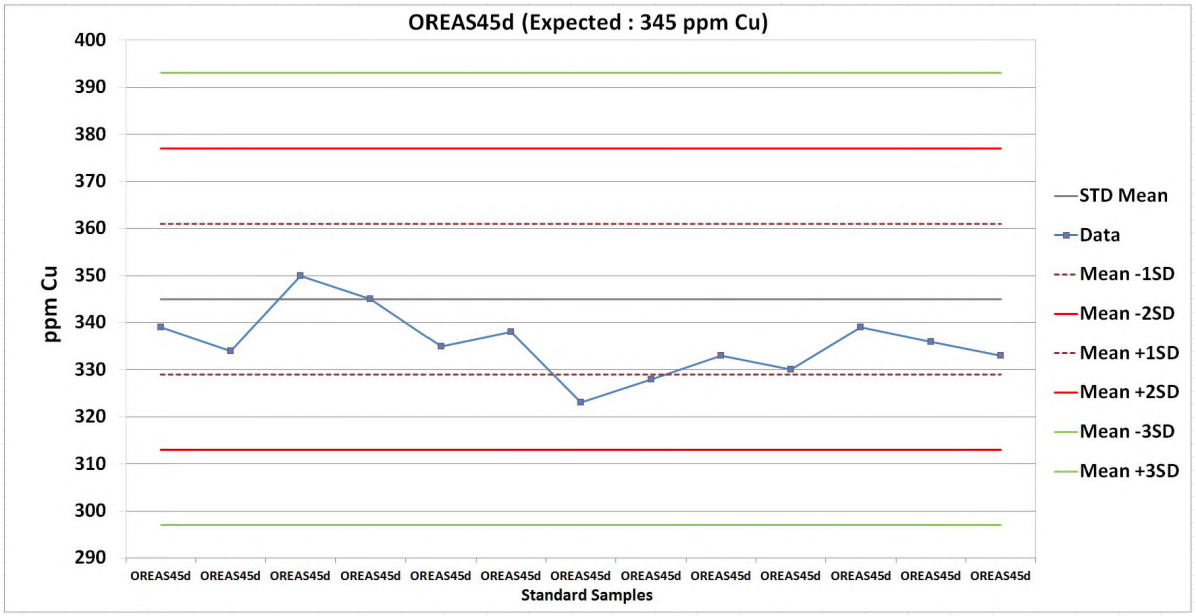

Figure 25: *Graph showing the ALS analysis of Cu in OREAS45d. Analytical results closer to certified mean and well within +/- 2standard deviations although low biased. For exploration purposes, the data is considered acceptable.*

Most assays for copper (85%) reported by ALS in OREAS45d lie within the first standard deviation limits with the rest falling in the second standard deviation limit. Assays from this standard show that the lab reported acceptable assays biased to low values.

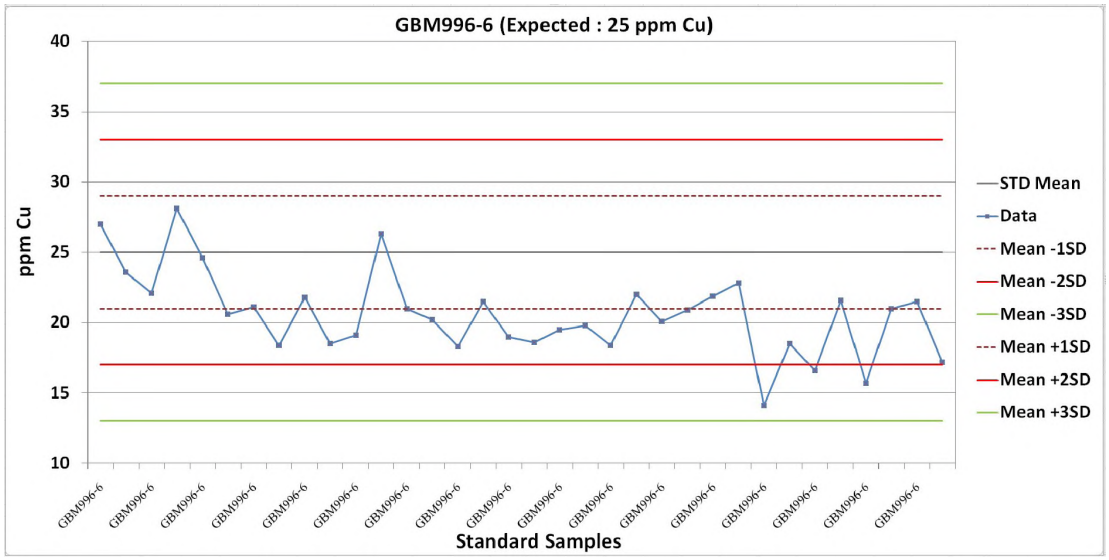

Figure 26: *Graph showing ALS analysis of Cu in GBM996-6. Analytical results mostly with 2SD limits with three samples reported outside the -2SD margin but well within 3SD limits. These results are acceptable for exploration purposes.*

Assays for GBM996-6 were consistently below the certified mean suggesting that samples in that batch were also lowly reported. Most sample aliquots for this CRM reported within 2SD with 3 samples reporting below the -2SD limit. Given the consistently low values for the complete batch, this is of no consequence, the data is considered acceptable.

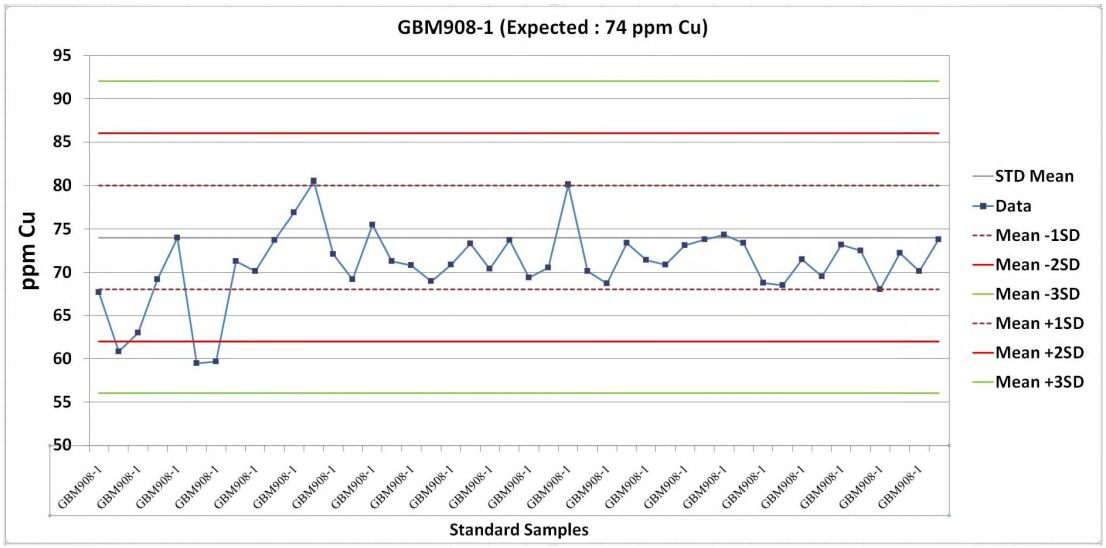

Figure 27: *Graph showing ALS analysis of Cu in GBM908-1. Most assays well within 1SD limits and close to the certified mean albeit consistently low biased. Three samples outside -2SD limit but given consistent low values in batch, this is inconsequential.*

Analytical precision was tested by insertion of field duplicates into sample batches and comparing results with "original" samples using ranked half absolute relative difference (HARD; **Figure 28**) and Q-Q plots (**Figure 29**).

A test applied to the ranked HARD chart is that 90% of the data should fall within a HARD value of 10% or less for very precise data. The chart below shows 83% of duplicate samples falling within the 10% HARD value. Considering that the field duplicates are not duplicates in the truest sense, this analytical precision is acceptable.

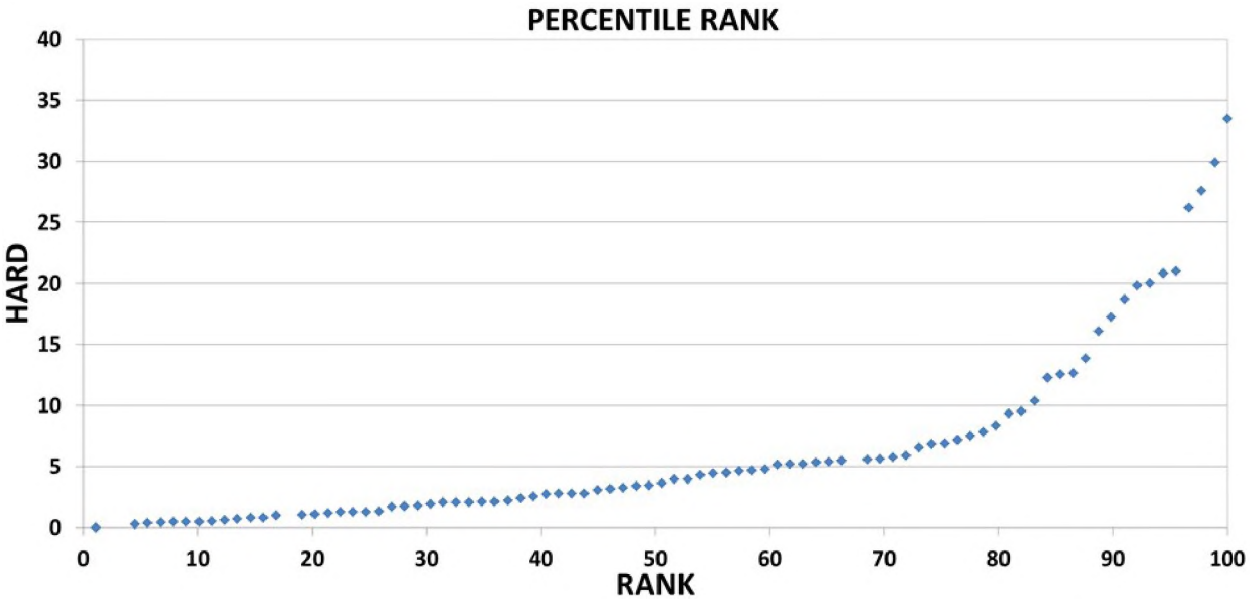

Figure 28: *Percentile Rank vs HARD chart for ALS copper duplicates. In exploration for sedimentary copper deposits, it is usual to accept analytical precision of 90% duplicate samples having a HARD value of 10-15%.*

Another method used to determine analytical precision is through Q-Q plots from where correlation coefficients (r) and coefficients of determinations (r^2) are calculated. R measures degree or strength of relationship between variables (in this case original and duplicate samples) whereas r^2 measures the percent of the variation in values of the independent variable (y/duplicate) that can be explained by variations in the value of the independent value (x/original).

The correlation coefficient (r) was determined to be 0.8 suggesting a strong correlation between duplicates and original samples (**Figure 29**). However, the coefficient of

determination (r^2 =0.69) suggests that only 69% of the duplicates are well correlated to original samples.

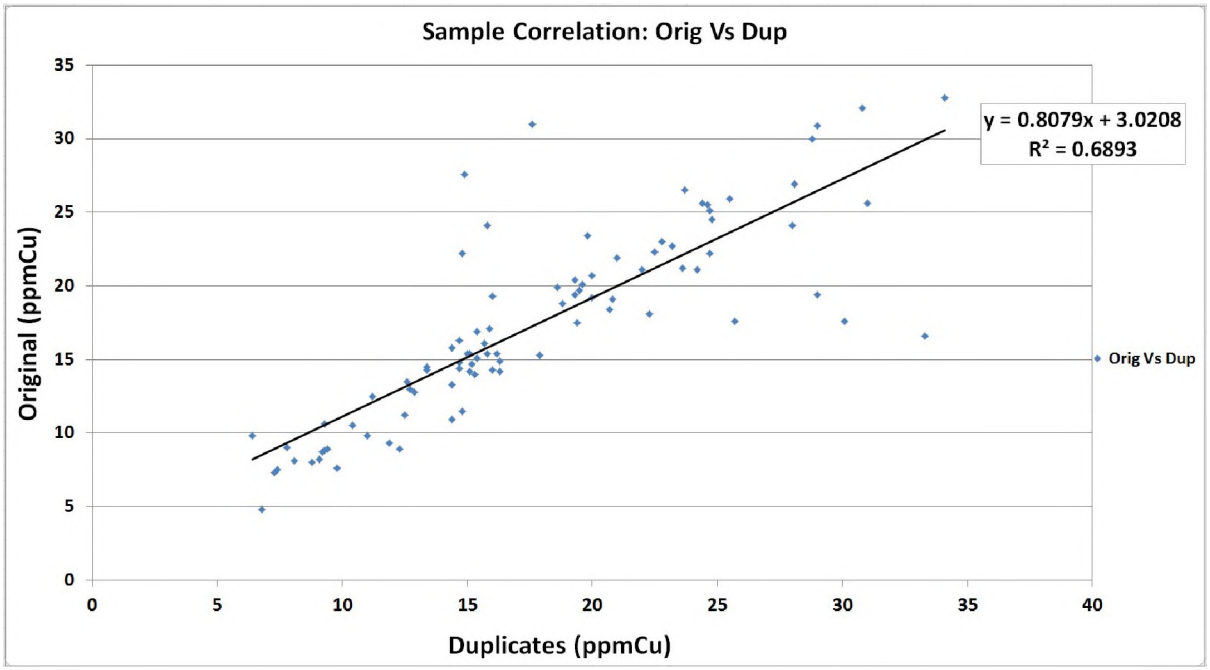

Figure 29: *Q-Q precision plot for ALS duplicate samples (r = 0.80, r^2 =0.69). Sixty-nine percent (69%) duplicates show strong correlation with original samples.*

6.2.2 Solwezi Tenement

Only the northern part of the tenement had easy vehicle access so sampling could only be done in this area. Two thousand one hundred and nineteen (2119) soil samples were collected between August 2012 and September 2013 (1279 soil samples collected in 2013 and 840 termite samples collected in 2012). All samples, except those from termite mounds, were screened to minus 180 µm.

The locations of sampling positions completed in this tenement are shown in Figure 30. Before giving up on the southern portion of the sampling grid, a helicopter visit was arranged to look for any rock exposures and any other interesting geological features such as signs of alteration, gossanous rocks and lithology that would suggest presence of copper mineralisation. Only laterite clearings, quartz-mica-schist float and quartzites were noted which were clearly barren and lacking any signs of copper mineralisation. A few termite

mounds were in the vicinity of these outcrops were sampled and analysed with handheld InnovX XRF spectrometer but the highest value obtained for copper was 20 ppm.

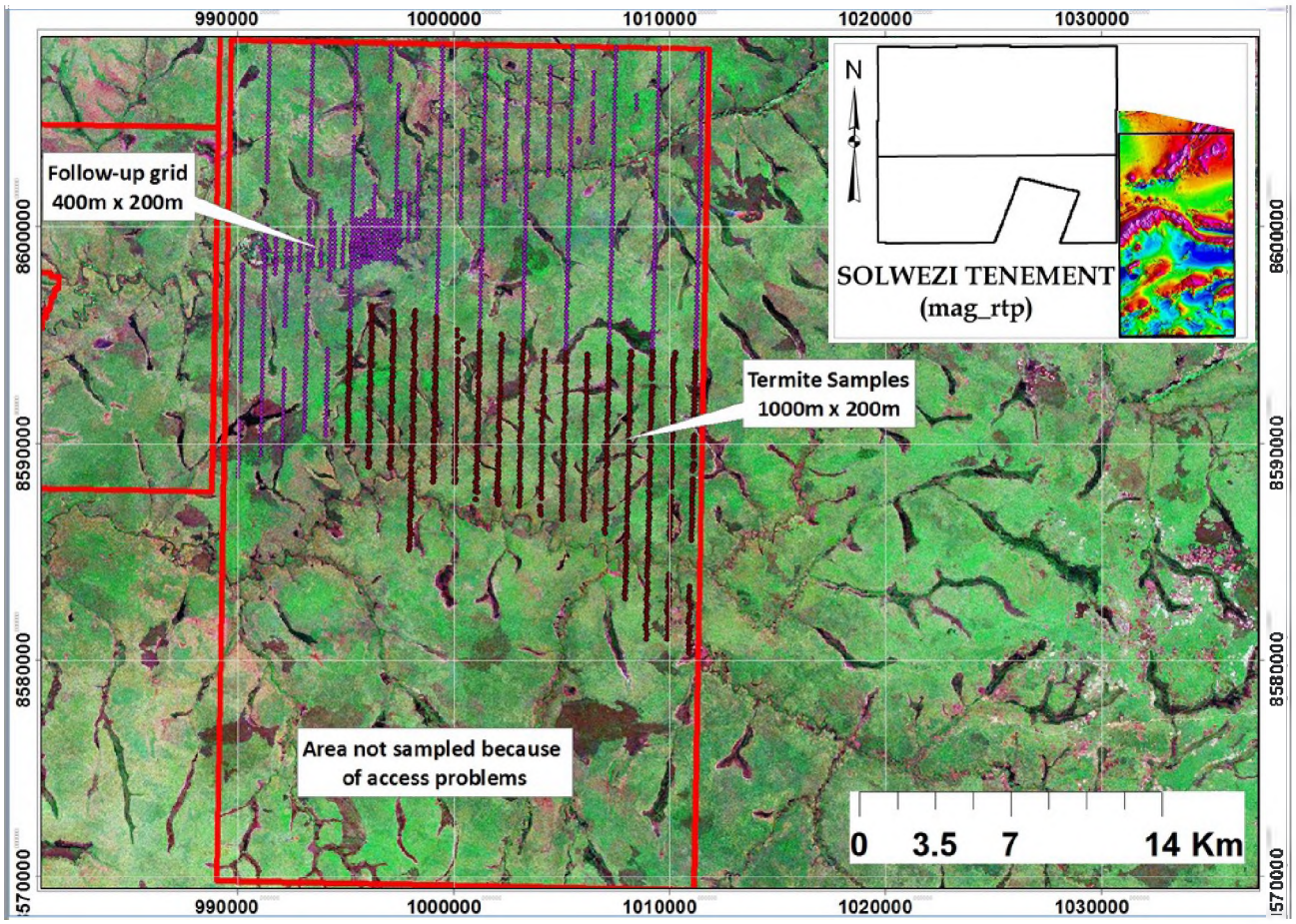

Figure 30: *Image showing combined termite and soil sampling campaign executed in Solwezi tenement with actual sampling specifications.*

The summary statistics for all the Solwezi samples analysed in the field are shown in Table 5. The results show a positive skewness indicating that the larger part of the sample population has concentrations approaching background concentrations. The upper background thresholds for the elements copper, cobalt and nickel are 43ppm, 30.4ppm, and 63ppm respectively. These values compare relatively well to those obtained at Sentinel, a copper deposits located 35km NW of the tenement (Background thresholds at the Sentinel deposit are; 43.13 ppm Cu; 21.04 ppm Co and 68.74 ppm Ni).

Table 5: *Descriptive statistics for elements of interest in Solwezi tenement*

Descriptive Statistics	Cu_ppm	Co_ppm	Ni_ppm	Fe_ppm
Count	2068	2068	2068	2068
Minimum	4	0.55	3	225
Maximum	142	292	451	117660
Range	138	291.45	448	117425
Skewness	1.86	6.51	3.2	1.50
Mean	31	13	35	21518
Unique Values	94	133	325	1999
Standard Deviation	15	22	32	10843
Median	28	8.4	31	19768
Confidence Level (95%)	0.66	0.97	1.37	467
75 percentile	36	12.62	50	26839
90 percentile	49	19.02	67	35066
95 percentile	58	27.48	81	41341
99 percentile	88	141.54	148.32	57124

From the summary statistics in Table 5 we can deduce the concentration range 4 – 43 ppm copper to be the regional background and 43 – 58 ppm copper to be the local background. A copper concentration of 58 ppm is the minimum anomaly threshold which coincides with 2 times the standard deviation and represents 5% of the total samples. A first order anomaly in the data would be in the range of 88 – 142 ppm copper; with the minimum threshold representing 4 times the standard deviation and comprising 1% of the total samples.

Cumulative frequency histogram, normal frequency histogram and probability plot for copper values in soil are shown in **Figures 31, 32** and **33**. Sample locations are shown on Landsat and magnetic image backgrounds respectively (**Figures 34 and 35**). A probability plot (**Figure 33**) gives an indication of sample population in the dataset. In probability plots, the assay value is plotted against the N score for that sample (where N= {X-mean}/standard

deviation). At most, samples below 43 ppm copper represents background populations whilst those with copper above 58 ppm could be regarded as anomalous. In this dataset 88 ppm copper represents first order anomaly minimum threshold.

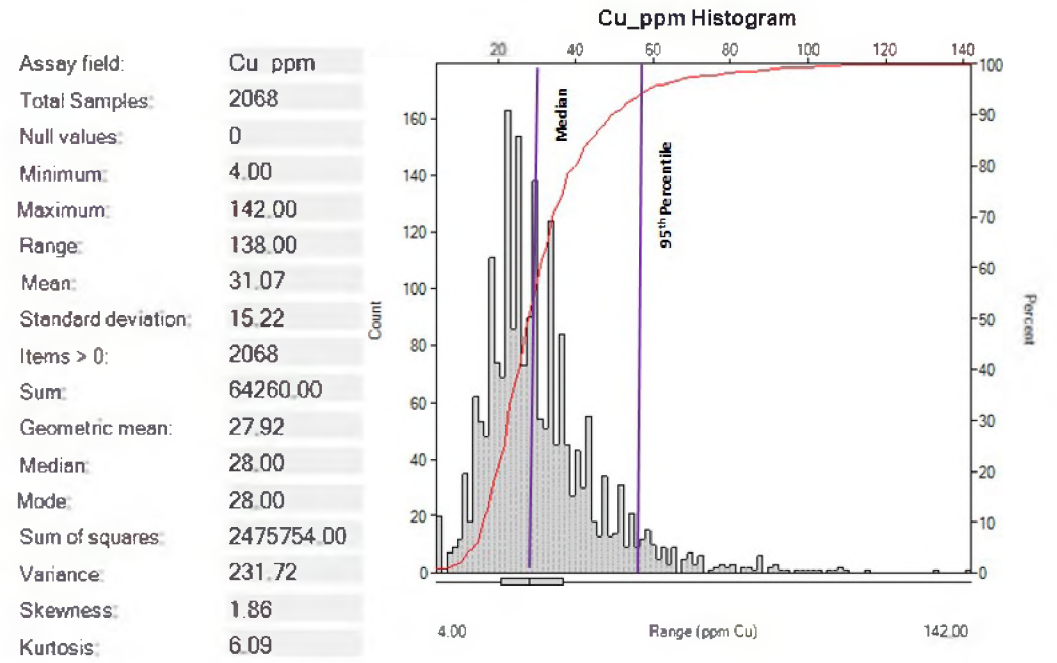

Figure 31: Cumulative frequency histogram showing copper in ppm over Solwezi tenement with associated summary statistics displayed showing sample mean, median and standard deviation.

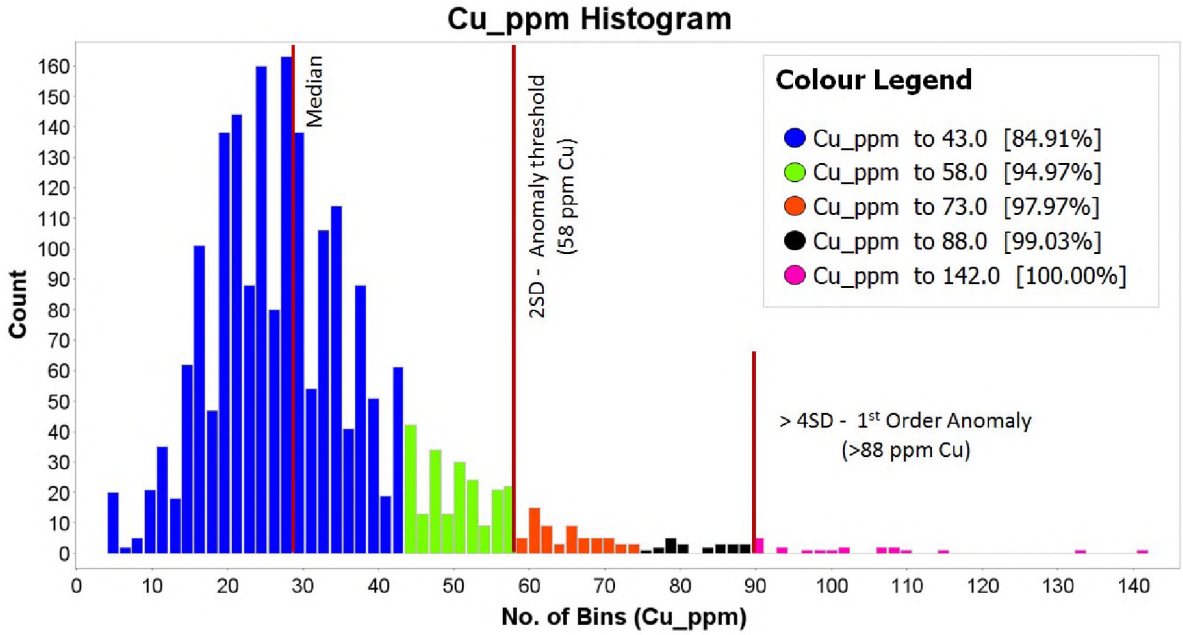

Figure 32: *Copper histogram for Solwezi samples: median = 28 ppm, minimum anomaly threshold (2SD / 95th percentile) = 58ppm, values above 88 ppmCu represent first order anomaly.*

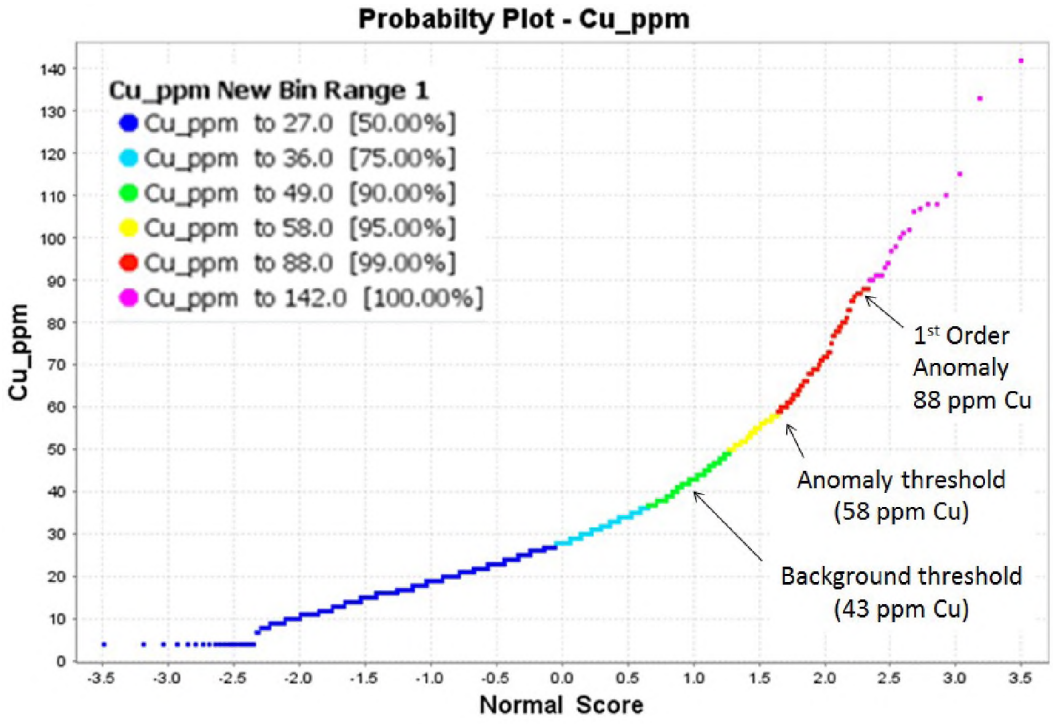

Figure 33: *Probability plot of copper ppm in soil identifying at least 3 sample populations (with intervals 0 – 27; 27 – 58, and 58 – 142ppm) and first order anomaly threshold at 88ppmCu.*

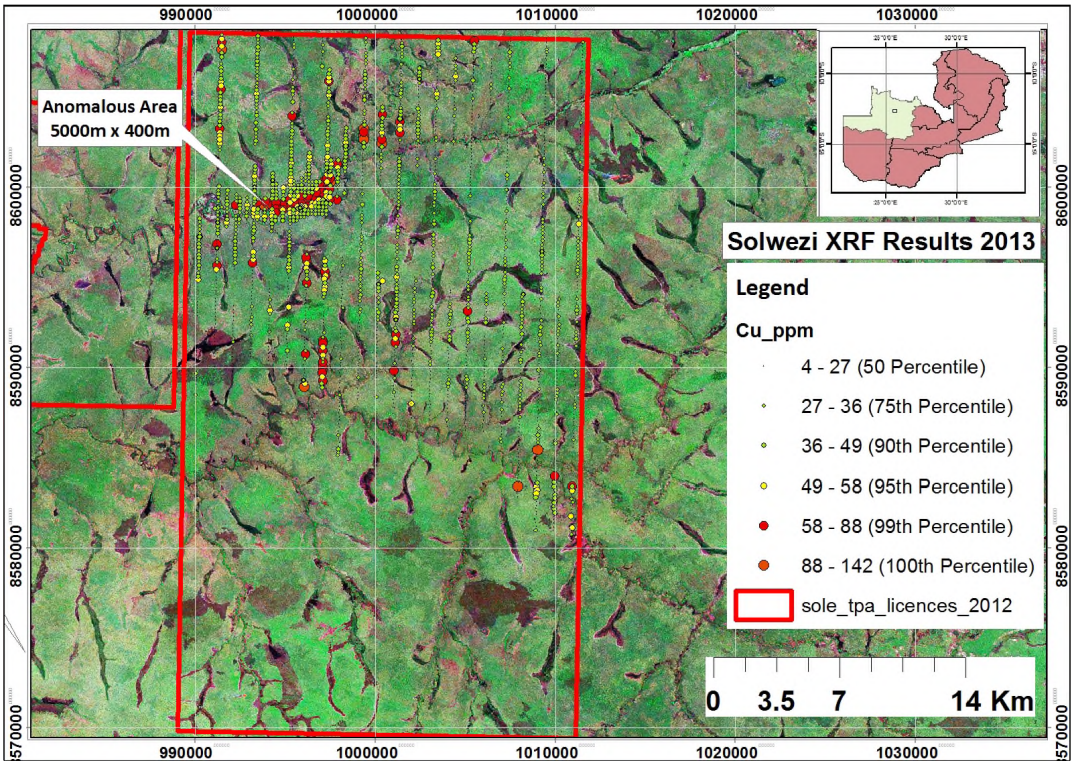

Figure 34: *Landsat image with sample locations showing anomalous copper values (red dots) whose concentrations range between 88 – 142 ppm.*

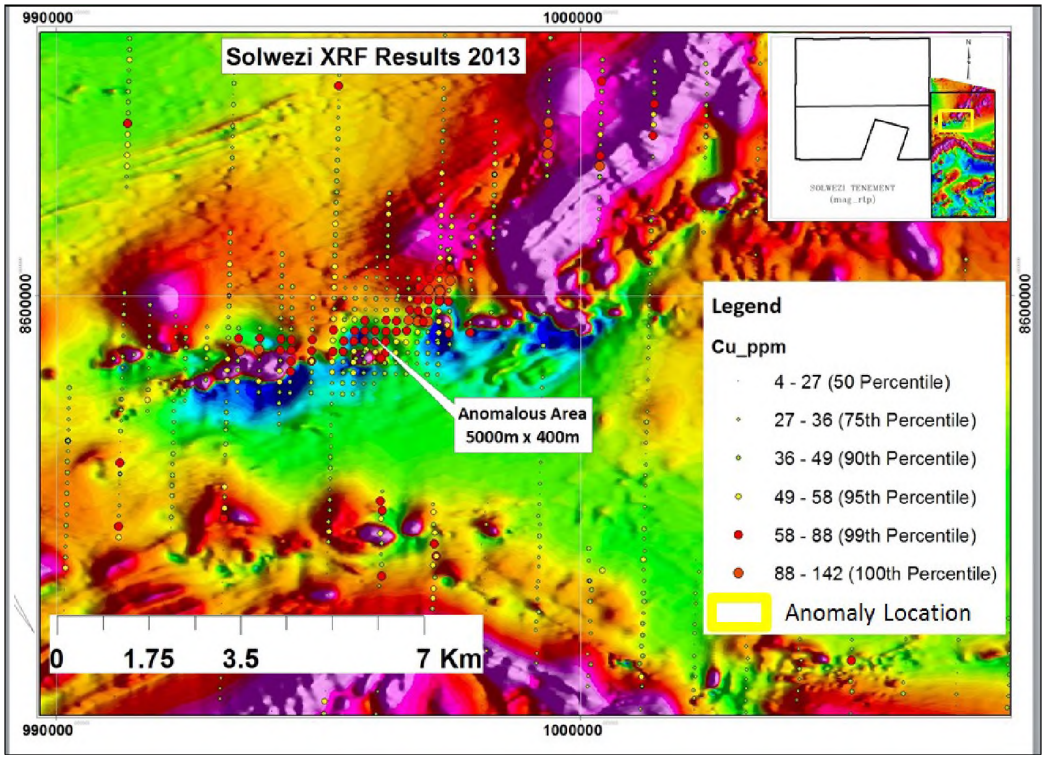

Figure 35: *RTP magnetic image with the location of anomalous samples. Anomalous zone measured 5000m x 400m and appear to align with a low magnetic domain proximal to high magnetic bodies.*

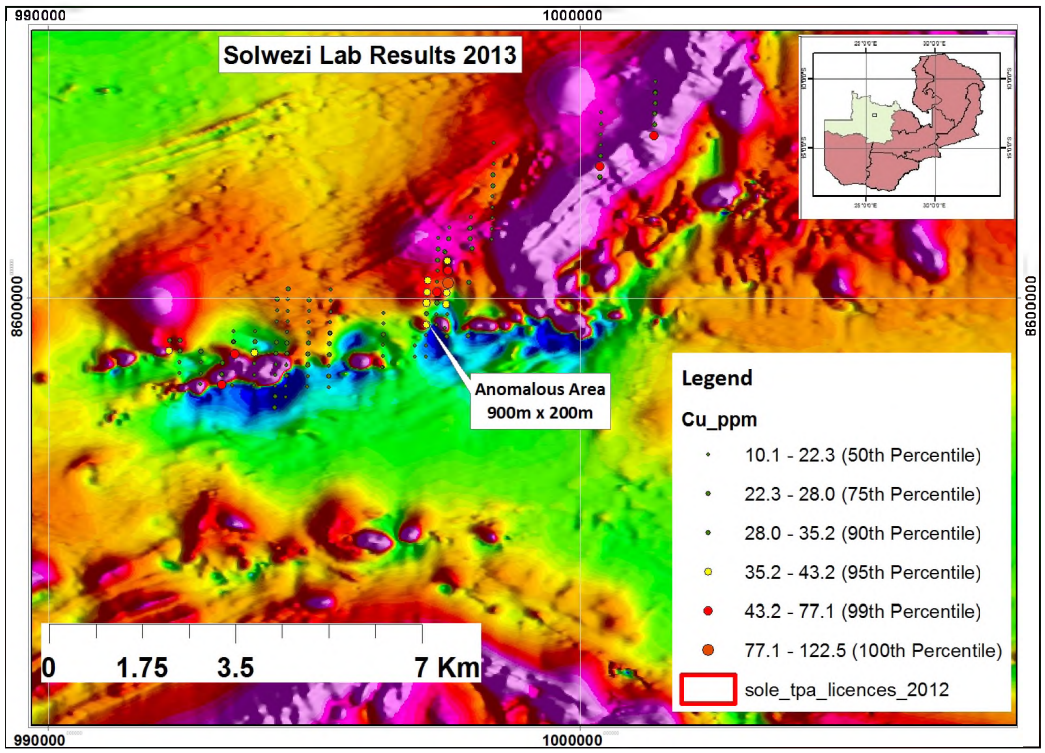

Figure 36: *Plot of laboratory assays on the backdrop of rtp magnetics. Anomaly size shrinks from 5000m x 400m to well below 900m x 200m.*

A correlation matrix for key target elements in the Solwezi soil samples is presented in Table 6. There is no strong correlation between elements in the analysed sample populations; increase or decrease in concentration of one element does not depend on increase or decrease of another element. However the moderate Cu/Co, Cu/Ni, Cu/Bi ratios are similar to what is observed at the Sentinel Copper deposits – where pair correlations between elements Cu/Co, Cu/Ni, Co/Ni and Co/V are in the order of 0.4 (See **Table 7** compared to **Table 8**; both laboratory assays).

Table 6: *Correlation matrix between some of the elements reported by portable XRF in Solwezi soil and termite mound samples (correlation coefficients, r).*

	Cu ppm	*Co ppm*	*Ni ppm*	*Fe ppm*	*Cr ppm*	*V ppm*	*Mn ppm*	*Rb ppm*	*Ag ppm*
Cu_ppm	1								
Co_ppm	0.29319	1							
Ni_ppm	0.01201	-0.2789	1						
Fe_ppm	0.22587	0.033	-0.1712	1					
Cr_ppm	0.16741	0.4189	-0.0786	-0.108	1				
V_ppm	0.50522	0.3991	-0.0446	0.58	0.2398	1			
Mn_ppm	0.11554	0.4083	-0.0248	-0.172	0.9569	0.1647	1		
Rb_ppm	0.08789	-0.3617	0.1106	0.3169	-0.2064	0.1429	-0.2192	1	
Ag_ppm	0.2035	-0.2888	0.3096	-0.028	-0.19	-0.126	-0.1555	0.01161	1

Table 7: *Pair correlation matrix for key target elements in Kalumbila geochem data (ICP-AES).*

Correlation	Cu_ppm	Co_ppm	Ni_ppm	Mo_ppm	V_ppm	Bi_ppm
Cu_ppm	1	0.45	0.27	0.23	0.47	0.36
Co_ppm	0.45	1	0.34	0.1	0.75	0.16
Ni_ppm	0.27	0.34	1	0.16	0.34	0.18
Mo_ppm	0.23	0.1	0.16	1	0.092	0.91
V_ppm	0.47	0.75	0.34	0.092	1	0.17
Bi_ppm	0.36	0.16	0.18	0.91	0.17	1

Table 8: *Pair correlation matrix for key target elements in Solwezi geochem data (ICP-MS).*

Correlation	Cu_ppm	Co_ppm	Ni_ppm	Mo_ppm	V_ppm	Bi_ppm
Cu_ppm	1	0.32	0.34	0.059	-0.033	0.14
Co_ppm	0.32	1	0.59	0.56	0.38	0.17
Ni_ppm	0.34	0.59	1	0.28	0.28	0.28
Mo_ppm	0.059	0.56	0.28	1	0.69	0.49
V_ppm	-0.033	0.38	0.28	0.69	1	0.36
Bi_ppm	0.14	0.17	0.28	0.49	0.36	1

The weak correlations between elements listed in Tables 6 and 7 are immediately apparent when the same data is presented on scatter plots – Figure 37 below. The key point is that the weak correlations observed in the Solwezi data for elements Cu, Co and Ni are similar to known copperbelt-style deposits such as First Quantum's Sentinel deposit. This gives hope for discovery of copper deposit in the area with a similar geochemical footprint as to that of Sentinel.

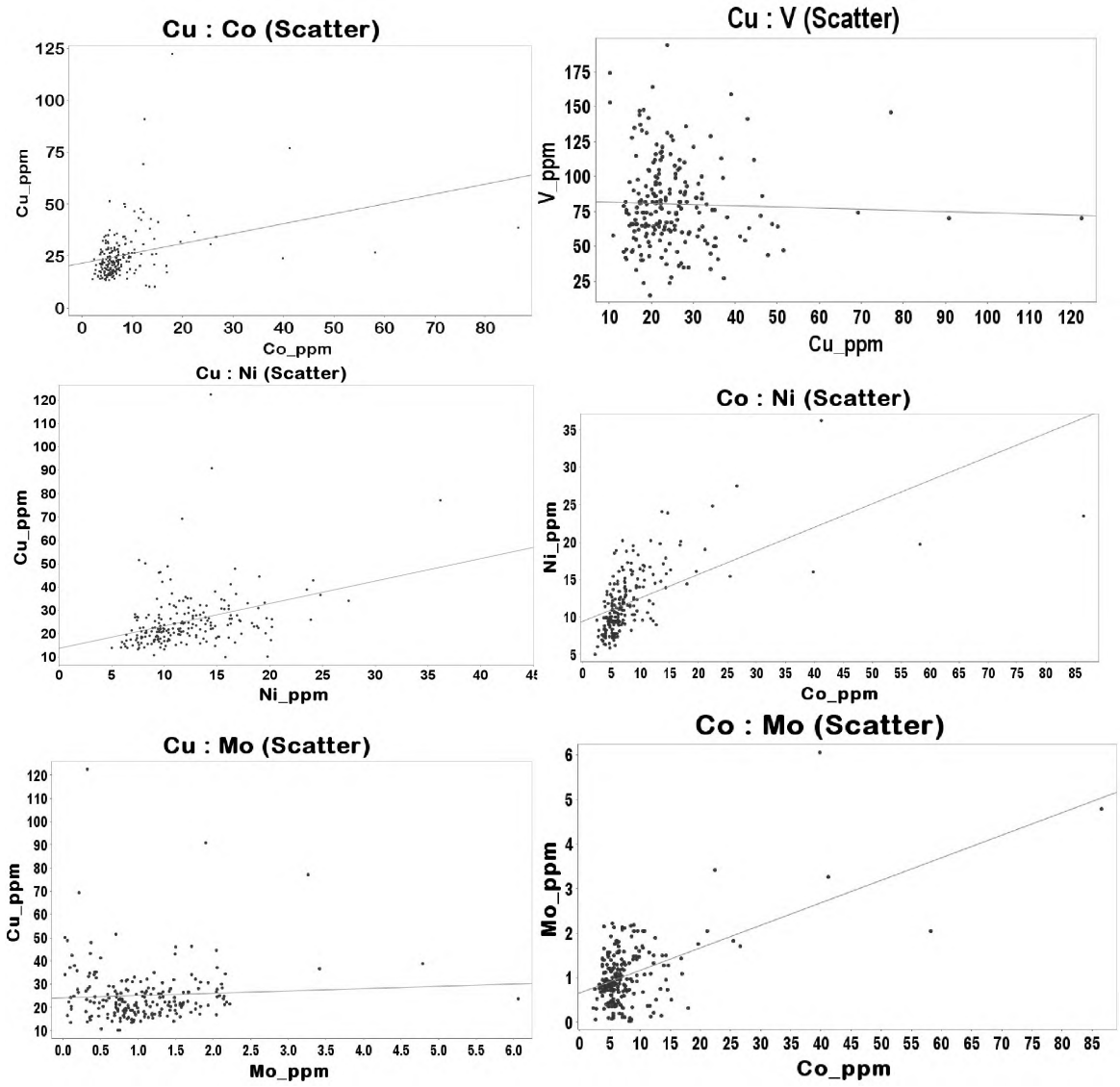

Figure 37: *Scatter plots of some of the key target elements in the Solwezi laboratory assays. Elements pairs depicted show weak correlations similar to the Sentinel Copper deposit's surface geochemical footprint.*

6.2.3 Matebo Tenement

Summary statistics for the Matebo assay data are presented in Table 9 below. These results show positive skewness in the data indicating that the larger sample population has concentrations approaching that of the background. The 3 key target elements in soil (Cu, Co & Ni) have very low concentrations whose upper background thresholds are 38.38 ppm Cu, 10.32 ppm Co and 58.53 ppm Ni respectively. Minimum anomaly thresholds - defined by median plus two times the standard deviation; for copper, cobalt and nickel are 50.76 ppm, 15.14 ppm and 77.06 ppm respectively. These figures are far less than those observed at Sentinel copper deposit (First Quantum's copper deposit – 35km north of Matebo) where minimum anomaly thresholds were defined as 71.7 ppm Cu, 28.4 ppm Co and 106.6 ppm Ni using similar criteria.

Table 9: *Summary Statistics for some elements in Matebo Samples*

Descriptive Statistics	Cu_ppm	Co_ppm	Fe_ppm	U_ppm	Ni_ppm	Bi_ppm	Mo_ppm	Ag_ppm
Count	1714	1714	1714	1714	1714	1714	1714	1714
Minimum	3.5	0.5	676	1.25	6.5	4.5	1.2	4.5
Maximum	177	52	156995	25	150	41	28	19
Range	173.5	51.5	156319	23.75	143.5	36.5	26.8	14.5
Skewness	2.56	2.15	0.41	2.96	0.41	1.55	3.47	22.84
Unique Values	68	201	1667	71	92	26	87	5
Mean	28.2	6.63	18267	2.26	40.24	8.12	2.31	4.53
Standard Deviation	12.38	4.82	14966	2	18.53	5.56	2.25	0.47
Mode	22	3.3	676	1.25	6.5	4.5	1.2	4.5
Median	26	5.5	13870	1.25	40	4.5	1.2	4.5
Confidence Level (95%)	0.59	0.22	709	0.09	0.88	0.26	0.11	0.02
75 percentile	34	8.92	24.393	3.1	51	12	3	4.5
90 percentile	43	12.4	36.251	4.9	61	16	5.35	4.5
95 percentile	50	15.2	43846.5	6.2	70	19	6.7	4.5
99 percentile	63.85	23.77	75638	10	89.85	26	10.485	4.5

The anomalous population consists of 79 samples which represents 4.6% of total samples. These can be further grouped by standard deviation into 2 main interval ranges as follows: 50.76 – 63.14 ppm Cu and 63.14 – 87.9 ppm Cu leaving 2 outlier samples (177 & 165 ppm Cu). This is illustrated graphically using frequency histograms (**Figure 38**) and probability plot (**Figure 39**) below.

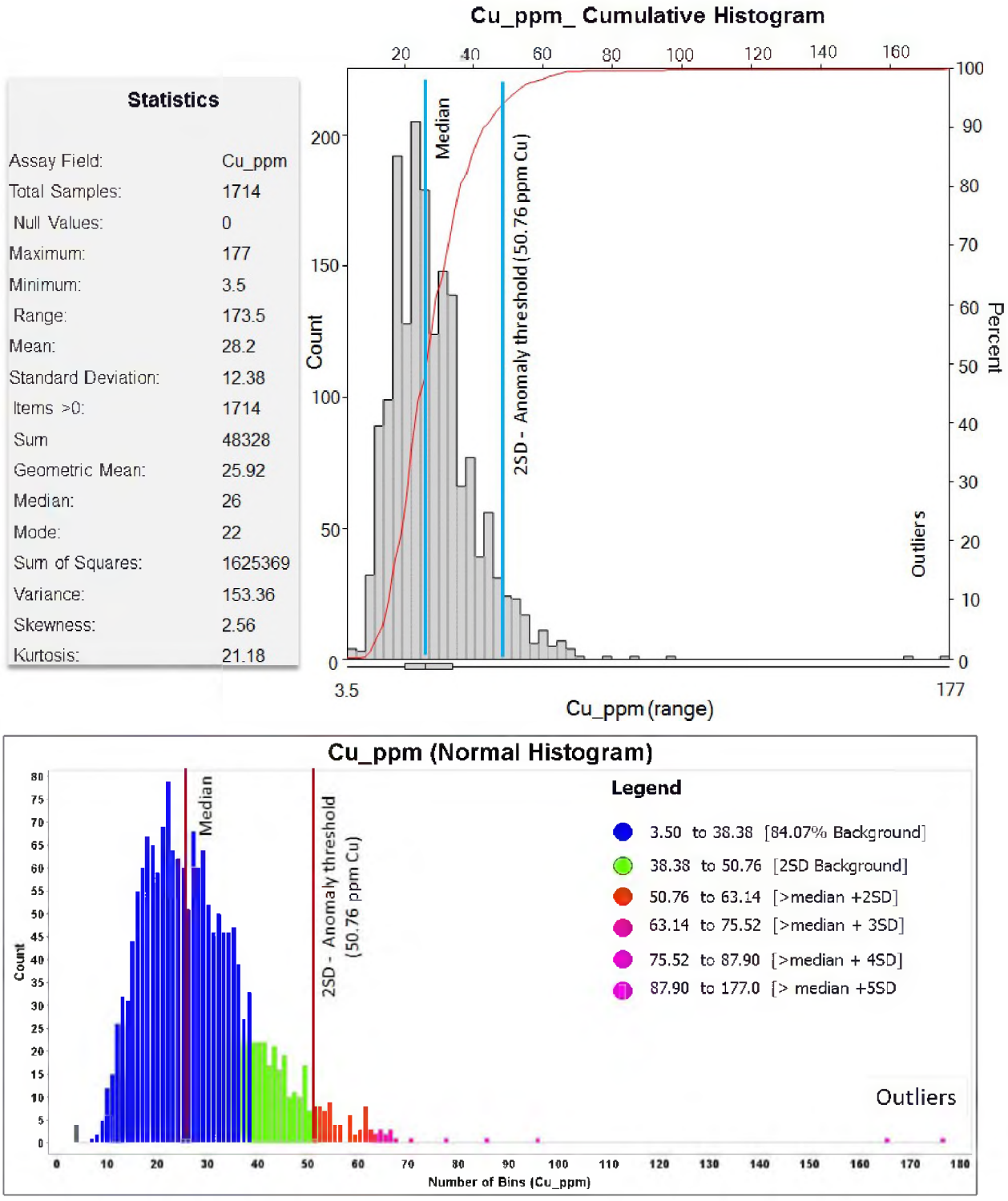

Figure 38: *Cumulative frequency histogram (top image) and normal frequency histogram plots for copper grades in Matebo soil samples. Median = 26ppm; anomaly threshold =50.76 ppm.*

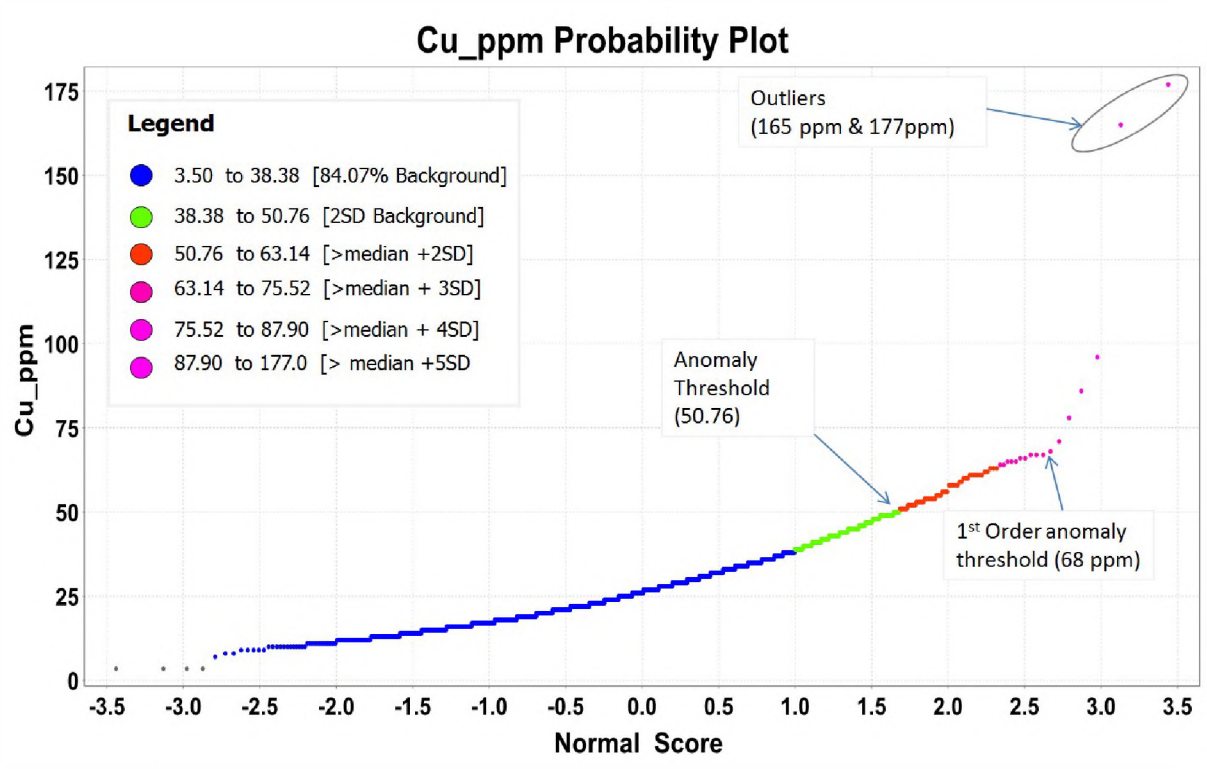

Figure 39: *Probability plot of copper assays in Matebo soil (assay value plotted against N score of that sample where N = (X-mean)/standard deviation). Minimum of three sample populations were identified in the dataset; Background (3.5 – 50.76 ppm) and anomaly populations (50.76 – 75.52ppm and 75.52 – 177 ppm).*

Table 10: *Pair correlation matrices(r) for some elements in Matebo xrf geochem data; note strong correlations between Cu/Co, Cu/V, Co/V and Co/Fe*

Correlation	Cu_ppm	Co_ppm	Ni_ppm	Fe_ppm	V_ppm	Mo_ppm
Cu_ppm	1	0.63	-0.076	0.6	0.65	0.008
Co_ppm	0.63	1	-0.5	0.94	0.79	0.089
Ni_ppm	-0.076	-0.5	1	-0.45	-0.26	-0.2
Fe_ppm	0.6	0.94	-0.45	1	0.81	0.0031
V_ppm	0.65	0.79	-0.26	0.81	1	0.094
Mo_ppm	0.008	0.089	-0.2	0.0031	0.094	1

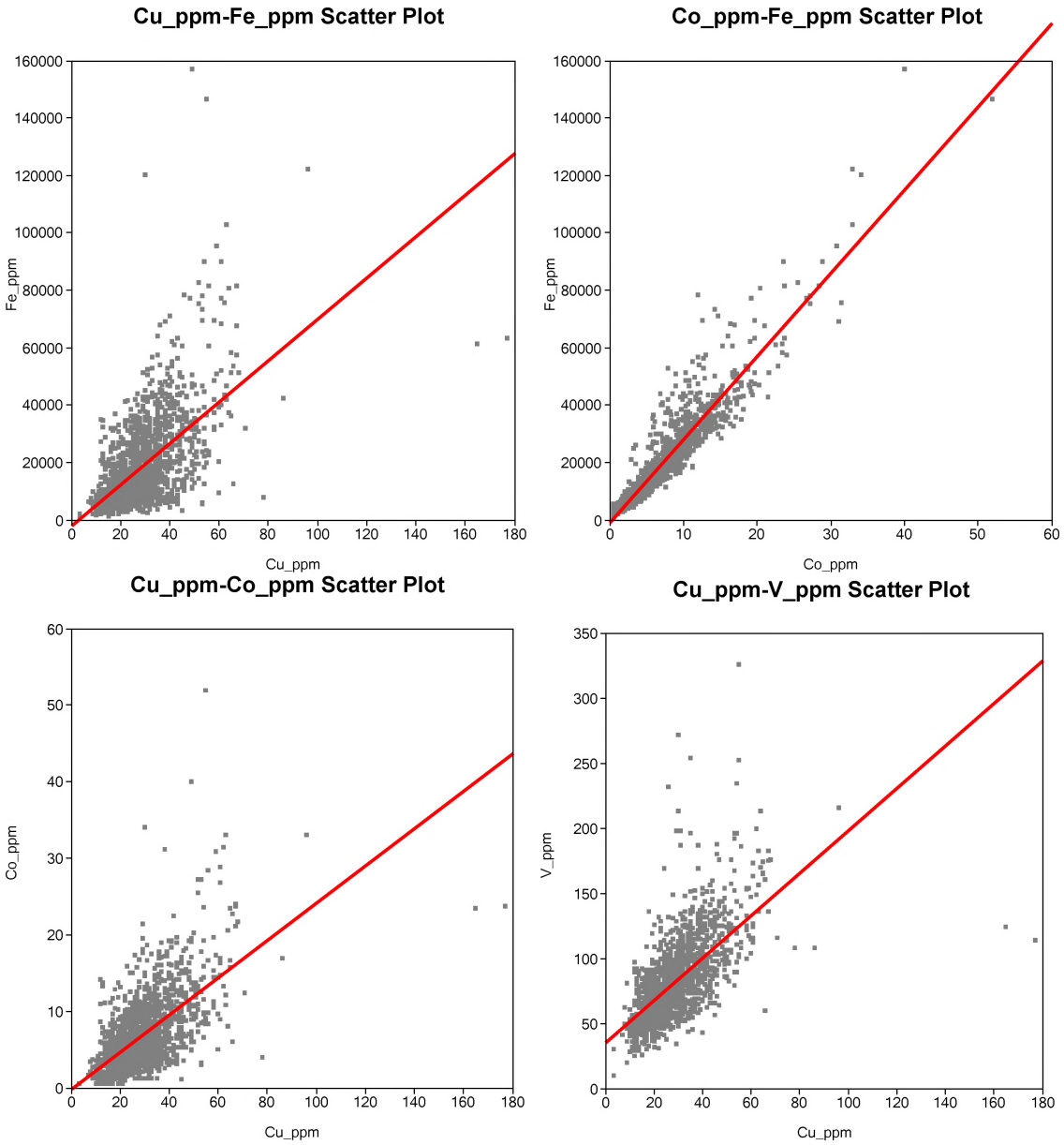

Figure 40: *XY Scatter plots of Pearson correlation matrices between some of the elements in the Matebo soil samples. Fe/Co, V/Co and V/Fe show a near linear correlation; suggesting that increase or decrease in one element corresponds to increase or decrease in the other.*

The high amounts of iron and low copper-cobalt content in the Matebo soil data may be indicating the level of leaching the area has undergone. In such strongly weathered environments copper and other elements that form complexes with chloride ions are and transported by oxidized, sulphate-rich fluids are depleted at the surface. This may potentially mask the geochemical response at surface of copper deposit in the subsurface. The strong Cu: Fe correlation (**Figure 40**) may not be attributed to the scavenging effects of iron oxides but rather a consequence of primary host rock composition since Cu and Fe tend to substitute for one another in silicate mineralogy. However, there is a significant cluster of points that

seem to be Cu depleted relative to Fe. This depletion could be a consequence of leaching. The V: Fe plot is very similar to the Cu: Fe pair correlation because vanadium can substitute for Fe in silicate minerals. In this way vanadium, and other soluble ions under oxidizing conditions, can be removed from surface soils by weathering processes and be retained in the groundwater or incorporated into clays.

Iron and cobalt are strongly correlated (**Figure 40**). This shows that the higher the iron content, the more cobalt is present. This seems to suggest iron is present mainly as iron oxides rather than as clays and may be adsorbing other elements. The strong positive correlation between Cu and Co is no surprise since Copperbelt style mineralisation often shows this geochemical relationship. Both Cu and Co are transported in oxidized fluids sourced from red beds in the Lower Roan and will precipitate together when they encounter reducing conditions.

Locations of anomalous samples are shown on geology and Landsat images in Figure 41 and Figure 42 respectively. These samples occur in areas underlain by stratigraphically higher rock units (Kundelungu) in the Katangan sequence not known to host mineralisation in the Zambian part of the Copperbelt. However, a giant copper deposit (Kamoa) was discovered recently hosted in the grand conglomerate (Schmandt et al., 2013).

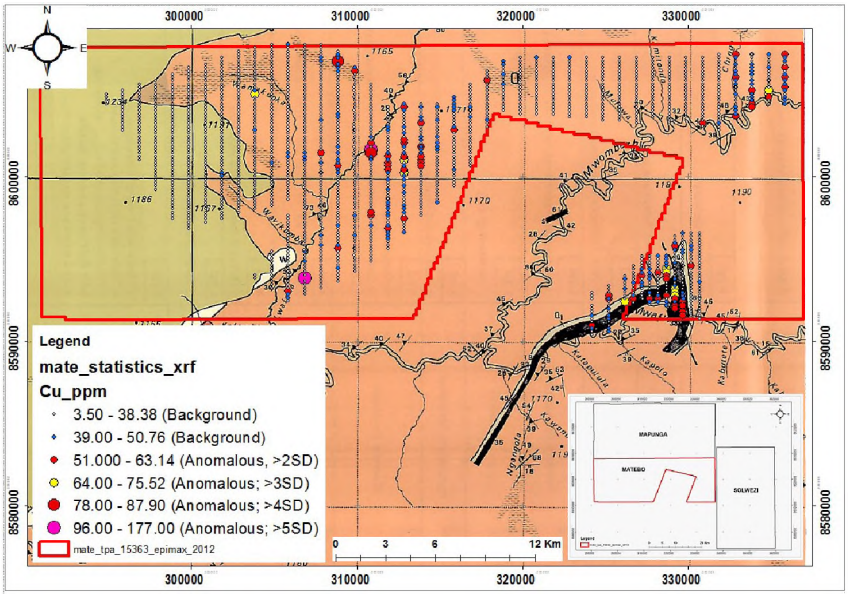

Figure 41: *Anomalous samples plotted on 250,000 scale geology map of the area (Yellow portion = Kalahari sand cover; Orange portion = Lower Kundelungu/Nguba; and thin black unit at the bottom right corner of grid is a siliceous shale outcrop).*

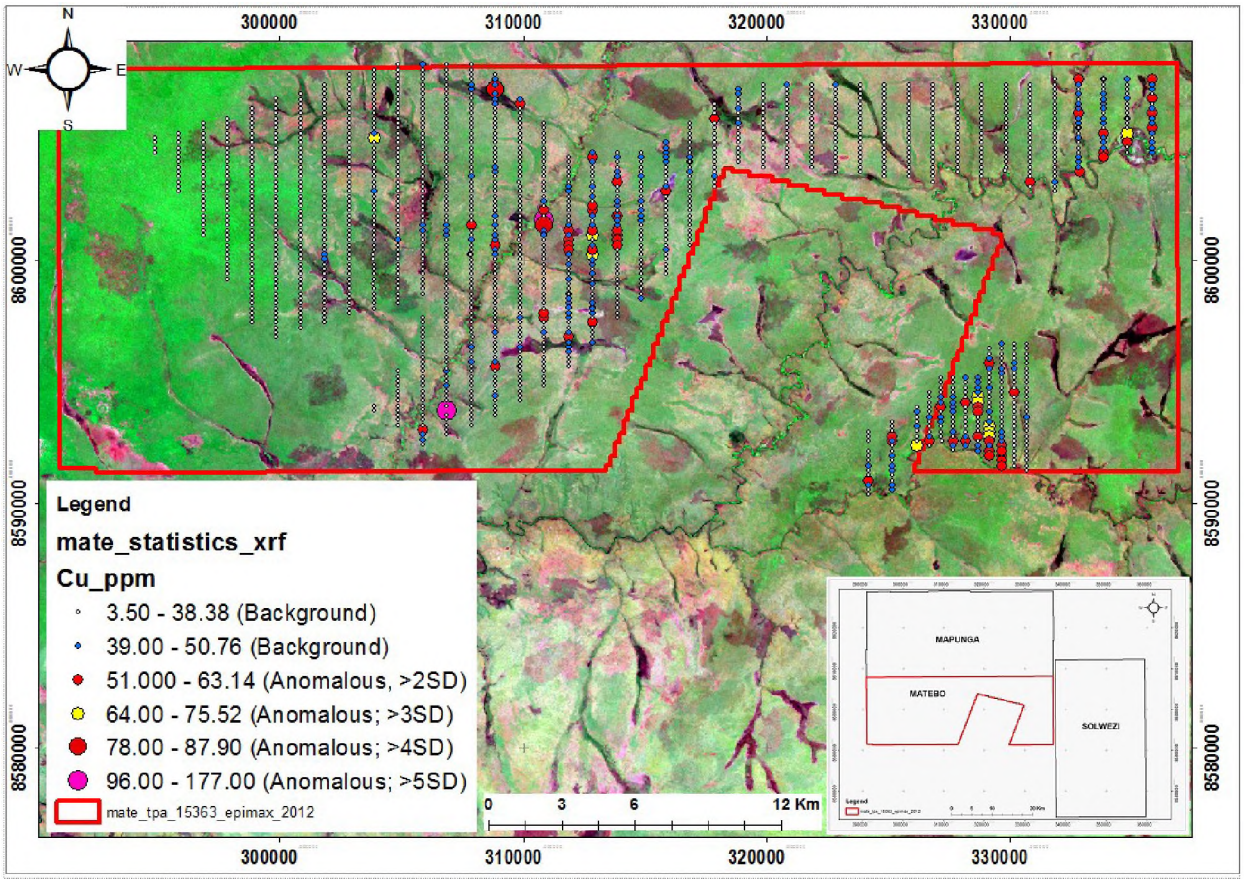

Figure 42: *Anomalous samples plotted on Landsat image; highest values in centre of grid falls on paleo dambo whilst those in southeast portion of the grid overlie shale and quartzite outcrops.*

6.2.4 Mapunga Tenement

This was the most northerly tenement closest to the deposits of Kalumbila (Sentinel Cu and Enterprise Ni) and is underlain by the most complete Katangan rock sequence characterised by prominent NW-SE trending structural features that appear to constrain mineralisation at the Sentinel deposit - 12 km north of this area. Descriptive statistics of key target elements in the Mapunga soil data are summarised in Table 11 below.

Table 11: *Descriptive summary statistics for Mapunga soil samples.*

Descriptive Statistics	Cu_ppm	Co_ppm	Ni_ppm	Fe_ppm	U_ppm	Pb_ppm	Bi_ppm	Mo_ppm
Count	4488	4488	4488	4488	4488	4488	4488	4488
Minimum	3.5	0.5	6.5	595	1.25	1	3.5	1.55
Maximum	297	175	237	658218	94	101	193	29
Range	293.5	174.5	230.5	657623	92.75	100	189.5	27.45
Skewness	2.46	2.65	0.83	3.5	37.7	9	4.3	2.83
Mode	28	0.5	6.5	595	1.25	1.7	4	1.55
Unique Values	130	438	149	4210	57	148	52	159
Mean	39.1	11.8	43.76	35160	1.59	3.6	8.21	3.05
Standard Deviation	20.03	14.6	29.46	48637	1.69	3.26	8.67	3
Median	35	5.8	42	15361	1.25	2.6	4	1.55
Confidence Level (95%)	0.59	0.43	0.86	1423	0.05	0.09	0.25	0.09
75th percentile	48	13.67	61	38456	1.25	4.7	11	3.4
90th percentile	64	32.41	80.1	102324	3	6.9	18.1	7.2
95th percentile	74	44	94	137914	3.9	8.65	27	9.3
99th percentile	104.11	67	130	199673	5.4	14.1	41	14.9

The data in **Table 11** shows overall low concentrations of Cu, Co and Ni in the soil positively skewed towards background concentrations for the majority of the samples. The upper background thresholds for Cu, Co and Ni are 55.03 ppm, 20.4 ppm and 71.46 ppm respectively. Minimum anomaly threshold for copper is 75.06 ppm; that of cobalt and nickel are 35 ppm and 100.92 ppm respectively. These anomaly threshold values give Co/Cu and Cu/Ni ratios as 0.37 and 0.74 in turn. These values closely resemble those calculated from the soil geochemical data at Sentinel where Co/Cu ratio was found to be 0.39 whilst the Cu/Ni ratio was 0.67. This implies brines of similar chemistry to those responsible for mineralisation at the Sentinel affected Mapunga area.

Grouping Mapunga copper geochemical data into class intervals by standard deviation gives 2 background populations and 6 anomaly populations with some outliers. These can be simplified into 4 main sample populations as follows: 3.5 – 75.06 ppm (background), 75.06 – 135.15 ppm (3^{rd} order anomaly), 135.15 – 195.24 ppm (2^{nd} order anomaly), and 195.24 – 297 ppm (1^{st} order anomaly). **Figures 43** (cumulative histograms), **44** (normal frequency histogram) and **45** (probability chart) below graphically illustrates this.

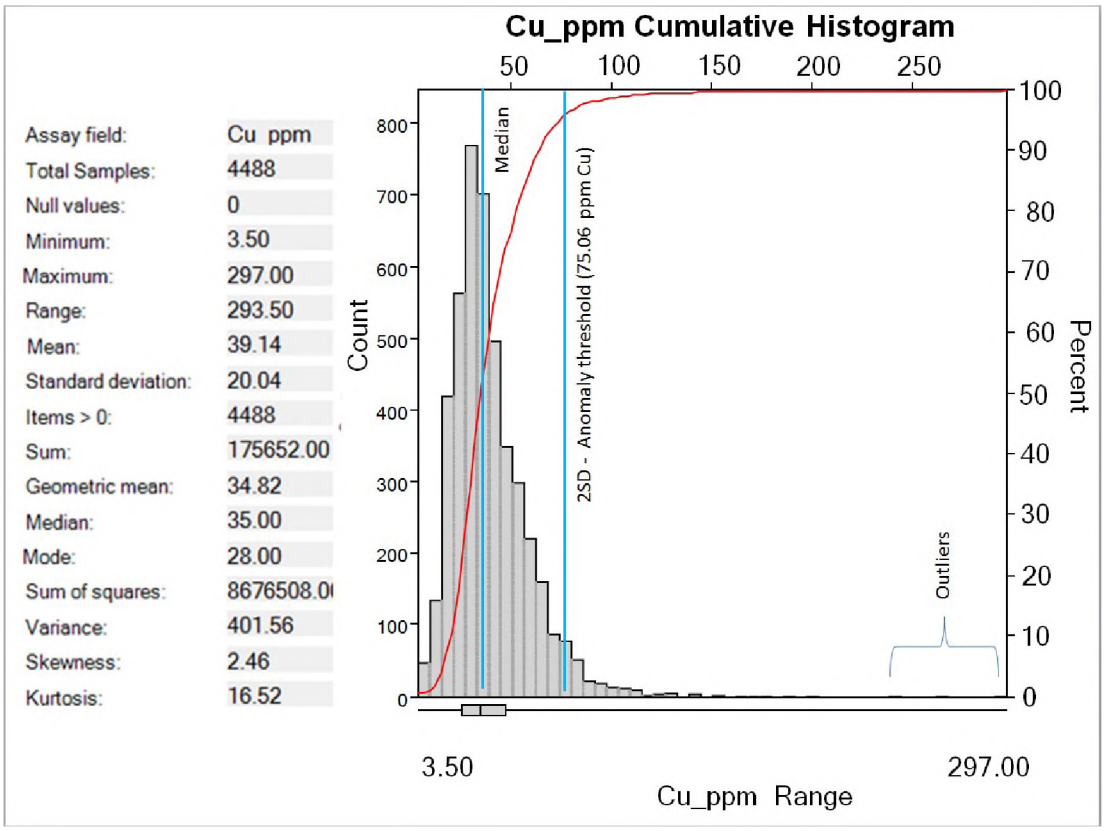

Figure 43: *Cumulative frequency histogram plot for Mapunga geochemical data; 95% of the samples lie in the background concentration whose upper limit is 75.06 ppm copper*

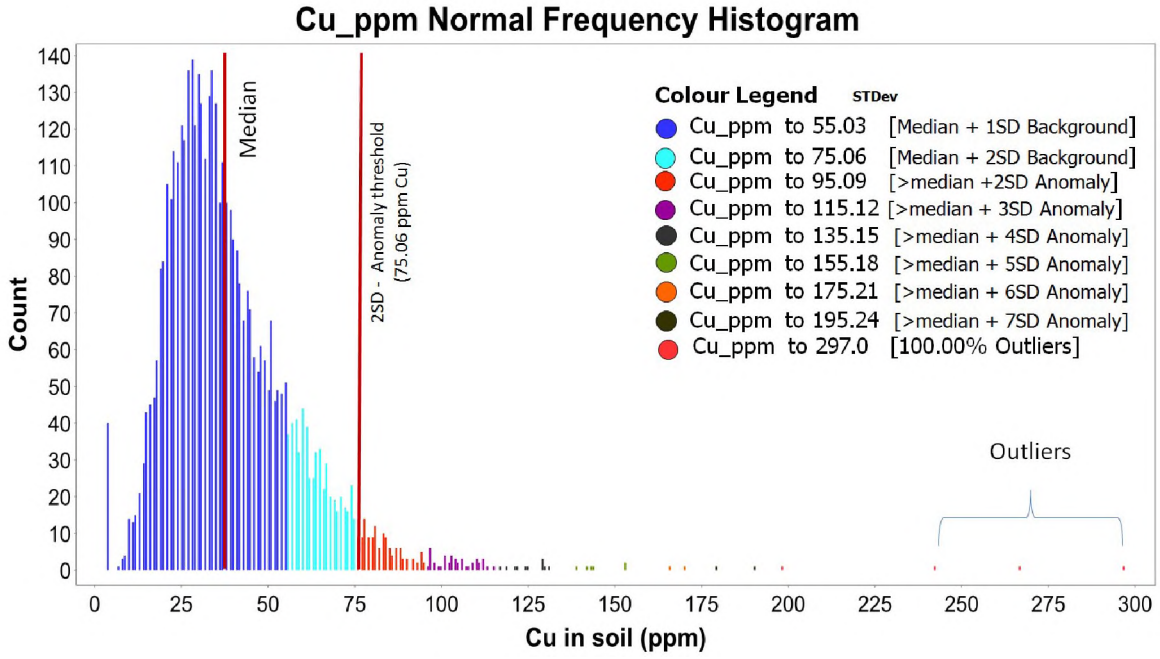

Figure 44: *Normal frequency histogram of copper concentrations in Mapunga soil; median =35 ppm; anomaly threshold = 75.06ppm. The legend in this plot groups sample populations by standard deviation into 2 background classes, 6 anomaly classes and some outliers.*

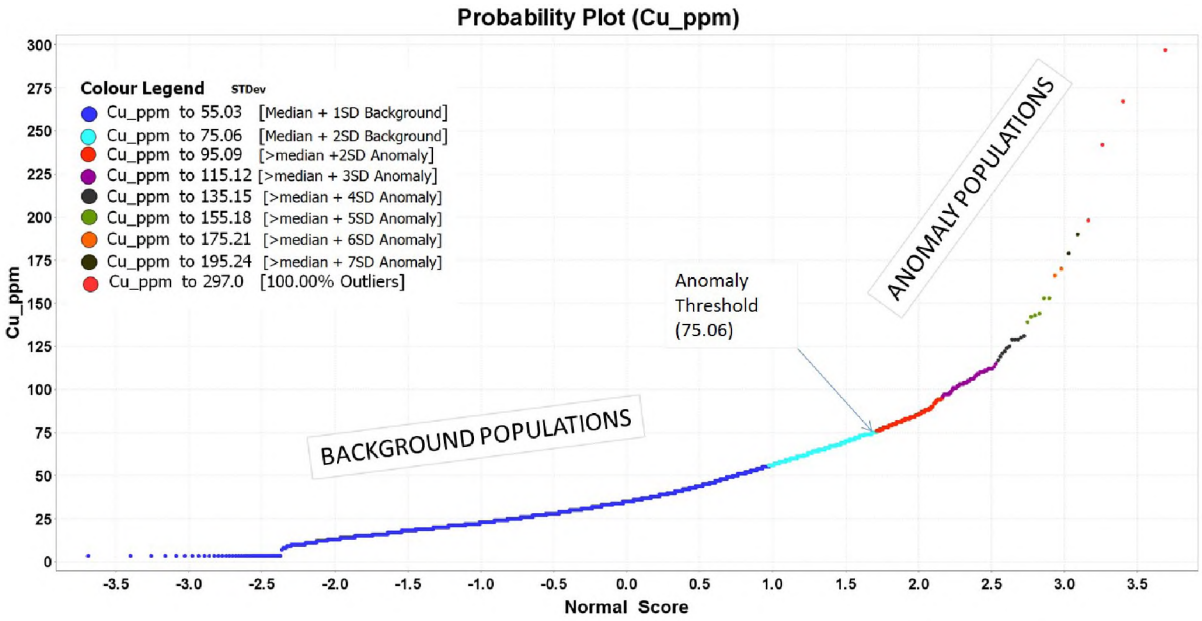

Figure 45: *Probability plot of copper concentration in soil (concentration, y-axis vs normal score, x-axis). At least three anomaly populations could be identified in the dataset (ranges from 75.06 – 135.15 ppm, 135.15 – 195.24 ppm and 195.24 – 297 ppm.*

The correlation matrix for important elements is depicted in **Table 12** and graphical view of element correlations are shown in scatter plots in **Figure 46**. As with Matebo samples, Mapunga samples show similar correlation between elements Cu/Co, Co/V and V/Ni to the copper deposit at Sentinel (Cu/Co = 0.45, Co/V = 0.75, V/Ni = 0.34). This level of copper in the Mapunga soil samples with its associated Co, Ni, Zn, Ag, V, Mo, Cd and Bi seem to point to shale or sandstone hosted sedimentary type copper deposit. Primary elements of interest (Cu, Co, Ni) show similar relationships seen with soils overlying Copperbelt deposit (Similar Cu/Co ratios; Cu/Mo ratios). This fact suggests possibility of Copperbelt style mineralisation in the tenement.

Table 12: *Pearson Correlation matrix between key target elements in Mapunga Soil samples (Laboratory assays).*

Correlation	Cu_ppm	Co_ppm	Ni_ppm	Mo_ppm	V_ppm	Bi_ppm
Cu_ppm	1	0.48	0.4	0.16	0.25	0.26
Co_ppm	0.48	1	0.68	0.12	0.45	0.063
Ni_ppm	0.4	0.68	1	0.11	0.47	0.2
Mo_ppm	0.16	0.12	0.11	1	0.23	0.13
V_ppm	0.25	0.45	0.47	0.23	1	0.29
Bi_ppm	0.26	0.063	0.2	0.13	0.29	1

Scatter plots in **Figure 46** show the content of iron and clays in the Mapunga soil data and the degree to which they affect target elements copper, cobalt and nickel. The Scandium-Copper (Sc/Cu) and Aluminium-Copper (Al/Cu) plots show significant populations of samples clustering along regression lines suggesting samples with background copper values occur in clay-rich samples. In these samples, an increase or decrease in clay content does not significantly increase or decrease the copper content. However, there are samples which are copper enriched relative to either scandium or aluminium – and so the copper values do not appear to be controlled by Al or Sc content.

The correlation between iron (Fe) and aluminium (Al) shows two trends. Above the regression line an increase in clay content (Al) corresponds to an increase in iron content. In this case Fe could be present as a clay rather than an oxide. Below the regression line Fe does not significantly increase with increase in Al. Fe is apparently present as iron oxide in these samples. This could explain why copper and cobalt show great affinity for Fe in the majority of samples although there are few samples that show Fe depletion relative to copper and cobalt trends. For this reason, it would imply Cu-Co concentrations in the Mapunga soils might not be reflecting the true original content as leaching could have depressed their amounts to present levels.

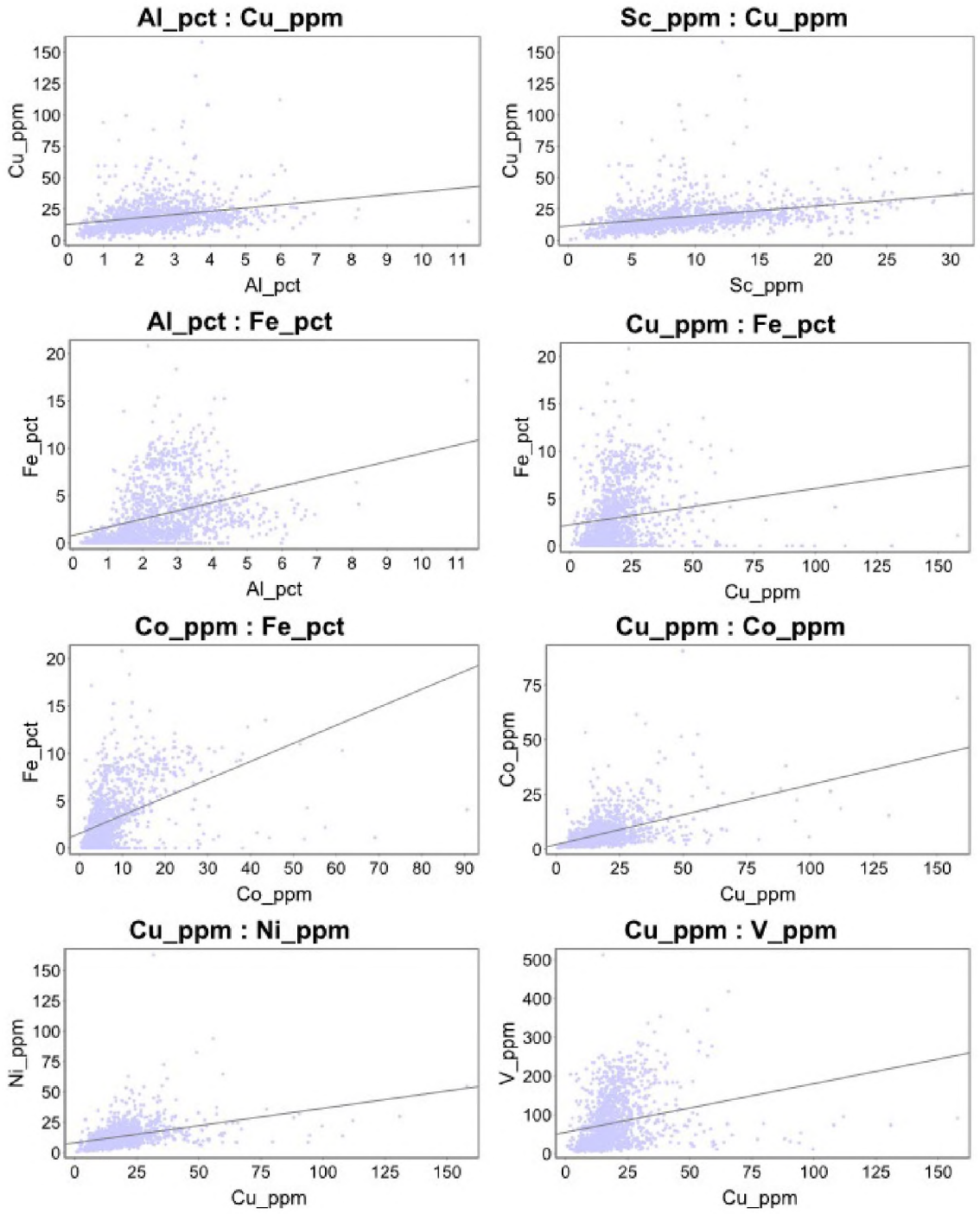

Figure 46: *XY Scatter plots of Pearson correlation matrices between some key target elements in the Mapunga soil samples. Cu/Co and Cu/Ni correlations show typical trends commonly observed on Sediment hosted copper deposits.*

Figures 47, 48 and 49 show the location of Mapunga samples plotted on geology, magnetic and Landsat images respectively. Most samples were collected over Upper Roan metasediments that underlie the greater portion of Mapunga tenement (area denoted by letter

J and shaded grey in **Figure 47**). The highest value of 989 ppm copper was obtained in a sample collected in the northeast corner of the tenement covered by Lower Roan metasediments overlying basement dome igneous rocks. This value was downgraded to 297-ppm copper when the location was re-sampled by extending initial the sample pit beyond the organic layer.

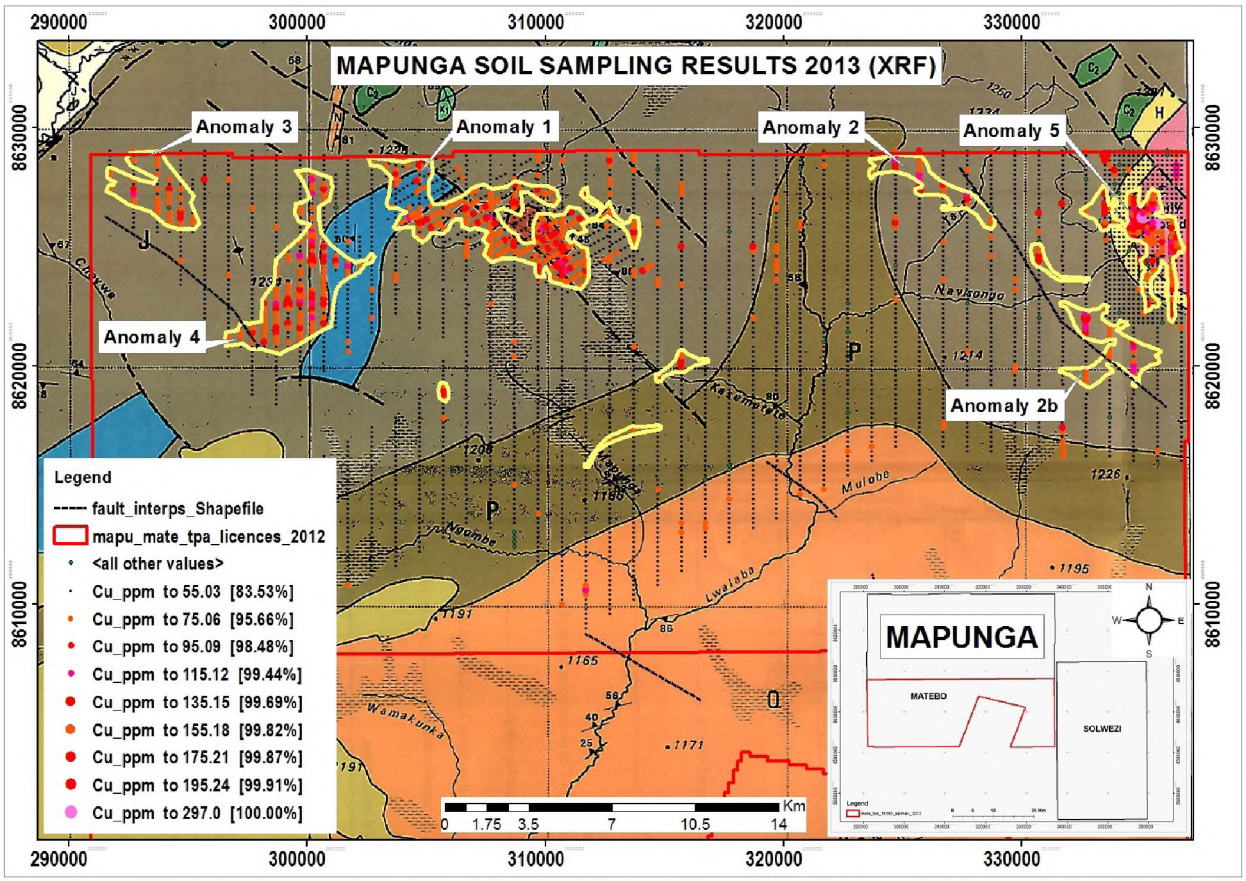

Figure 47: *Clusters of Cu anomalies, grouped on the basis of standard deviation, plotted on 1:250,000 scale geology map of Ntambu area (grey area =Upper Roan units; brown area = Mwashia age sequences; orange area = Lower Kundelungu calcareous, dolomitic, non-calcareous meta-argillite, meta-siltstones and quartzites).*

Anomaly clusters shown in Figure 47 were identified based on definition by standard deviation with median plus two times standard deviation used as a minimum cut-off. Tighter sampling grid spacing was employed in areas 1, 4 and 5 to delineate the anomalies further. Infill samples more or less retained similar levels of copper concentrations as in the original samples in regional lines. Copper anomalies in clusters 1 and 2 follow the trend of interpreted regional structures which run NW-SE and separates high magnetic domains from

low magnetic units (see **Figure 48**). These structures were interpreted from airborne regional magnetic.

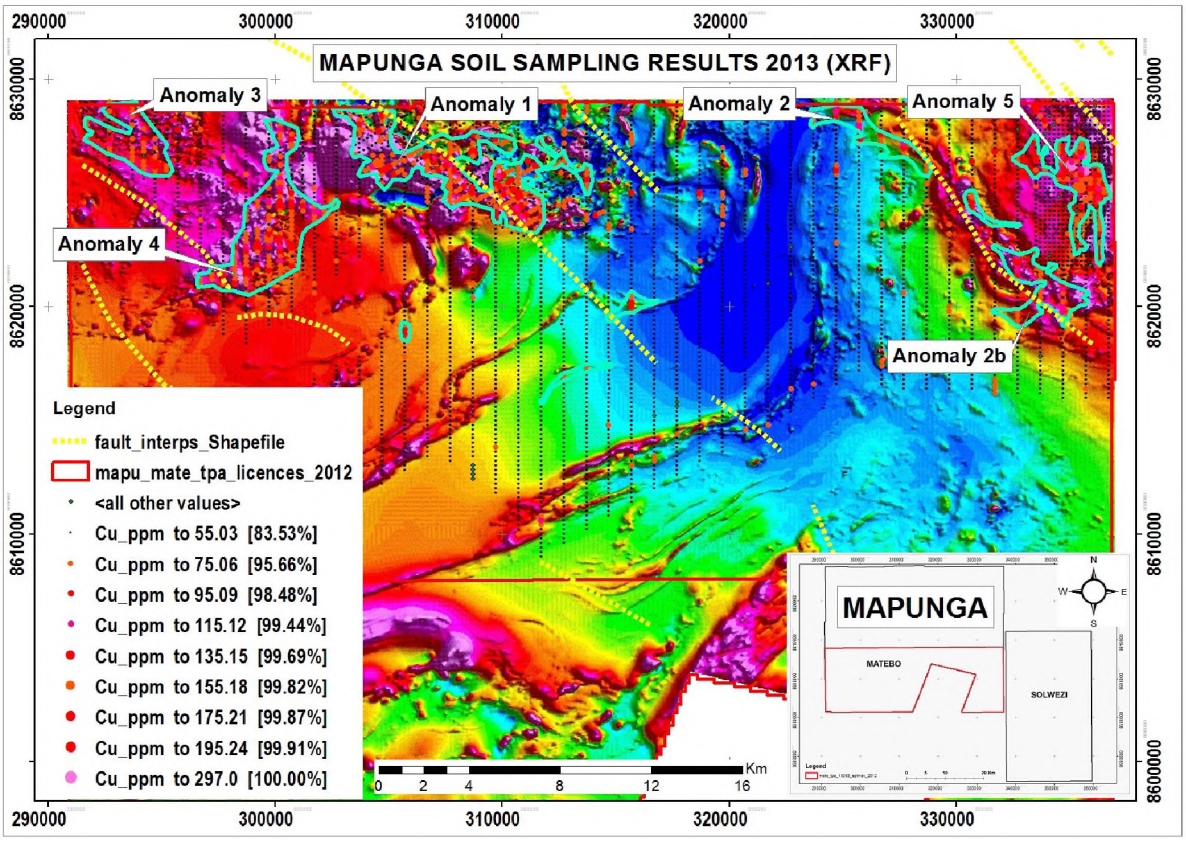

Figure 48: *Anomalous Copper clusters (blue polygons) plotted on magnetic image (rtp) with interpreted fault lines shown as yellow dashed lines. Anomaly clusters 1 and 2 follow NW-SE trending interpreted fault lines.*

There is very minimal rock outcrop in the area which makes it difficult to discern whether lithological interferences have an effect on soil geochemical results. Topography is relatively flat even though it is inundated with many streams and shallow water bodies which gently slope to the south at shallow gradient (**Figures 49 and 50**). For this reason, identified anomalies are not expected to have shifted far from their original positions, and therefore, could be related to "orebodies" in the immediate subsurface.

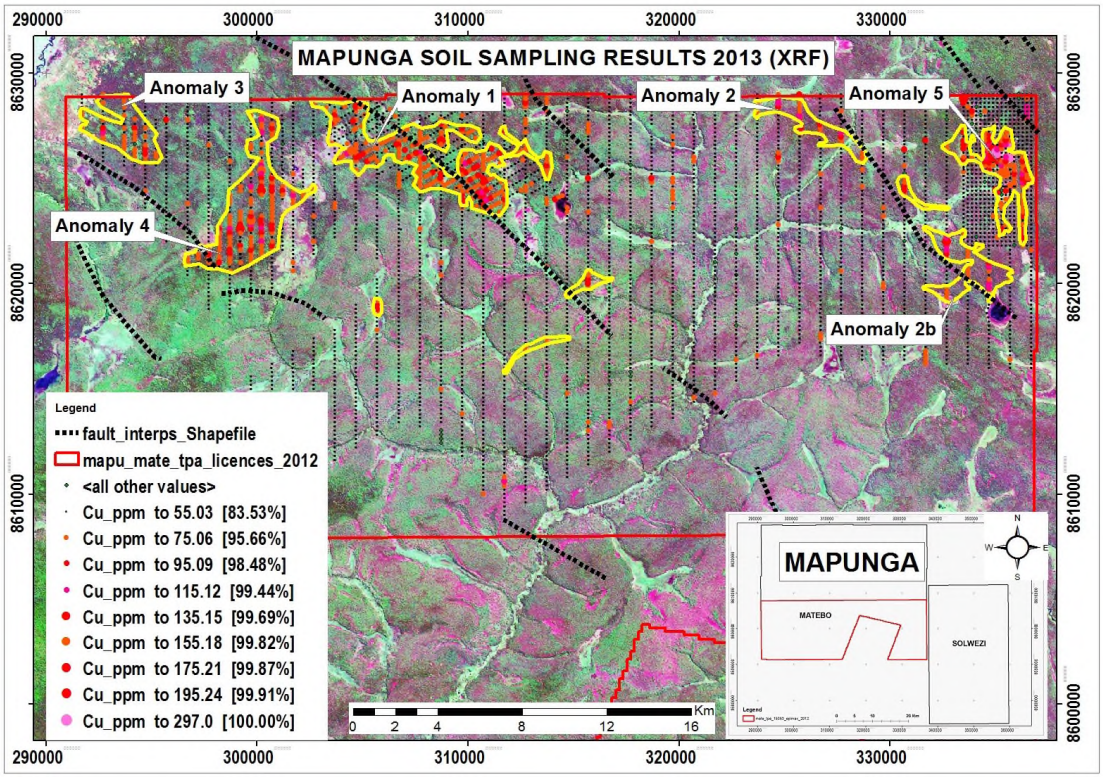

Figure 49: *Landsat image showing relief of the area and anomalous copper clusters (yellow polygons). Topography drops gently to the southwest.*

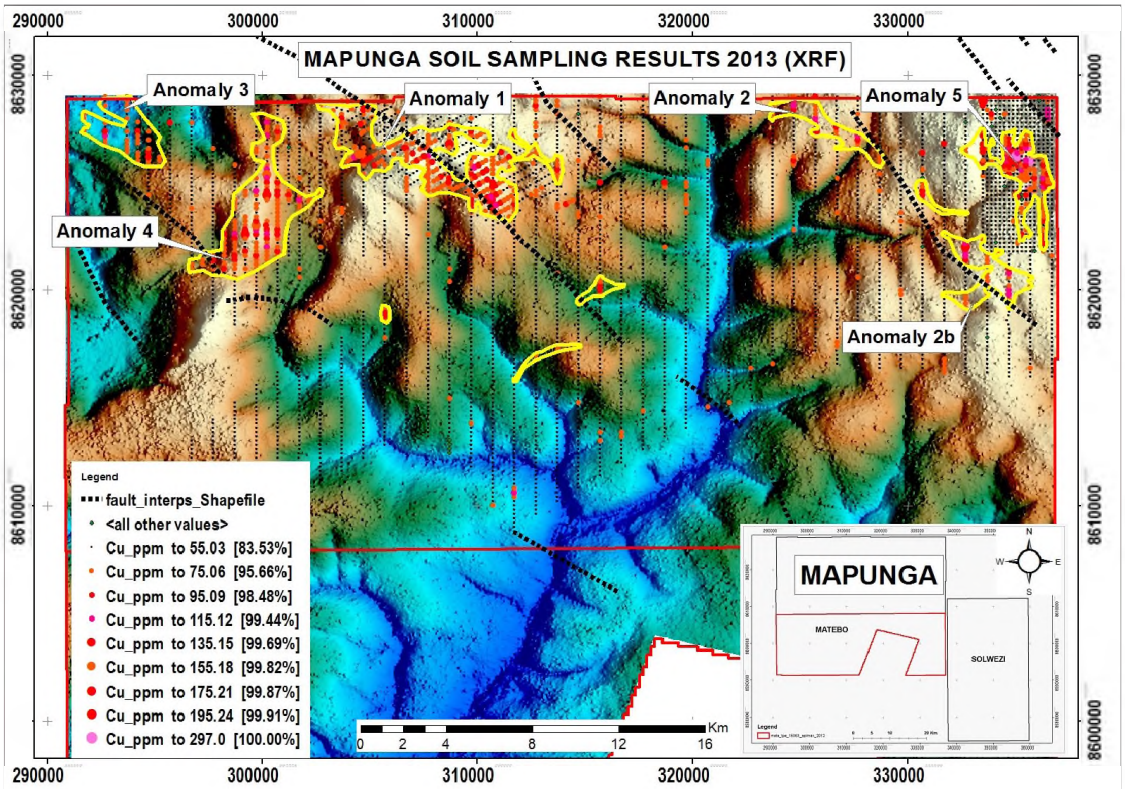

Figure 50: *Clusters of anomalous copper shown on DTM image.*

The following comments provide a summary of observations on samples in each of the anomaly clusters shown in Figures 47 to Figure 50.

Anomaly 1 – located in the central area and associated with a NW-SE trending structural lineament which demarcates high from low magnetic domains. This geochemical anomaly extends for approximately 10km strike length by 2km width. Mapping at 250k scale identified a small outcrop of syenite near the southeast end of this anomaly (sitting just north of the lineament). The small size of the syenite outcrop relative to the soil anomalism suggests it is unlikely to be the source. The low levels of Ti and Cr in the soil discounts this outcrop to be the source of the geochemical anomaly. Also, most elements expected to be high in soil of igneous origin such as chromite; titanium and manganese are low suggesting soil developed from metasedimentary source rather than from weathered syenite. Samples in this cluster have anomalous cobalt concentrations (xrf: 35.4 ppmCo – 175 ppmCo; laboratory: 14.6 – 90.6 ppm).

Anomaly 2 – located near the top right corner of the grid, is a thin linear soil anomaly averaging 0.50km width and a discontinuous strike length of roughly 14km. Along this deep seated structural feature most clearly identifiable on first derivative of magnetics, there are two main anomaly subsets: the northern-most cluster - a more coherent anomaly and measuring 5.6km in length and 0.6km in width; and the anomaly cluster **2b** to the south which measures 4km strike length by 0.7km width. This latter anomaly subset occupies a broad fold nose where Katangan rock sequence curves around the pre-Katangan basement changing strike direction from NW-SE to E-W.

Anomaly 3 – located in the top left corner of the tenement, appear to follow a NW-SE trending lineament best observed on first derivative of magnetics (TMI). The anomaly cluster roughly measures 4.0km in strike by 1.5km width. A few meters west of this soil geochemical anomaly (outside the study area), another exploration company was drilling for nickel mineralisation and going by discussions with supervising geologists on that drilling programme it seems the drill holes were intersecting mineralisation. A few samples in this cluster have anomalous cobalt concentrations.

Anomaly 4 – located between anomaly clusters 3 and 1 but separated by a barren gap of 4km on either side, this cluster has a NNE-SSW orientation and sits on the shoulder of a mapped carbonate unit to the east. The anomaly spans a distance of roughly 7.0km length by 2.5km width and is well defined by the 75 – 135 ppm copper contour lines. Over a 100 anomalous sample points are located in this anomaly cluster; although there are one or two samples that appear to fall within re-vegetated paleo-dambos where surface influences to the geochem signature cannot be ruled out. However, even by discounting these few samples from statistical analysis, the size of the anomaly remains unchanged. High Ca, Fe, Mn, V, Co, Zn, with moderate Cr is characteristic feature of this anomaly. These elements are typical in sedimentary type deposits. Zinc contents in this cluster (152 ppm) are well above normal levels in soil developed from limestone (25 ppm Zn background) or shales (100 ppm Zn background). The presence of vanadium and zinc without uranium discounts black shale as the underlying lithology. Samples in this cluster pass the test often applied to SEDEX Pb-Zn-Ag deposits where the index 100Zn/(Zn+Pb) falls within the range 60 – 77 with standard deviation not exceeding 15 (Houston and Large, 1987). Nearly all samples in this cluster have anomalous cobalt levels. This cluster should be treated as a potential Cu-Zn-Co target.

Anomaly 5 – is located in the top right corner of the grid in an area with the most identical geological setting to majority of the Cu-Co deposits of the Zambian Copperbelt. Anomalous samples fall on a thin curvilinear sliver of Lower Roan unit that wraps around the pre-Katangan basement dome. This soil geochemical anomaly roughly measures 2.8km by 1.2km. Majority of the samples overlie a high magnetic domain which probably represents the basement units. However, a plot of **Ti/Zr** ratio, an index commonly used to identify igneous rocks in deeply weathered terrains (Hallberg, 1984) does not suggest soil developed from igneous rocks. Extensive "ground-truthing" traverses in the area concluded surface weathering activities had some influence on the soil geochemistry especially on soils developed in dambos. This conclusion was arrived at when a previously sampled point with 989 ppmCu reported a much reduced chemical response when the same hole was deepened (297 ppmCu and 16 ppmCu in B- and C-horizons respectively).

7. DISCUSSION AND INTERPRETATIONS

It is worth noting that studies on the Copperbelt have established a regional zonation of mineralisation from the paleo-shoreline close to the Kafue anticline westwards (Mendelssohn, 1961). We can deduce that the grade of copper deposits would most likely decrease from the established paleo-shoreline westwards. Therefore, the soil geochemical footprint in the areas to the west of the Copperbelt cannot (and must not) be expected to be of similar geochemical concentrations as those from the Copperbelt even though the deposits may be of a similar mode of occurrence. Furthermore, we know that depths of ore deposits and weathering activity will have an impact on the type and strengths of the geochemical surface expression.

This aside, comparisons with existing deposits in the vicinity of study areas will give pointers of what geochemical footprint to expect in the soil anomalies that are related to mineralisation. For instance at the nearby Sentinel copper deposit a regional sampling campaign (1000 m x 100 m) defined the copper–hosting carbonaceous phyllite with a 60 ppm Cu contour whilst the 100 – 200 ppm Cu contour highlighted and constrained the host unit further. On the other hand, the Enterprise Nickel deposit was outlined by the greater than 80 ppm Ni contours. All anomalous samples directly overlying the deposit had concentration levels in between the range 80 – 695 ppm Ni. At Kansanshi copper deposit on the northern flanks of the Solwezi Dome, the >200 ppm Cu contour defined the deposit for over a strike length of 7.0 km by 3.0 km width. A halo of manganese enveloping the deposit is one of the characteristic features of Kansanshi.

In the Kalumbila area, soils have a correlation ratio in the order of 0.4 for Fe/Cu, Cu/V, Cu/Co and Cu/Bi. In soils overlying Copperbelt deposits Co/Cu ratios range from 1:10 to 0.3 with anomalous cobalt concentrations ranging between 20 – 80 ppm and background values falling within 7 – 14 ppm. In assessing soil anomalies for potentially representing buried deposits in the study areas, these figures have been referenced.

7.1. Solwezi Tenement

The Solwezi tenement has virtually no exposures of lithology save for few places along river channels. Calcareous siltstones, siliceous shales and dense moderately magnetic dolomites were the only rock types observed on the Mushingashi, Mwafwe and Maheba river banks. Laterite cappings are very widespread in this concession.

The area was explored with two deposit models in mind; sedimentary stratiform copper style and vein style mineralisation. Priority targets were low magnetic domains in close proximity to magnetic highs (refer to Figure 51 below).

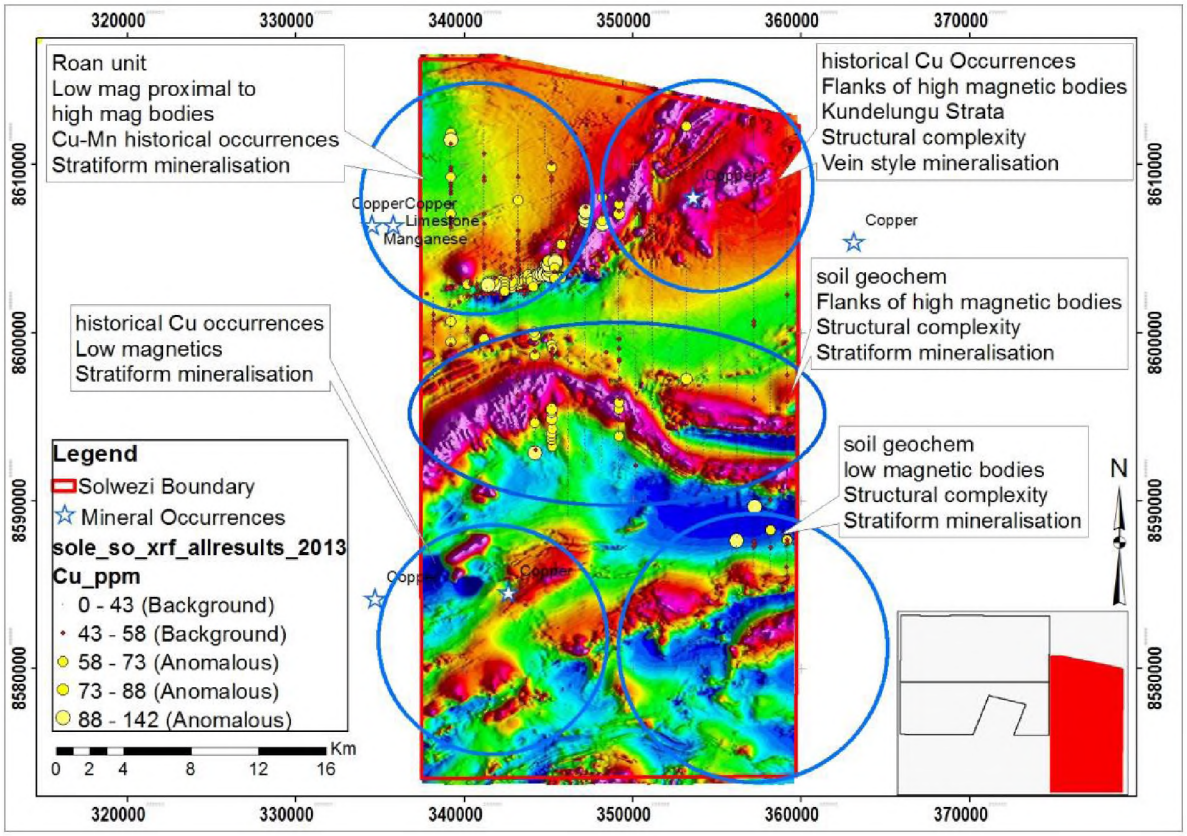

Figure 51: *Magnetic image (rtp) with summary motivation for targeting strategy employed in Solwezi tenement.*

Results from the geochem sampling programme reviewed a small anomalous area measuring **5.0** km by **0.40** km defined by copper in soil values ranging between 58 – 142 ppm (**Figures 34, 35, 51**). This range was statistically calculated using the median plus two times the standard deviation as minimum anomaly threshold. The anomaly was highlighted by 210 samples making up 11% of total samples collected. For size comparison, Sentinel Copper deposit, 50 km northwest of this area, occurs in the 11 km long Mwashia carbonaceous shale with copper mineralisation confined to the 4.0 km x 1.0 km portion of that carbonaceous shale. Sentinel occurs on a pronounced magnetic low in close proximity to high magnetic bodies, just like this soil geochemical anomaly in Solwezi. The Sentinel host shale has a high electromagnetic response. This geophysical technique could be employed in the Solwezi tenement to further scrutinise the identified geochemical target.

Maximum metal concentrations in the soils were 142 ppm Cu, 292 ppm Co, 11.7% Fe, 113 ppm Zn, 686 ppm Pb, 495 ppm V, 78 ppm Mo, 14 ppm Ag and 223 Bi among other elements. Certainly 142 ppm copper concentration is not very classical when looked at in terms of typical Copperbelt soil concentration levels, but in this region (~200km west of the Copperbelt); 142 ppm copper in soil can be significant. These values, with the exception of vanadium, appear to be above the level of abundances expected in soils and shales (Levinson, 1974). Levinson's listing of average abundances of elements in various materials is shown in **Table 13**.

Table 13: *Tabulation of range of average abundances for selected minor and trace elements in various media (Levinson, 1974). All values are in ppm except those on water which are in ppb. (*) indicate no data available.*

Element	Earth's Crust	U/mafic	Basalt	Granodiorite	Granite	Shale	Limestone	Soil	River Water
Ag	0.07	0.06	0.1	0.07	0.04	0.05	1	0.1	0.3
As	1.8	1	2	2	1.5	15	2.5	1.5	2
Au	0.004	0.005	0.004	0.004	0.004	0.004	0.005	*	0.002
Ba	425	2	250	500	600	0.004	100	100-300	10
Bi	0.17	0.02	0.15	*	0.1	700	*	*	*
Co	25	150	50	10	1	20	4	1.4	0.2
Cr	100	2000	200	20	4	100	10	5-1000	7
Cu	55	10	100	30	10	50	15	2-100	7
Hg	0.08	*	0.08	0.08	0.08	0.5	0.05	0.03	0.007
Mn	950	1300	2200	1200	500	850	1100	850	7
Mo	1.5	0.3	1	1	2	3	1	2	1
Ni	75	2000	150	20	0.5	70	12	5-500	0.3
Pb	12.5	0.1	5	15	20	20	8	2-200	3
Pd	0.004	0.02	0.02	*	0.002	*	*	*	*
Pt	0.002	0.02	0.02	*	0.008	*	*	*	*
Sb	0.2	0.1	0.2	0.2	0.2	1	*	5	1
Sn	2	0.5	1	2	3	4	4	10	*
Ti	5700	3000	9000	8000	2300	4600	400	5000	3
U	2.7	0.001	0.6	3	4.8	4	2	1	0.4
V	135	50	250	100	20	130	15	20 - 500	0.9
W	1.5	0.5	1	2	2	2	0.5	*	0.03
Zn	70	50	100	60	40	100	25	10-300	20

Plot of copper values using a split probability curve graphically illustrates sample clustering by standard deviation. The graph shows five sample populations in the dataset subdivided

into three clusters of background 3 clusters of anomalous populations (**Figure 52**). When samples in the anomaly clusters were treated by aqua regia digestion (partial digestion technique) and ICP-MS finish, retained assays were very depressed by as much as 79% compared to HHXRF results. It is usual for portable xrf spectrometers to indicate higher concentrations of elements because they are a total 'digestion' technique which measure total available elements in the sample at the point measured. However, this magnitude of difference in concentration levels was not anticipated. This had an effect of reducing the anomaly size from 5.0 km by 0.40 km to just well above 0.90 km by 0.20 km. Another likely cause for this difference in assay magnitude, apart from digestion method, could be insufficient homogenisation in the field prior to analysis.

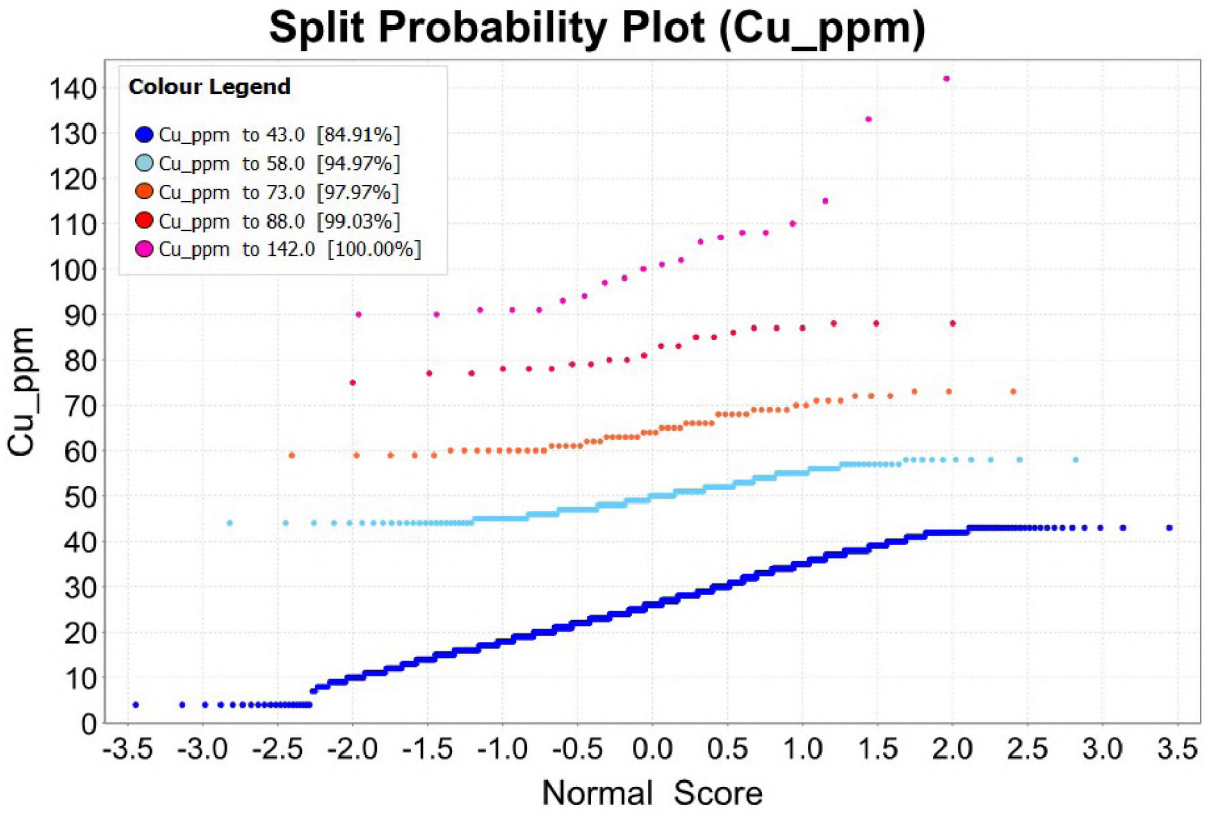

Figure 52: *Split probability plot defining sample population in Solwezi soil geochem XRF data: 2 clusters of background and 3 clusters of anomaly populations.*

7.2. Matebo Tenement

Very limited outcrops exist in this grid which has topography that gently slopes to the south. A ridge of Quartz Mica Schist interlayered with Quartzite and a thin band of siliceous Shale occurs at the bottom portion of the tenement. Other outcrops of siltstones and shales are only exposed in river channel. Analysis of soil samples established a statistical anomaly of values ranging between 50.76 – 177 ppm copper using the median and two times standard deviation as minimum anomaly threshold. The highest copper value came from a river catchment area where influence of surface weathering processes cannot be discounted. However, high iron content (0.3% to 27.3%) probably masks copper concentration levels in the soils as interpreted from Figure 40 above, where increase in iron does not significantly increase copper content. Geochemical anomaly defined by statistics occupies 3.0km stretch overlying thin black shale of probable Mwashia age at the bottom of the grid. Five sample populations were identified in the data and these are categorised into 2 background and 3 anomalous clusters (see **Figure 53**).

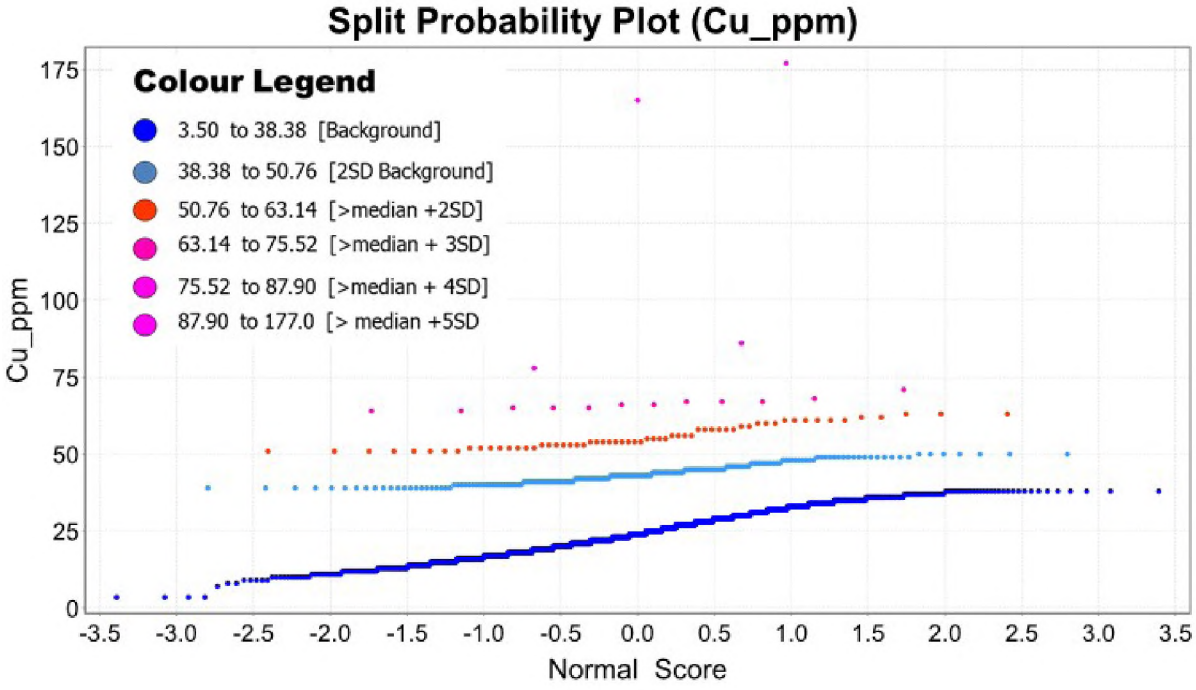

Figure 53: *Split probability plot defining sample populations in Matebo soil geochem data (xrf). Two sample anomaly populations and 4 background populations.*

This grid is in a very remote place far removed from any infrastructural utilities such as electricity, road network etc., so any deposit to be discovered in this area must be large

enough to offset infrastructural development costs. The geochemical anomalies observed in the grid do not suggest presence of such large deposits. In this regard, there is very little potential for finding economically viable deposit in this grid.

7.3. Mapunga Tenement

Mapunga was explored with the aim of finding Copperbelt-Style stratiform and IOCG type deposits. This area has all the characteristics observed on Copperbelt and Kalumbila deposits: Katangan strata proximal to Mwombezhi Basement Dome; NW-SE trending structural features known to be associated with mineralisation in the region; and low to high magnetic domains observed on other deposits within the Lufilian Fold Belt (**Figure 54**).

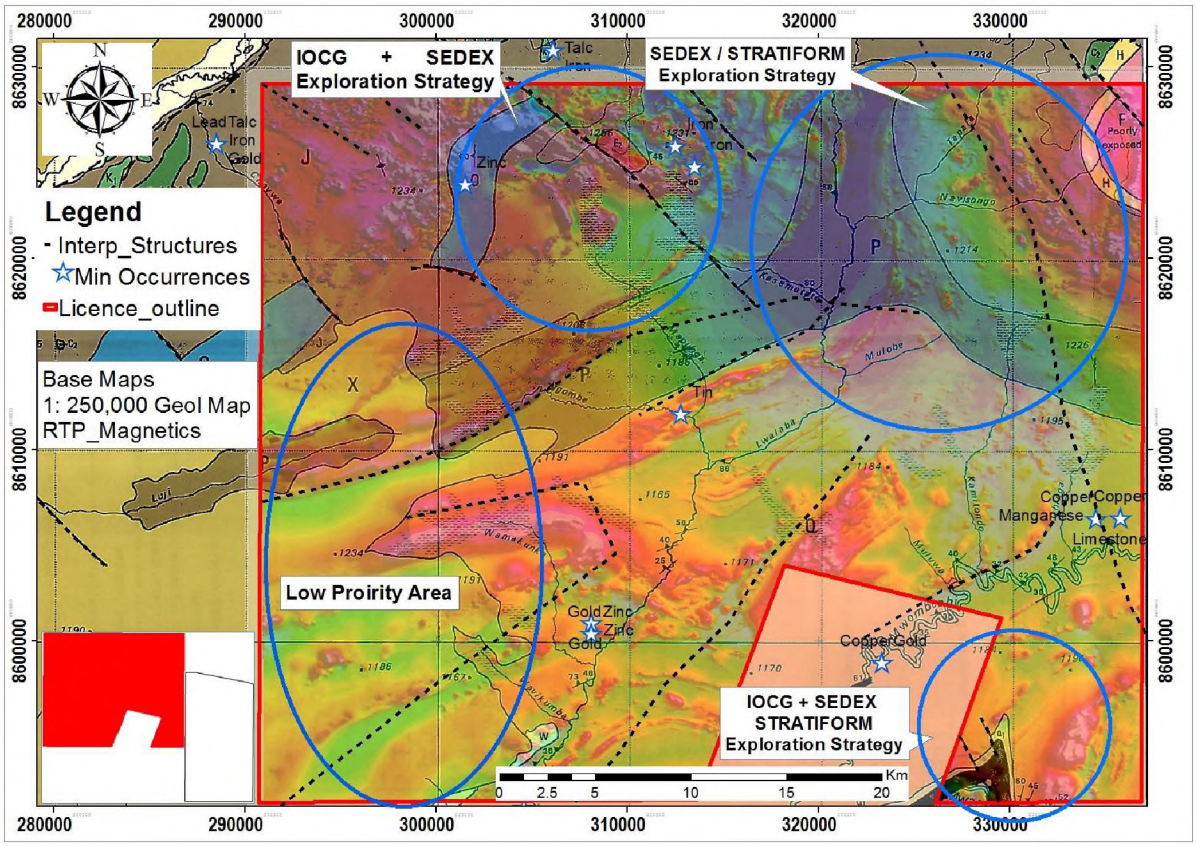

Figure 54: *Summary map showing priority targeting areas in Mapunga-Matebo tenements depicted on AS Magnetic image draped on 250k Geology map.*

The deep reddish-brown to yellowish orange colouration of Mapunga soils is due to the high iron content which ranges from 0.1% to 65.8%. These levels of iron indicate intense leaching of the area. This might explain the low levels of copper observed in the soils of the area and a number of false positive anomalies observed in the surrounding areas particularly on carbon-

rich (darker) soils. The Cu/Fe scatter plot in Figure 46 shows the majority of samples with copper concentrations in the background ranges have very high Fe content whilst all samples with anomalous copper concentrations are depleted with regards to Fe content.

When laboratory assays are plotted using anomaly thresholds established with HHXRF spectrometer results, the geochemical footprints of the 5 anomaly clusters shrink in size. Laboratory assays peaked at 158 ppm Cu compared to 297 ppm Cu by HHXRF. Anomaly cluster number 3 disappeared completely whilst clusters 1 and 2 remain as point anomalies (**Figure 55**). However, this does not portray an entirely accurate picture since only samples from anomalous populations defined by HHXRF were subjected to laboratory analysis.

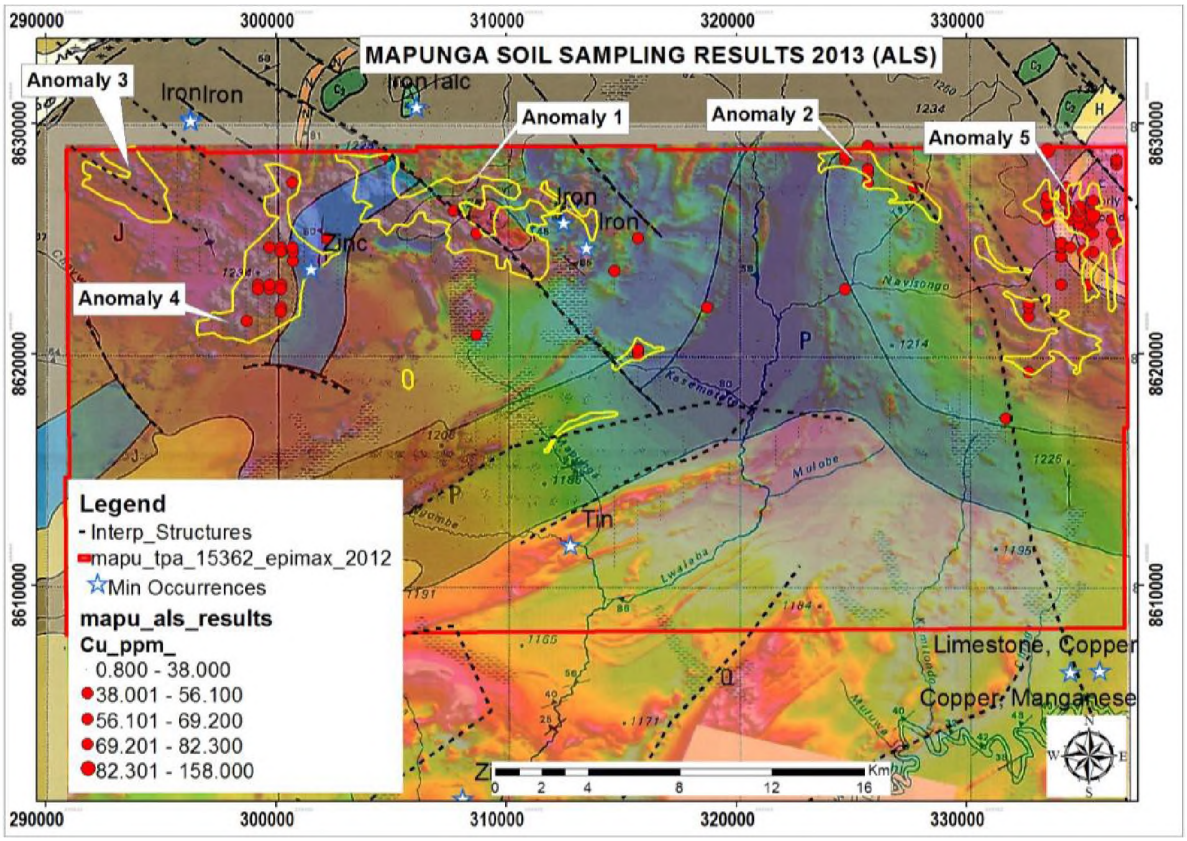

Figure 55: *Laboratory assays plotted on geology and magnetic image backdrop. Anomaly cluster 3 disappears; clusters 1 and 2 are reduced to point anomalies whilst cluster 4 and 5 shrinks in size.*

These anomaly clusters are located in very interesting positions. Geochemical cluster number 1, located on a structure close to the syenite intrusion, is very conducive to IOCG type deposits. Cluster 1 is a copper – cobalt target. Soils in this tenement are low in Cr, Mn and Ti which discounts lithological weathering contributions from intrusive units and thus, suggest development from metasedimentary rock types. Considering laboratory assays, point

anomalies in cluster number 2 covers an area of just over 1.0km length by 0.2km width in the fringes of the basement dome. Though the geochemical footprint is not large enough to suggest giant buried deposit, it is still an anomaly requiring further exploration testing. Both clusters 1 and 2 are Cu-Co targets with cobalt concentrations between 14.6 ppm to 90.6 ppm (laboratory assays).

Anomaly Cluster 4 is a Cu-Zn-Co target located on the margin of the Marble band within the Biotite-Garnet schist of the Upper Roan. Anomalous Zn varies from 56.4 ppm to 182 ppm whereas cobalt values are in the range 35.4 ppm to 79.5 ppm. This area has a known Zn mineral occurrence which is confirmed by anomalous Zn in the soils.

Anomaly cluster 5 seems to occupy an area known to be underlain by sub-outcropping basement sequences of the Mwombezhi Dome enveloped by Katangan rocks of the Lower Roan and Upper Roan groups. However, field traverses highlighted numerous excavations and shallow shafts in banded ironstones exposed by previous explorers. Since banded ironstones are a constant feature in the Mwashia Group of the Katangan stratigraphy, that portion of Mapunga could be covered by Mwashia age metasediments.

Anomaly cluster 5 had the highest copper value of 989 ppm reported in the dambo environment. This value was deemed too high even for black cotton soils in this region so a follow-up exercise was instituted aiming to establish the source of the anomalous concentration. A fence of pits around the 989 ppm Cu point were sampled at base of A-horizon and within the B-horizon of the soil profile and results compared (**Figure 56**). It is clear surface weathering processes are either responsible for anomalous copper in black cotton soils, or there is a narrow weathered mineralised vein completely obscured by eroded surface material. Source of anomalous copper in this sample certainly needs further investigation.

Figure 56: *Sample pits dug in dambo to ascertain source of anomalous copper. In all the pits copper concentration decreased from the surface downwards.*

Overall, Mapunga soil geochemical data identified at least 4 anomaly clusters that need further exploration testing. Anomaly clusters 1, 2, 4, and 5 all copper-cobalt targets established by both XRF and wet chemistry results. Grouping laboratory assays by standard deviation (**Figure 57**) gives 2 background and 3 anomalous populations with the interval 69.2 – 158ppm Cu as the first order anomaly in the data.

Pearson correlation for pairs Cu/Co, Cu/Ni, Cu/Ag, Cu/Pb and Cu/V are in the range 0.25 to 0.48 (Table 12 above) typical for Copperbelt style sediment hosted copper mineralisation. Most elements associated with Copperbelt style mineralisation (Co, Cu, Pb, Zn, Ni, Ag and V) converge in these 4 anomaly clusters. Anomalous cobalt values in the Copperbelt deposits fall with the range 20 – 80 ppm. In this tenement anomalous cobalt values from laboratory assays vary between 19.9 – 90.6 ppm.

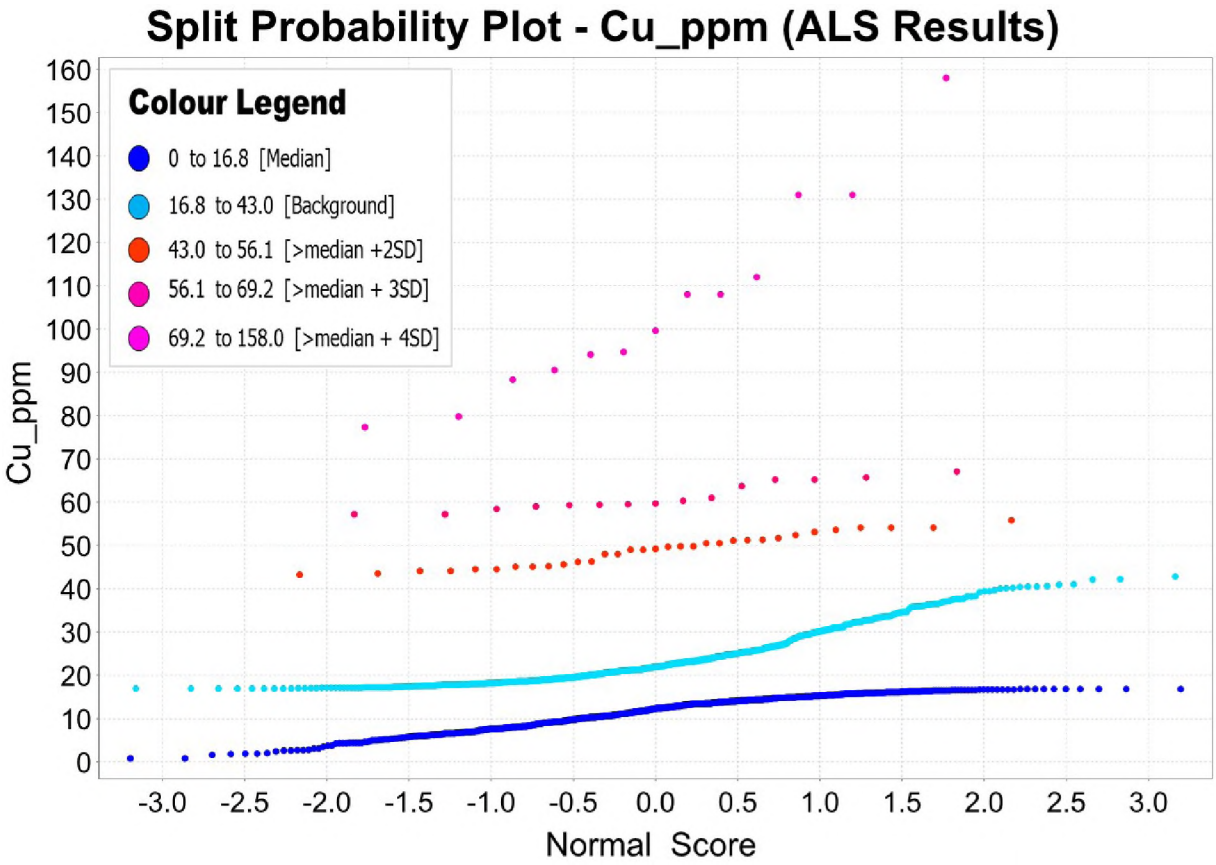

Figure 57: *Split probability plot of laboratory results defining 4 background populations and 2 anomalous populations. Anomalous concentrations fall between 43 – 158 ppm copper, 19.9 – 90.6 ppm cobalt, and 20.6 – 91 ppm zinc.*

8. CONCLUSIONS

There has been very limited historical exploration works carried out in the study areas. Historical explorers, who were mainly focused on finding economic quantities of iron ore, identified isolated occurrences of banded iron formations which they exposed by trenching and pitting. Occurrences of zinc, tin, manganese, gold, copper and limestone were also identified during this historical exploration. However, prior to this study, no recent exploratory works have been carried out in the study which employ modern techniques of soil geochemistry.

This study noted many geological attributes inherent in the NW Province of Zambia that are conducive for hosting copper-cobalt mineralisation: strategic location within the mineral district of the Domes Region proximal to Sentinel copper and Enterprise nickel deposits; comparable geophysical attributes to those observed at existing mines in the region; similar structural complexities known to be associated with mineralising events in the region; and the wide range of deposit styles possible in the region as evidenced by Vein-style deposit of Kansanshi, Stratiform style at Kalumbila, basement hosted copper at Lumwana, and a horde of many other oxide copper mineralisations dotted all over NW Province (Kalaba, Kalengwa, Zambesia, Luamata, Lalafuta, etc.).

Geochemical surveys completed in the study areas generated statistical anomalies that require further evaluation with particular consideration to anomaly size, anomaly location, associated elements in the anomaly cluster as well as to the strengths of elemental concentrations. Anomaly clusters in the Mapunga grid are located on either linear structural features or sit at lithological boundaries within Katangan strata. Though conceptual exploration approach is useful in NW Province, it should be noted that the geology of the province is poorly known comparable to that of the Copperbelt Province. This is due to deep soil cover in NW Province except in Basement highs where the geology is exposed somewhat. Empirical exploration approach needs to go hand in hand with conceptual approach in order to generate large number of geochemical targets for further screening. Geochemical anomalies identified in Mapunga need to be scrutinised further before they can be dismissed.

The geochemical anomaly established in the Solwezi grid shrunk in size from 5000m x 400m (xrf results) to 900m x 200m (laboratory results). Location of this anomaly in the low

magnetic domain shadowing high magnetic bodies is similar to Sentinel Copper deposit owned by First Quantum Minerals Limited. The chemical footprint (Cu, Co, Ni, V, and Ag) is typical of sedimentary type deposits found in the Zambian Copperbelt and the Cu/Co, Cu/Ni, Co/Ni, and Co/V are within typical ranges of Copperbelt style mineralisation.

Great potential of finding copper-cobalt deposits in the study areas exist. The soil geochemical anomalies must be further tested by trenching and pitting prior to drilling. The anomalous clusters are well place on structural features that can be interpreted to be physical traps that, perhaps, helped to transport and focus Cu, Co, and Ni bearing brines into the area. Banded ironstone exposed in excavations help us to place the underlying geology in the study area of Mapunga in the Mwashia stratigraphic Group where we know chemical traps exited that helped trap the copper-nickel-cobalt deposit at Sentinel.

9. RECOMMENDATIONS

The statistical anomalies generated in the soil geochemical data must be followed up to checked whether they are indicative of underlying economic deposits. The anomaly cluster in Solwezi which has a closest resemblance to the Sentinel deposit in terms of its geophysical character can easily be checked by acquiring airborne electromagnetics data. Sentinel copper deposit is a low magnetic signature deposit but responds strongly to electromagnetics. If the soil anomalism coincides with strong electromagnetic response, drilling can then follow.

Relatively cheap ground Induced Polarisation and Gravity surveys should be executed over the anomaly clusters in Mapunga and Solwezi to check for vein and massive sulphide mineralisation. A couple of lines, 2 or 3, over each anomaly cluster should be enough to give good data to enable make informed decision whether or not to proceed with drill testing.

The cheapest screening tool that need to be performed prior to any of the methods mentioned above should be trenching and pitting across all established geochemical anomalies. Auger drilling to base of saprolite would also be a quick way of testing whether chemical responses obtained in surface soils would be replicated, if not bettered, at depth. In the case of anomaly cluster 5 in Mapunga where a 989 ppm copper value was obtained in the dambo, further rings of pits around this sample must be dug and sampled to ascertain provenance of copper anomalism. A closely spaced infill sampling grid must be executed in the surrounding areas up-slope of this sample to try and trace surface passage of this copper anomalism.

10. REFERENCES

Anand, R.R., Lintern, M.J., Noble, R.R.P., Aspandiar, M., Macfarlane, C., Hough, R., Stewart, A., Wakelin, S., Townley, B., and Reid, N., 2014, Geochemical Dispersion Through Transported Cover in Regolith-Dominated Terrains-Toward Understanding of Process, Society of Economic Geologists, Inc., Special Publication 18, p1-000 (Draft Copy).

Anand, R.R., Lintern, M.J., Townley, B., Noble, R.R.P., Wakelin, S., Macfarlane, C., Hough, R., Smith, P., Aspandiar, M., Carr, G., Korsch, M., Reith, F., Phang, C., Reid, N., Gray, D.J., Soongpankhao, S., Soto, M. C., López, L. F., Luca, R., Hill, S., Pinchand, T., Gregg, A., and Reich, M., 2009, Predictive geochemistry in areas of transported overburden: CSIRO/AMIRA Final Restricted Report P2009/1788, 138p.

Annels, A.E., 1974, Some aspects of the stratiform ore deposits of the Zambian Copperbelt and their genetic significance,In: Bartholome P. (Ed), Gisements stratiforms and Provinces Cupriferes, p.235-254, Societe Geologique de Belgique, Liege.

Appleton, J.D., 1978, The geology of the Kabompo Gorge area; explanation of degree sheet 1225 NW Quarter, Report of the Geological Survey of Zambia, no.40, Government Printer, Lusaka, 48p.

Armstrong, R. 2001, The Western Arm of the Lufilian Arc in NW Zambia and its potential for Copper mineralisation. Journal of African Earth Sciences, v. 33, p. 503-528.

Armstrong, R.A., Master, S., and Robb, L.J., 2005, Geochronology of the Nchanga Granite, and constraints on the maximum age of the Katanga Supergroup, Zambian Copperbelt: Journal of African Earth Sciences, v. 42, p. 32-40.

Armstrong, R.A., Robb, L.J., Master, S., Kruger, F.J., Mumba, P.A.C.C. 1999, New U-Pb age constraint on the Katangan sequence, Central African Copperbelt, Abstracts, IGCP 418, 2nd Field Meeting, Kitwe, Zambia, p. 48-49.

Barrick Gold Corporation, 2016, Annual Report, A Company of Owners (http://barrick.q4cdn.com/808035602/files/annual-report/Barrick-Annual-Report-2016.pdf).

Barron, J.W., 2003, The Stratigraphy, Metamorphism and Tectonic History of the Solwezi Area, NW Province, Zambia: Integrating Geological Field Observations and Airborne Geophysics in the Interpretation of Regional Geology. PhD thesis (unpublished), Colorado School of Mines, Golden, Colorado, USA, 233p.

Barron, J.W., Broughton, D.W., Armstrong, R.A., Hitzman, M.W., 2003, Petrology, Geochemistry and Age of Gabbroic Bodies in the Solwezi Area, North-western Zambia, in Contributions presented at the 3rd IGCP-450 Conference, Proterozoic

Sediment-hosted Base Metal Deposits of Western Gondwana; Conference and Field Workshop, Lubumbashi, Democratic Republic of Congo, p. 75–77.

Bartholome, P., Evrard, P., Katekesha, F., Lopez-Ruiz, J., Ngongo, M., 1971, Diagenetic ore-forming processes at Kamoto, Katanga, Republic of the Congo, In: Amstutz G. C. And Bernard, A.J., (Eds), Ores in sediments, International Union of Geological Sciences, Series A, No.3, Springer-Verlag, New York, p.21-41.

Bateman, A. M., 1930, Ores of the Northern Rhodesian Copperbelt, Economic geology, v.25, p.365-418.

Bau, M., 1999, Scavenging of dissolved yttrium and rare earths by precipitating iron oxyhydroxide: Experimental evidence for Ce oxidation, Y-Ho fractionation, and the lanthanide tetrad effect, Geochimica et Cosmochimica Acta, v.63, p. 67-77.

Bernau, R. 2007, The Geology and Geochemistry of the Lumwana Basement-hosted Copper-Cobalt (Uranium) Deposits, NW Zambia: PhD thesis (unpublished), Southampton, U.K., University of Southampton, School of ocean and Earth Sciences, 187p.

Binda, P. L., 1994, Stratigraphy of Zambian Copperbelt orebodies, Journal of African Earth Sciences, v.19, no.4, p. 251-264.

Binda, P., & Van Eden, J. 1972, Sedimentological evidence on the origin of the Precambrian great conglomerate (Kundelungu tillite), Zambia, Paleogeography, Paleoclimatology, Paleoecology, v.12, no. 3, p. 151-168.

Brems, D., Muchez, Ph, Sikazwe, O., Mukumba, W., 2009, Metallogenesis of the Nkana copper-cobalt South Orebody, Zambia, Journal of African Earth Science, vol.55, p.185 - 196.

Brown, A.C., 1997, World-class sediment-hosted stratiform copper deposits: characteristics, genetic concepts and metallotects, Australian Journal of Earth Science, vol.44, p. 317-328.

Brown, A.C., 2005, Refinements for footwall red-bed diagenesis in the sediment-hosted stratiform copper deposits model, Society of Economic Geologist, Inc., vol.100, p. 765 - 771.

Broughton, D., Hitzman, M., & Stephens, A., 2002, Exploration History and geology of the Kansanshi Cu(-Au) deposit, Zambia, Society of Economic Geologists, Special Publication, v.9, p. 141-153.

Brummer, J.J., Woodward, G.D., 1999, A history of the Zambian Copper Flower, Becium Centraliafricanum (B. Homblei), Journal of Geochemical Exploration, vol.65, p.133-140.

Cahen, L., Snelling, N.J., Delhal, J., Vail, J.R., Bonhomme, M., and Ledent, D., 1984, The geochronology and evolution of Africa, Clarendon Press, Oxford, 512p.

Cailteux, J., Binda, P., Katekesha, W., Kampunzu, A., Intiomale, M., Kapenda, D., 1994, Lithostratigraphical correlation of the Neoproterozoic Roan Supergroup from Shaba (Zaire) and Zambia, in the Central African Copper-Cobalt Metallogenic Province, Journal of African Earth Sciences, v.19 no.4, p. 265-278.

Capistrant P. L., Hitzman W. M., Wood, D., Kelly, N. M., Williams, G., Zimba M., Kuiper Y., Jack, D., Stein H., 2015, Geology of the Enterprise Hydrothermal Nickel Deposit, North-Western Zambia, Economic Geology, v. 110, p. 9-38.

Carey H., Cevallos C, Feijth, J., 2012, Fundamental Geological Interpretation of helicopter electromagnetic, Magnetic, and Radiometric Data North of Chililabombwe, Zambia. Fugro Airborne Surveys, Summary Report, Project # 2301, Konnoco Zambia Limited (Unpubl. Internal Report), 87p.

Coward, M., & Daly, M. 1984, Crustal lineaments and shear zones in Africa: Their relationship to plate movements, Precambrian Research, v. 24, no.1, p. 27-45.

Davidson, C.M., 1931, The geology and deposits of Chambeshi, Northern Rhodesia, Economic Geology, Vol.26, p. 131 - 154.

De Swardt, A.M.J., Drysdall, A.R., 1964, Precambrian Geology and Structure in Central Northern Rhodesia, Memoirs of the Geological Survey North Rhodesia, 2, 82p.

De Waele, S., Muchez, P., Vets, J., Fernandez-Alonzo, M., & Tack, L., 2006, Multiphase origin of the Cu–Co ore deposits in the western part of the Lufilian fold-and-thrust belt, Katanga (Democratic Republic of Congo), Journal of African Earth Sciences, v. 46 no.5, p. 455-469.

Diederix, D., 1977, The Geology of the Nchanga Mining Licence Area, Nchanga Consolidated Copper Mines Limited, Chingola Division, Geology Department, 79p., (Internal report, copies available from the Geological Survey of Zambia).

Drysdall, A.R., Johnson, R.L., Moore, T.A., Thieme, J.G., 1972, Outline of Zambian Geology, Geologie en Mijnbouw, v.51, p. 265-276.

Edmonds, A.C.R., 1976, The Vegetation Map (1:500, 000,) of Zambia, Forestry Department, Ndola, Government of Zambia, sheet 1.

Fairchild, I. J., & Kennedy, M. J., 2007, Neoproterozoic glaciation in the Earth System, Journal of the Geological Society, London, Vol.164, p. 895 – 921.

First Quantum Limited, 2012, Update on Kansanshi and Enterprise Mineral Resource and Reserve Estimates, Marketwire, December 4, Vancouver, British Columbia; (http://www.first-quantum.com/Media-Centre/Press-Releases/Press-Release-Details/2012/First-Quantum-Minerals-Provides-Update-on-Kansanshi-and-Enterprise-Mineral-Resource-and-Reserve-Estimates1132197/default.aspx).

First Quantum Limited, 2012, Mineral Resource and Reserve Estimates for Sentinel Copper Project, Marketwire, March 26, Vancouver, British Columbia; (http://www.mining.com/first-quantum-minerals-provides-mineral-resource-and-reserve-estimates-for-its-sentinel-copper-project-zambia/).

Fleischer, V.D., Garlick, W.G., Haldane, R., 1976, Geology of the Zambian Copperbelt, In: Wolf, K.H. (Ed.), Handbook of stratabound and stratiform ore deposits, Vol. 6, Elsevier, New York, pp 223-352.

Fleischer, V.D., 1984, Discovery, geology and genesis of copper-cobalt mineralisation at Chambeshi Southeast prospect, Zambia, Precambrian Research, vol.25, (1-3), p. 119 - 133.

Freeman, P.V., 1988, Description of some mineral deposits discovered or re-investigated in the post-world war II period, Geological Survey of Zambia, 205p.

Garlick, W.G., 1961, The Syngenetic theory, In: The geology of the Northern Rhodesian Copperbelt (Edited by Mendelsohn, F.), McDonald, London, p. 146 – 165.

Garlick, W.G. and Fleischer, V.D., 1972, Sedimentary environment of the Zambian copper deposition, Geologie Mijnbouw, vol.51, p.271 – 299.

Govett, G.J.S., 2010, Early years in geochemical prospecting research, Centre, Imperial College of Science and Technology, London: Exploration geochemistry in Zambia in the 1950s; personal recollection, Geochemistry, Exploration, Environment, Analysis, vol.10 no.3, p. 237 – 249.

Gray, A., 1929, The outline of the geology and ore deposits of the Nkana concession, 15th International Geology Congress.

Greyling, L.N., Rob, L.J., Master, S., Boiron, M.C., Yao, Y., 2005, The nature of early basinal fluids in the Zambian Copperbelt: A case study from Chambeshi deposit, Journal of African Earth Sciences, v.42, p. 159-172.

Hallberg, J.A., 1984, A geochemical aid to igneous rock identification in deeply weathered terrain, Journal of Geochemical Exploration, v.20, p. 1-8.

Hayes, T.S., 1990, A preliminary study of thermometry and metal sources of the Spar Lake stratabound copper-silver deposit, Belt Supergroup, Montana, U.S. Geological Survey Open File Report 90-0484, 30p.

Hitzman, M.W., Kirkham, R.V., Broughton, D.W., Thorson, J., and Selley, D., 2005, the sediment-hosted stratiform copper ore system: Economic Geology 100th Anniversary Volume, p. 609-642.

Hitzman, M.W., 2011, Observations on a visit to First Quantum's Trident Project and on Fishtie Project Drillcore, 20p., (Unpubl. Internal Report).

Houston, D.L., and Large, R.R., 1987, Genetic and Exploration Significance of the Zinc ratio (100Zn/(Zn+Pb)) in massive sulphide systems, Economic Geology, v.82, p. 1521-1539.

Jackson, G.C.A., 1932, The geology of the Nchanga district, Northern Rhodesia, Quarterly journal of the Geological Society of London, vol.88, p.443 - 514.

John, T., Schenk, V., Haase, K., Scherer, E., Tembo, F., 2003, Evidence for a Neoproterozoic ocean in south central Africa from MORB-type geochemical signatures and P-T estimates of Zambian eclogites, Geology, v.31, p. 243-246.

John, T., Schenk, V., Mezger, K., and Tembo, F., 2004, Timing and PT evolution of whiteschist metamorphism in the Lufilian Arc-Zambezi belt Orogen (Zambia); implications for the assembly of Gondwana, Journal of Geology, v.112, p. 71-90.

Johnson, P.S., Rivers, T., and De Waele, B., 2005, A Review of the Meso-proterozoic to Early Palaeozoic Magmatic and Tectonothermal History of South-Central Africa: implications for Rodinia and Gondwana, Journal of the Geological Society, London, v.162, p. 433-450.

Kabengele, M., Mashala, T., Loris, N.B.T., 2003, Geochemistry of the Lower Mwashya pyroclastic rocks in the Likasi-Kambove area (Democratic Republic of Congo), Contributions presented at the third IGCP-450 Conference: Proterozoic Sediment-hosted Base Metal Deposits of Western Gondwana, Conference and Field Workshop Lubumbashi, Democratic Republic of Congo, p. 69–74.

Kampunzu, A.B., 1998, Intraplate Magmatism and Tectonics of Southern Africa, Gondwana Research (Gondwana Newsletter Section), v.1, nos. 3/4, p. 424-425.

Kampunzu, A., Cailteux, J., Kamona, A., Intiomale, M., & Melcher, F., 2009, Sediment-hosted Zn–Pb–Cu deposits in the central African Copperbelt, Ore Geology Reviews, v.35 no.3, p. 263-297.

Kampunzu, A.B. and Cailteux, J., 1999, Tectonic evolution of the Lufilian Arc (Central Africa Copper Belt) during Neoproterozoic Pan African Orogenesis, Gondwana Research, v.2, no.3, p. 401-421.

Key R. M., De Waele, B., Liyungu, A. K., 2004, A multi element baseline geochemical database from the western extension of the central African Copperbelt in north western Zambia, Applied Earth Sciences, v.113, 22p.

Key, R.M., Liyungu, A.K., Njamu, F.M., Somwe, V., Banda, J., Mosley, P.N. and Armstrong, R.A., 2001, The Western Arm of the Lufilian Arc in NW Zambia and its potential for copper mineralisation, Journal of African Earth Sciences, v.33, p. 503-528.

Key, R., and Banda, J., 2000, The Geology of the Kalene Hills area, Explanation of those parts of quarter degree sheets 1124NW, 1023SE and 1024SW that lie in Zambia, report of the Geological Survey of Zambia, no.107, 56p.

Key, R.M., Liyungu, A.K., Njamu, F.M., Somwe, V., Banda, J., Mosley, P.N. and Kirkham, R.V., 1989, Distribution, settings and genesis of sediment-hosted stratiform copper deposits, Geological Association of Canada, Special Paper, v.36, p. 503-528.

Kirkham, R.V., 1989, Distribution, settings and genesis of sediment-hosted stratiform copper deposits, Geological Association of Canada, Special Paper v.36, p. 3-38.

Klinck, B.A., 1977, The Geology of the Kabompo Dome area: Explanation of quarter degree sheet 1227NE, Report of the Geological Survey of Zambia, no.44, 44p.

Kokonyangi, J., Kampunzu, A.B., Armstrong, R., Yoshida, M., Okudaira, T., Arima, M., and Ngulube, D.A., 2006, The Mesoproterozoic Kibaride belt (Katanga, SE, D.R. Congo), Journal of African Earth Science, v.46, p. 1-35.

Legg C.A., 1973, Provisional Mineral Map of the Republic of Zambia (1:1,500,000) Geological Survey Department, government printer, Lusaka, sheet 1.

Levinson, A. A., 1974, Introduction to Exploration Geochemistry, 2nd Edition, Applied Publishing Limited, Wilmette, Illinois, USA, 924p.

Loughlin, W.P., 1978, Geology of the Matebo and Luma River areas, explanation of degree sheet 1225, SE quarter and 1226, SW quarter, Report of the Geological Survey of Zambia, no.90, 19p.

Maisse, F., Gregoire, J., Brooks, R. R., Morrison, R. S., and Reeves, R. D., 1978, Aeolanthus biformifolius De Wild, a hyper-accumulator of copper from Zaire, Science, v.199, no. 4331, p. 887-888.

Master, S., Rainaud, C., Armstrong, R.A., Phillips, D., Robb, L.J., 2005, Provenance ages of the Neoproterozoic Katanga Supergroup (Central African Copperbelt), with implications for basin evolution, Journal of African Earth Sciences, v.42, p. 41-60.

McGoldrick, P., Scott, R., Selley, D., and Broughton, D., 2003, Minor Element Geochemistry of Zambian Copperbelt Deposits, AMIRA P544 Final Report, 12.1-12.6.

Mendelssohn, F., 1961 (Editor), The geology of the Northern Rhodesia Copperbelt Macdonald Publishing Company, London, 523p.

Mendelssohn, F., 1989, Central/Southern Africa Ore shale deposits, special paper v.36, p. 453-470.

Moon, C.J, Whateley, M.K.G., and Evans, A. M., 2006, Introduction to Mineral Exploration, 2nd Edition, Blackwell Publishing, Malden, USA, 499p.

Notebaart, C.W., Vink, B.W., 1972, Ore minerals of the Zambian Copperbelt, Geology en Mijnbouw v.5, p. 337-345.

Porada, H., 1989, Pan-African Rifting and Orogenesis in Southern to Equatorial Africa and Eastern Brazil, Precambrian Research, v.44, no.2, p. 103-136.

Porada, H., Berhorst, V., 2000, Towards a new understanding of the Neoproterozoic-Early Palaeozoic Lufilian and northern Zambezi Belts in Zambia and the Democratic Republic of Congo, Journal of African Earth Sciences v.30, p. 727-771.

Rose, A.W., 1989, Mobility of copper and other heavy metals in sedimentary environments, Geological Association of Canada, Special Paper v.36, p. 97-110.

Ryan, R., Fraser, B., Chapman, M., and Stevens, D., 2004, Field Guide for Geoscientists and Technicians, A Practical Guide to Working in the Bush, The Australian Institute of Mining and Metallurgy, Spectrum Series v.12, 418p.

Sales, R.H., 1962, Hydrothermal versus Syngenetic theories of ore deposition, Economic Geology, vol. 57, p. 721 - 734.

Salisbury, 1961, Secondary Geochemical Dispersion on Copperbelt (unpubl. Internal report), Kalulushi Technical Services Library, 85p.

Saraswatibhatla S., 2012, Solwezi Airborne Magnetic and Radiometric survey, Results and Recommendations, (unpublished confidential report to Vale), 15p.

Saraswatibhatla S., 2013, Lualaba Airborne Magnetic and Radiometric survey, Results and Recommendations, (unpublished confidential report to Vale), 11p.

Schmandt, D., Broughton, D., Hitzman, M.W., Plink-Bjorklund, P., Edwards, D., and Humphrey, J., 2013, Kamoa Copper Deposit, Democratic Republic of Congo, Stratigraphy, Diagenetic and Hydrothermal Alteration, and Mineralisation, Economic Geology, v.108, p. 1301-1324.

Selley, D., Broughton, D., Scott, R., Hitzman, M.W., Bull, S., McGoldrick, L.P., Croaker, M., Pollington, N. and Barra, F., 2005, A New Look at the Geology of the Zambian Copperbelt, Economic Geology, 100th Anniversary volume, p. 965-1000.

Sillitoe, R. H., Perello, J., Creaser, R.A., Wilton, J., Wilson, A.J., Dawborn, T., 2017, Age of the Zambian Copperbelt, Miner Deposita, Springer-Verlag Berlin Heidelberg, 24p.

Snowden, 2011, Quality Assurance and Quality Control of assay data: QAQC concepts Manual.

Steven, N., and Armstrong, R., 2003, A metamorphosed Proterozoic carbonaceous shale hosted Cu-Co-Ni deposit at Kalumbila, Kabompo Dome: The Copperbelt ore shale in north-western Zambia: Economic Geology, v.98, p. 893-909.

Surveyor General, 1986, Physical map of Zambia, Ministry of Lands and Natural Resources, Survey Department, Lusaka.

Sutton, S.J., and Maynard, J.B., 2005, A fluid mixing model for copper mineralisation at Konkola North, Zambian Copperbelt, Journal of African Earth Sciences v.42, p. 95 – 118.

Sweeney, M.A., and Binda, P. L., 1994, Some constraints on the formation of the Zambian Copperbelt deposits, Journal of African Earth Sciences, vol.19 No.4, p. 303 – 313.

Sweeney, M.A., Binda, P. L., Vaughan, D. J., 1991, Genesis of the ore of the Zambian Copperbelt, Ore Geology Reviews, v.6, p. 51-76.

Tooms, J. S., and Webb, J. S., 1961, Geochemical Prospecting Investigations in the Northern Rhodesian Copperbelt. Economic Geology, v.56, p. 815 - 846.

Unrug, R., 1982, The Lufilian Arc, A Microplate in the Pan-African Collision Zone of the Congo and Kalahari Cratons, Precambrian Research, v.21, p. 181-196.

Unrug, R., 1988, Mineralization controls and source of metals in the Lufilian fold belt, Shaba (Zaire), Zambia, and Angola, Economic Geology, v.83, no.6, p. 1247-1258.

Unrug, R., 1996, The Assembly of Gondwanaland, Scientific Results of IGCP Project 288, Gondwanaland Sutures and mobile belts, v.19, p. 11-20.

Watts, Griffis and McQuat Limited, 1991, Assessment of Mineral Opportunities in Zambia, confidential report to Zambia Consolidated Copper Mines Limited, 566p (Copies available from the Geological Survey of Zambia).

Wendorff, M., 2005a, Evolution of Neoproterozoic-Lower Palaeozoic Lufilian arc, Central Africa: a new model based on syntectonic conglomerates, Journal of the Geological Society of London, Vol. 162, pp. 1- 4.

Woodhead, J., 2011, Mwombezhi Dome PLLS148 Quarterly Report: July to September, Zamanglo prospecting Limited, Kitwe.